Appendix 1

Från:
Till:

Datum:
Ärende:

Till: :@karolinska.se>
Från: '@landspitali.is>
Datum: 2014-09-11 19:07
Ärende: Ang: Re: bronkoskopier och spirometrier

Hej

Det tog lite tid, men jag hittade följande:

29. okt 2009 fannst PAD med bitar ifran min acut op dar diagnosed bekraftades.

27. nov 2009 togs det benmerg som var normal

8. jan 2010 gjordes det CT biopsi av cavitet i lungan som visade granuloma i lungor som pa odling var miliary TBC infection

11 feb 2011 bestallde min kollega pa onkologen bronchosckopi dar man hittade massiv förtrangning i trachea. Biopsier togs, men de var inte av bra kvalitet och visade enbart granulomatös vavnad. Sa nagon cancer-diagnos fanns inte har i vara journal fran den perioden. Patienten skickades jo till Er och jag kom ihag att tanken var att ny bronchoscopi och biopsier skulle tas hos Er.

mvh

Karolinska Universitetssjukhuset 11002521SV1
Öron-,näs- och halskliniken, Huddinge
Avdelning B82
141 86 STOCKHOLM
tel: 08-585 877 91 fax:08-585 873 25

Appendix 2

2011-05-24 10:10 Jan-Erik Juto, Läk H - ÖNH-avd B82 (låst)

INTAGNINGSANT.

Patientansvarig läkare Jan-Erik Juto (läk) /1f3x/

Intagningsorsak Pat kommer på remiss från Reykjavik för att dels gå igenom röntgenundersökningar här samt gå igenom en bronkoskopi av trakea, larynx och bronker. Detta inför planerad stor kirurgi om cirka 2 v.

Socialt Universitetsstuderande i Reykjavik. Bördig från Eiritrea. Varit på Island vid Universitetet, studerat där sedan cirka två år tillbaka. Är gift. Har hustru och två barn hemma i Eiritrea. Det yngre barnet som nyligen fötts har han inte sett.

Tobak Icke rökare.

Tid/nuv.sjukdomar För cirka 19 mån sedan i Reykjavik, efter att tidigare ha varit väsentligen helt frisk anamnestiskt, får han stridor. Undersöks och det befinns att han har en mucoepidermoid cancer distalt i trakea som förtränger. Man bulkar pat i samband med provtagning och man får en stor blödning och det krävs en öppen thorakirurgi för att stoppa blödningen. Trots trycklöshet i under 15-20 min är pat efter op neurologiskt intakt. Härefter upptäcks en lungturberkulos och han får behandling under några månader för detta. Därefter startar en strålbehandling till 66 gray. Tumören går tillbaka på detta. Åter recidiv av tumör med viss stridor våren 2011.

Kontakt med Karolinska sjukhuset efter att man har i en bedömning i Boston beslutat därifrån att en palliativ behanling bör göras. Pat har nu bedömts av Paolo Macchiarini, härvarande .....dent kirurg på kliniken och han skall nu under denna vårdtid bedöma CT-bilder och även PET CT-bilder som skall tas under vårdtiden under 2-3 dagar och bedöma möjligheten till radikal kirurgi vilken planeras med utrymning av tumör och transplantation, med en transplantat polymer med överdragen av patientens egna stamceller.

Pat har någon slags bronkvidgande inhalationsmedicinering. Han har vissa svårigheter att andas pga sekretstagnation men han lyckas hosta upp det så det blir klart lindrigare.

Ingen känd allergi.

Karolinska Universitetssjukhuset 11002521SV1
Öron-,näs- och halskliniken, Huddinge
Avdelning B82
141 86 STOCKHOLM
tel: 08-585 877 91 fax:08-585 873 25

Överkänslighet Ingen känd.

Status

Allmäntillstånd	Gott. Inga kardiopulmonella inkompensationstecken i vila i stolen. Rör sig obehindrat på golvet.
Munhåla och svalg	Retningsfria slemhinnor. Egna sanerade tänder.
Näsa	Lite intorkat sekret. I övrigt retningsfritt bilat.
	Epi-, oro- och hypofarynx u a.
Larynx	Normal stämbandsrörlighet och normalt larynx.
Halsens mjukdelar	Palperas u a.
Hjärta	Regelbunden rytm. Inga bi- eller blåsljud hörbara.
Blodtryck	110/80 mmHg
	i vila vä arm.
Lungor	Fys u a, dock lite bronkiella andningsljud av och till en del stridor hörbara på båda sidor.

Preliminär bedömning Man med ett recidiv av ett mucoepidermoid cancer i distala trakea. Inkommer nu för DT och PET scan samt en bronkoskopi med kartläggning endoskopiskt av utbredning av tumören. Allt inför planerad radikal kirurgi om cirka 2 v.

---------- slut utskrift ----------

SVAR RÖNTGEN/ISOTOP

Appendix 3

FRÅN

Karolinska Universitetssjukhuset
Röntgenavd, Huddinge
Röntgen C146
141 86 Stockholm
Tel 08-585 808 50

B: 11002-521-M01
S: 11002-521-M01
F: 11002-521-M01
R: 1026-7213120-2
L: 4327139001

TILL

Karolinska Universitetssjukhuset
Öron-,näs- och halskliniken, Huddinge
Öron-, näs- och halsmottagningen
141 86 STOCKHOLM
Tel: 08-585 814 30 Fax:

Prioritet: Normal
Patienten bör undersökas på: Röntgen
Patienten kallas från: Vårdavd.

Remissdatum: 2011-05-19 13:41 Remittent: Jan-Erik Juto
Till sektion: Datortomografen
Önskad undersökning: CT hals och thorax.
Frågeställning: artärer, venös return, aneurysm? fistlar?
Anamnes, status: Ref till samtal med Bertil Leidner den 19/5:

Patienten skall undersökas med thorax preop. spec protokoll. Har tid bokad för undersökningen tisdagen den 24/5 kl 15.00 på datortomografen, HS.

För 20 månader sedan livräddande öppen thoraxkirurgi pga av profus blödning i samband med rigid bronkoskopi med biopsi från distalt i trachea sittande tumör, mucoepidermoid cancer. Man hade vid biopsitagningen perforerat ut i mediastinum och fått skada på lungartär.
Härefter har strålbehandling givits till 66 Gray, fulldosbehandling.
Nu recidiv av tumör distalt i trachea och ev i bronk/bronker, eventuellt utanför luftträdet.

Patienten finns på avd B82
Patienten är planerad för radikal kirurgi till den 7/6 på Huddinge sjh med rekonstruktion av luftvägar.
Inför denna operation behövs klarläggande CT undersökning.

SVAR

Undersökning påbörjad: avslutad: 2011-05-24 13:29 Rek. C-koder:

Undersökningskod: D47. DT Thorax

Utlåtande: Datortomografi thorax

Undersökningen är utan och med i.v. kontrast och med tredimensionella rekonstruktioner över trachea över carina och höger och vänster stambronk:

En expansivitet ventrolateralt till höger om distala trachea gående ned till carina. Expansiviteten är cirka 7 x 10 mm i tvärsnittsdiametrar och i kraniokaudal riktning cirka 9 mm. Tumöravgränsningen är dock svårbedömbar. Mjukdelsmassor finns fram mot arteria pulmonalisgren och emot artärgrenen mot höger överlob. Likaså finns mjukdelsmassor fram emot vengrenen till höger överlob av höger vena pulmonalis, dessa ovan beskrivna mjukdelsmassor utgörs sannolikt av fibros postoperativt och/ eller efter

FRÅN Karolinska Universitetssjukhuset
Röntgenavd, Huddinge
Röntgen C146
141 86 Stockholm
Tel 08-585 808 50

B: 11002-521-M01
S: 11002-521-M01
F: 11002-521-M01
R: 1026-7213120-2
L: 4327139001

TILL Karolinska Universitetssjukhuset
Öron-,näs- och halskliniken, Huddinge
Öron-, näs- och halsmottagningen
141 86 STOCKHOLM
Tel: 08-585 814 30 Fax:

Prioritet: Normal
Patienten bör undersökas på: Röntgen
Patienten kallas från: Vårdavd.

strålbehandling. Ingen förträngning av kärllumen. Däremot föreligger en förträngning av distalaste delen av trachea inom främre delen och strax ovanför carina. Strax nedanför carina finns det två mjukdelsmassor som laddar kontrast, båda ca 1,5 cm stora som kan vara lymfkörtlar. Dwet finns en 0,5 x 2 cm stor mjukdelsmassa som laddar kontrast strax till vänster om trachea ovanför carina som kan vara postoperativt betingad eller vara flera tätt intilliggande små lymfkörtlar. Det finns metallclips i området för expansiviteten efter tidigare operation. Det finns en mjukdelsmassa paravertebralt medialt på höger sida i höger lunga med en del fibrösa förändringar dorsalt om denna, förändringarna är sannolikt strålningsinducerade. Inget aneurysm i något av kärlen påvisade. Inga fistlar påvisade. Ordinär kontrastfyllnad av hjärtats förmak och kamrar, inga tecken till högerkammarbelastning.

Herlin, Gunnar

13:52 2011-05-27 Signering 1 Preliminärt svar: Herlin, Gunnar

Fallet demonstrerades för Prof. Machiarini 2011-05-24 avseende frågor inför tillverkning av artificiell trachea- huvudbronk implantat. Mätvärden avseende längd och diameter av trakea och huvudbronker, carinavinkel mm registrerades./ pg
07:07 2011-06-14 Signering 2 Slutgiltigt svar: Güntner, Peter
----------slut----------

SVAR RÖNTGEN/ISOTOP

Appendix 4

FRÅN

Karolinska Universitetssjukhuset
Centrala Röntgen
Solna
171 76 Stockholm
Tel 08-517 757 01

B: 11001-521-M02
S: 11002-521-DK1
F: 11001-521-M02
R: 1026-7205799-3
L: 4326905201

TILL

Karolinska Universitetssjukhuset
Öron-,näs- och halskliniken, Huddinge
B84
141 86 Stockholm
Tel: 08-585 895 55 Fax: 08-585 895 50

Prioritet: Normal
Patienten bör undersökas på: Röntgen
Patienten kallas från: Vårdavd.

Remissdatum: 2011-05-18 11:50
Remittent: Richard Kuylenstierna
Till sektion: NuklearMed. - PET/CT
Önskad undersökning: PET-CT
Frågeställning: Spridning av primärtumör från distala trakea
Anamnes, status: Pat med en låggradig mucoepidermoid cancer i distala trakea som tidigare opererats och erhållit fulldos radioterapi i Island för ca ett år sedan. Även behandlad för lungtbc och utläkt.

Nu recidiv av den distala trakealtumören med andningssvårigheter.

Vi planerar en trakealtransplantation (ej tidigare utförd i Sv)

Mycket angeläget att snarast bedöma om tumören är dissiminerad eller ej. Har informerat prof Hans Jacobsson.

Pat är inlagd på Huddinge avd B82 eller B84 från v 21.

Kontrastallergi: Nej
Diabetes: Nej

SVAR

Undersökning påbörjad: avslutad: 2011-05-25 13:32 Rek. C-koder:

Undersökningskod: N93. NM PETCT F18 FDG

Utlåtande: POSITRONEMISSIONSTOMOGRAFI med 18F-FDG samt DATORTOMOGRAFI efter

tillförsel av intravenöst kontrastmedel (hals, thorax och buk/bäcken):

Anteriort om carina finns en något svåravgränsad mjukdelsökning med inbäddade clips samt sträckande sig aningen in i den högra huvudbronken. Området svarar mot ett rundat, kraftigt ökat FDG-upptag med en diameter på halvannan cm. Fyndet tolkas som det kända tumörrecidivet.

Sträckande sig ungefär från tumörområdet snett lateralt caudalt, paravertebralt ut i höger lunga finns en skrumpnande, fibrotisk, delvis organiserad förändring med oregelbundet, lätt ökat spårämnesupptag. Perifert om detta finns medialt i de 5:e - 7:e högra revbenen uppdrivna, frakturer med karaktär av fördröjd läkning. Frakturerna visar kraftigare ökat spårämnesupptag. Samtliga dessa förändringar förklaras med stor sannolikhet av den tidigare radioterapin. Sådan ger permanenta lungförändringar och kan också försvaga skelettet med ökad frakturrisk. Stämmer det utifrån kännedom om strålfältet?

Aktiviteten i höger tonsill är något högre än kontralateralt (alternativt

Framställd
11-05-26 11:26

FRÅN Karolinska Universitetssjukhuset
Centrala Röntgen
Solna
171 76 Stockholm
Tel 08-517 757 01

B: 11001-521-M02
S: 11002-521-DK1
F: 11001-521-M02
R: 1026-7205799-3
L: 4326905201

TILL Karolinska Universitetssjukhuset
Öron-,näs- och halskliniken, Huddinge
B84
141 86 Stockholm
Tel: 08-585 895 55 Fax: 08-585 895 50

Prioritet: Normal
Patienten bör undersökas på: Röntgen
Patienten kallas från: Vårdavd.

är aktiviteten nedsatt inom vänster tonsill). Inget avvikande morfologiskt varför fyndets kliniska signifikans är liten. Status efter sternotomi.

- Metabolt aktiv tumör i nivå med carina. Föga misstanke på tumörspridning utanför detta.

Undersökningen kan rekvireras digitalt via Röntgenklinikens Solna expedition, telefon
08 - 517 745 97 eller fax 08 - 517 745 83.

Vänliga hälsningar,

Hans Jacobsson, Professor, specialist i radiologi och nukleärmedicin, 08 - 517 735 81

11:26 2011-05-26 Signering 2 Slutgiltigt svar: Jacobsson, Hans
----------slut----------

Clinical Radiology 66 (2011) 366–382

Contents lists available at ScienceDirect

Clinical Radiology

journal homepage: www.elsevierhealth.com/journals/crad

Pictorial Review

False-positive uptake on 2-[^{18}F]-fluoro-2-deoxy-D-glucose (FDG) positron-emission tomography/computed tomography (PET/CT) in oncological imaging

A.D. Culverwell [a], A.F. Scarsbrook [a,b], F.U. Chowdhury [a,b,*]

[a] *Department of Clinical Radiology, Leeds Teaching Hospitals NHS Trust, UK*
[b] *Department of Nuclear Medicine, Leeds Teaching Hospitals NHS Trust, UK*

ARTICLE INFORMATION

Article history:
Received 13 September 2010
Received in revised form
14 December 2010
Accepted 21 December 2010

With the increasing utilization of integrated positron-emission tomography/computed tomography (PET/CT) using the glucose analogue 2-[^{18}F]-fluoro-2-deoxy-D-glucose (FDG) in oncological imaging, it is important for radiologists and nuclear medicine physicians to be aware that FDG uptake is not specific for malignancy, as many different physiological variants and benign pathological conditions can also exhibit increased glucose metabolism. Such false-positive FDG uptake often arises outside the area of primary interest and may mimic malignant disease, thereby confounding accurate interpretation of PET/CT studies. With the use of illustrative clinical cases, this article will provide a systematic overview of potential interpretative pitfalls and illustrate how such unexpected findings can be appropriately evaluated.

Introduction

Integrated positron-emission tomography/computed tomography (PET/CT) using the glucose analogue 2-[^{18}F]-fluoro-2-deoxy-D-glucose (FDG) is established in the imaging procedures of oncological patients. The recognition that combined metabolic and morphological information yielded by PET/CT can have a significant impact on tumour staging and re-staging, detection of recurrent disease and optimization of therapy in a wide variety of solid-organ malignancies, along with increased access to this imaging technique, has led to greater utilization of PET/CT in oncological patients in recent years.[1–5] It has become apparent, however, that due to the non-specific nature of FDG uptake (which is the key to its successful use as a radiotracer in a wide range of clinical indications), there are many physiological variants and benign (although often clinically significant) pathological entities that also demonstrate augmented glucose metabolism.[6–11] Accurate interpretation relies on detailed knowledge of (a) technical artefacts that may arise from integrated PET/CT; (b) physiological uptake patterns of FDG; and (c) the causes of "false-positive" FDG uptake. This article provides an overview of the common causes of potential pitfalls that may be encountered on FDG PET/CT studies undertaken in oncological patients and attempt to describe how such findings can be evaluated accurately and confidently, thereby avoiding interpretative error and inappropriate management.

Mechanism of FDG uptake

FDG is a non-physiological analogue of glucose that varies only slightly from the chemical structure of the glucose molecule. It undergoes normal cellular transport and metabolic pathways.[12] Once injected, FDG is taken up

* Guarantor and correspondent: F.U. Chowdhury, Departments of Clinical Radiology and Nuclear Medicine, Bexley Wing (Level 1), St James's University Hospital, Beckett Street, Leeds LS9 7TF, UK. Tel.: +44 113 2068260.
E-mail address: fahmid.chowdhury@leedsth.nhs.uk (F.U. Chowdhury).

0009-9260/$ – see front matter © 2011 The Royal College of Radiologists. Published by Elsevier Ltd. All rights reserved.
doi:10.1016/j.crad.2010.12.004

by cell membrane glucose receptors (principally, the glucose transporter-1 molecule, GLUT-1) that transport it into the intracellular compartment, where it is phosphorylated into FDG-6-phosphate by the enzymatic action of hexokinase. As early as 1924, the Nobel laureate Otto Heinrich Warburg hypothesized that malignant cells generated energy by the preferential non-oxidative breakdown of glucose.[13] At a cellular level, it has subsequently been shown that most malignant cells express high concentrations of GLUT-1 receptors and hexokinase while showing reduced expression of the dephosphorylating enzyme, glucose-6-phosphatase. The overall effect is that FDG becomes trapped in the cancer cell, failing to undergo further metabolism; consequently, this can be exploited to visualize the metabolic activity at sites of tumoural involvement. However, it has long been recognized that active benign pathological conditions, such as inflammatory and infective processes, may also show increased accumulation of FDG. This is largely due to the enhanced glycolytic metabolism that accompanies inflammatory cellular infiltrates, incorporating activated macrophages, monocytes, and polymorphonuclear cells, which are all actively involved in the recruitment, activation, and healing phases of tissue inflammation.[11]

Physiological biodistribution of FDG

The physiological biodistribution of FDG reflects the utilization of glucose as a substrate by normal body tissues and organs. The brain is an obligate user of glucose regardless of substrate availability and high FDG uptake is routinely seen within the basal ganglia and the cortex. Activity within the ocular muscles can be quite intense due to active eye movements during the uptake period following injection of FDG. The lympho-epithelioid tissue in the head and neck, including the tonsillar tissue of Waldeyer's ring and in the nasopharynx, palate, and at the base of the tongue, shows symmetric and moderate tracer uptake, especially in younger patients. Asymmetric tonsillar uptake is not uncommon, and although it has been suggested that a difference in maximum standardized uptake value (SUVmax) between left and right sides is a useful parameter for distinguishing between normal FDG uptake in pharyngeal palatine tonsils from primary cancer, it is

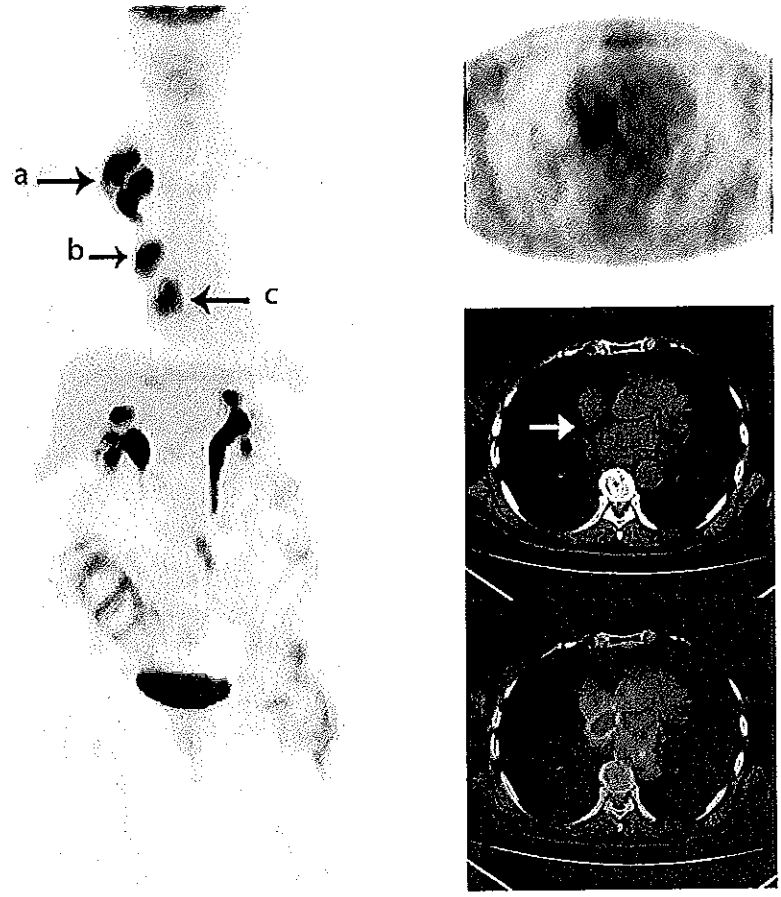

Figure 1 Lipomatous hypertrophy of the interatrial septum. Maximum intensity projection (MIP) PET image shows a primary lung cancer (a), an FDG-avid node at the right hilum (b) and a further focus of FDG uptake in the right side of the mediastinum (c). Selected axial PET, CT, and fused PET/CT images show that this area (c) corresponds to fatty hypertrophy of the interatrial septum (arrow), a recognized benign variant appearance.

generally the case that in the absence of a morphological abnormality, asymmetrical uptake is almost always benign.[14,15] The salivary glands also commonly show low-grade diffuse FDG activity.[16] Muscles in the oropharynx and hypopharynx often demonstrate symmetrical physiological FDG uptake, including the pterygoid muscles and the muscles of the oral floor. When asymmetrical, uptake in these locations may mimic focal areas of malignancy.[17] Low-grade diffuse uptake in the thyroid is also recognized as a normal finding in patients who are euthyroid.

Uniform and low-grade activity is seen within the mediastinal vascular structures, and this low-level uptake is usually accepted as a background reference level for characterizing abnormal FDG uptake elsewhere in the thorax, e.g., in mediastinal nodes in lung cancer or in solitary pulmonary nodules[2]. In the fasting state, the heart theoretically switches to fatty acids rather than glucose as its preferred substrate, but the degree of left ventricular myocardial uptake on FDG PET is highly variable even with a standard 4–6 h fast prior to FDG injection (Fig 1).[18] Normal thymic activity may be seen in young patients or following chemotherapy, so-called "thymic rebound", which may persist for several months after treatment, manifesting as an inverted "V" area of uptake in the anterior mediastinum.[10,19,20]

The liver, spleen and haematopoietic bone marrow usually show low-grade and homogeneous uptake of FDG, with activity in the liver being slightly more than that in the spleen and bone marrow.[10] Diffuse and moderate gastric uptake (especially when the stomach is non-distended) and low-grade activity in the oesophago-gastric junction are frequently encountered, and do not usually carry any clinical significance. Physiological uptake within the small and large bowel is highly variable, being more pronounced in the caecum and ascending colon, and adopts a diffuse pattern with no corresponding morphological abnormality on CT. It is speculated that bowel uptake is related to a combination of factors, including activity within intestinal contents, lymphoid tissue, gut microorganisms, and smooth muscle activity. Extremely avid and diffuse uptake of FDG throughout the colon, and to a lesser extent in the small bowel, is frequently seen in diabetic patients on the oral biguanide drug, metformin, which has several effects including inhibition of intestinal glucose reabsorption and

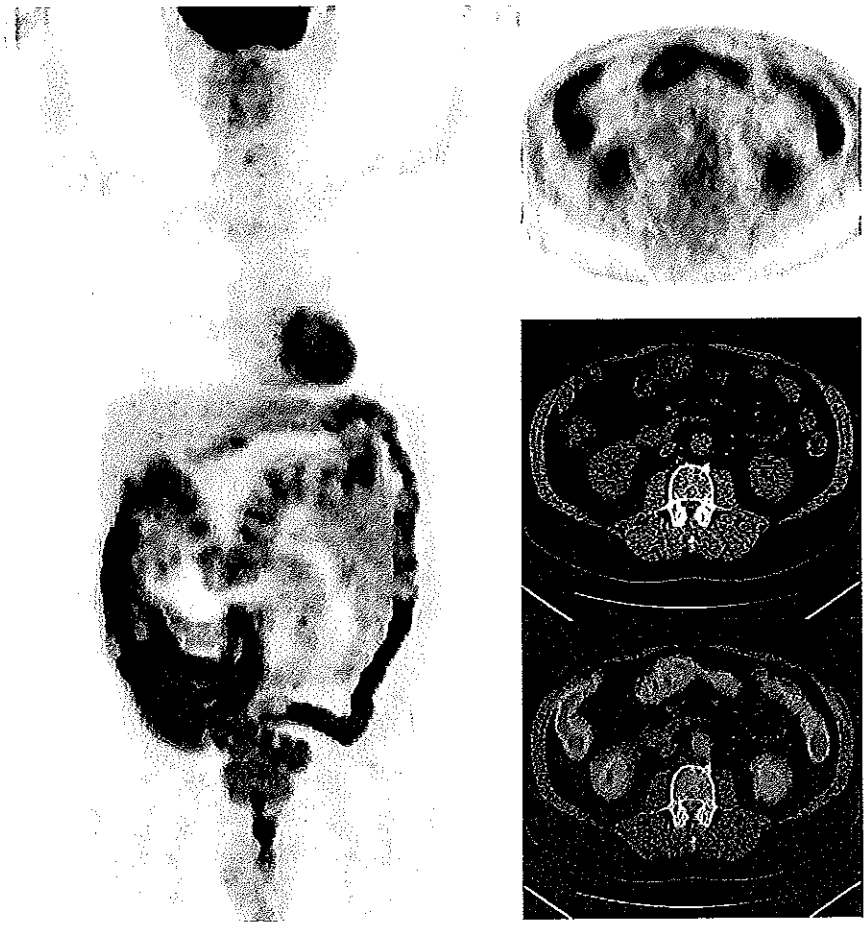

Figure 2 Metformin-induced bowel uptake. MIP PET image demonstrates extremely avid and diffuse FDG activity throughout the colon and also involving some small bowel loops. Selected axial PET, CT, and fused PET/CT images show no corresponding morphological abnormality in this diabetic patient on metformin treatment.

augmentation of glucose utilization by intestinal mucosa (Fig 2).[21,22]

FDG is a small molecule that readily undergoes glomerular filtration, but unlike normal glucose, the tubular cells fail to reabsorb it leading to urinary excretion, which is the principal mechanism of FDG clearance from the body. Hence it is not surprising that high levels of FDG activity are routinely seen in the renal collecting system, ureters, and urinary bladder. FDG activity within redundant ureter, bladder diverticula, and in the prostatic urethra (e.g., following trans-urethral resection, TURP) frequently gives rise to variant appearances that should not be misinterpreted as pathological findings. Physiological endometrial FDG activity varies cyclically in pre-menopausal women, peaking during the ovulatory and menstrual phases. Similarly, ovarian uptake and activity within the corpus luteum is normal in pre-menopausal women, particularly mid-cycle.[23,24] Documentation of the menstrual history of pre-menopausal women by technologists at the time of imaging can provide corroborative clinical information in this situation. Symmetric uptake within the testes is also a common physiological finding, especially in younger men.[25,26]

Prominent muscle activity may be seen in anxious patients or in those who have been undertaking muscular activity during the FDG uptake period, e.g., chewing leading to avid uptake in the muscles of mastication (Fig 3). Extensive activity may also be seen in the accessory muscles of respiration in dyspnoeic patients. Prominent activation of sympathetically innervated brown adipose tissue is a well-recognized phenomenon that is particularly problematic in younger female patients with low body-mass index (Fig 4).[27] These areas of physiological uptake can be minimized by keeping the patient rested, warm, and comfortable during the uptake period.[28,29] Some advocate the use of beta-blockers to further ameliorate this problem, although this is not routine practice in the UK.[30]

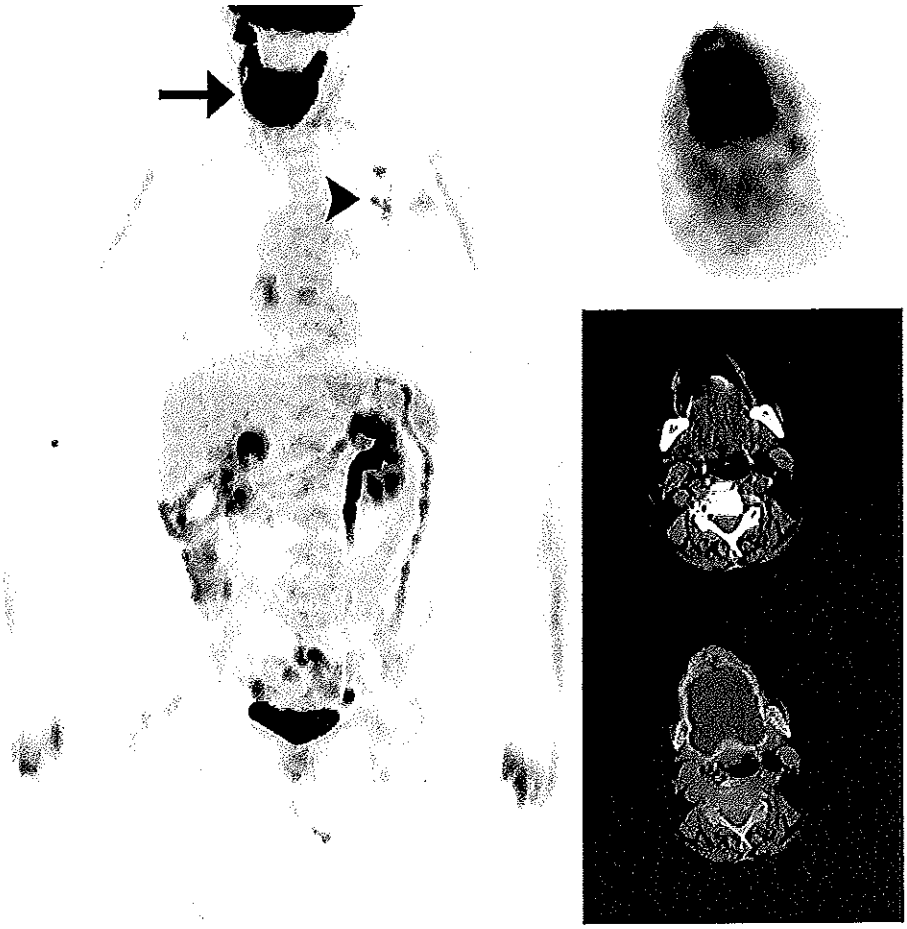

Figure 3 Prominent physiological uptake in the head and neck. MIP PET image and selected axial PET, CT, and fused PET/CT images show extremely avid and diffuse uptake throughout the tongue (arrow) with no corresponding morphological abnormality. This was caused by uncontrolled tongue movement during the FDG uptake period, which may be seen in patients who are anxious or suffering with neuromuscular conditions, such as tardive dyskinesia. This should not be confused with lingual disease. Note the inflammatory-looking nodular uptake in the left lung apex (arrowhead).

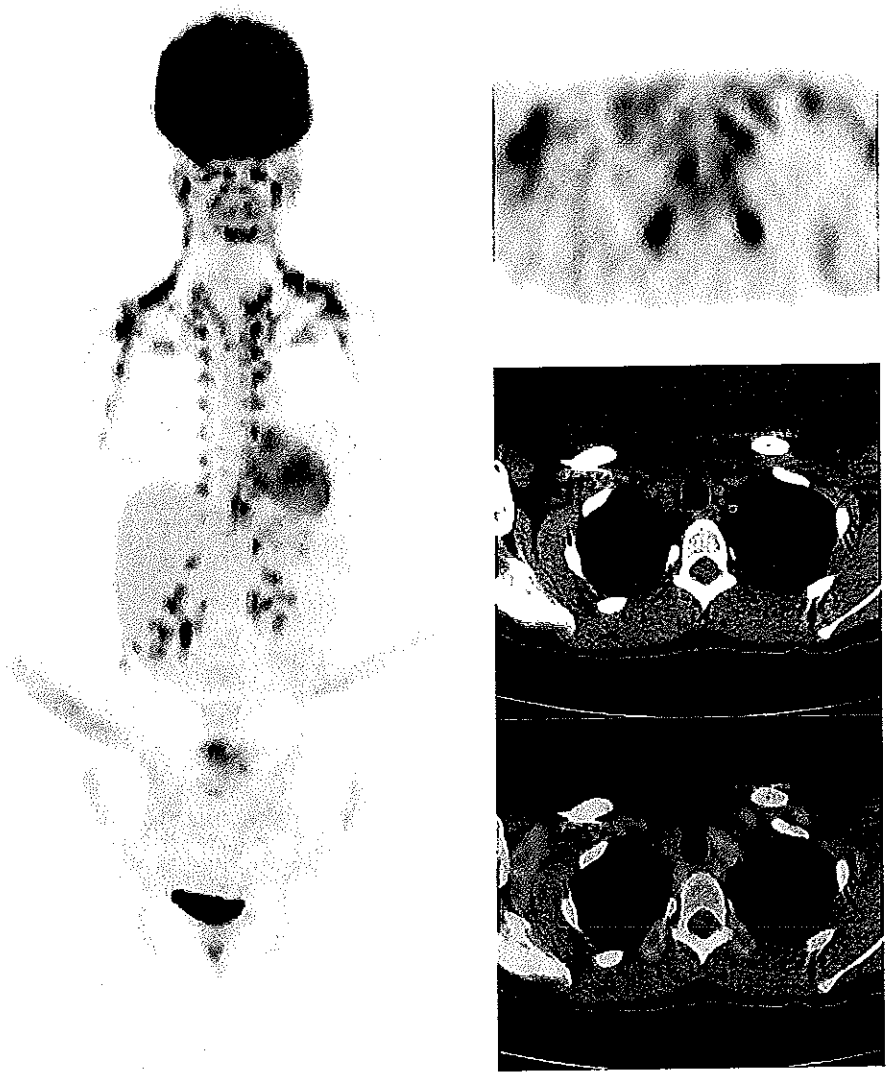

Figure 4 Physiological brown adipose tissue activation. MIP PET and selected axial PET, CT, and fused PET/CT images depict the typical distribution of activated brown fat in a young female patient, affecting the extra-cranial head and neck, supraclavicular fossae, axillae, mediastinum, paravertebral, and sub-diaphragmatic areas. Note the "step-ladder" or "lobster-claw" configuration of the paravertebral brown fat.

Technical artefacts

Integrated PET/CT has the potential to generate several types of technical artefacts. Incorporation of the low-dose CT component allows rapid attenuation–correction of the PET data, which significantly shortens study acquisition time compared with performing additional rotating-source transmission PET. However, CT attenuation correction may generate artefacts in areas with high CT attenuation values, e.g., around metallic implants. Review of the non-attenuation corrected PET images can prove helpful in this situation. The PET data, which requires between six to nine bed positions for a standard acquisition from skull base to upper thighs, is obtained during free tidal breathing, and this can lead to respiratory motion artefacts in the lungs and around the diaphragmatic domes. This may cause the artificial impression of a lesion in the liver dome misregistering to the lung, or vice versa, on the fused PET/CT.[31,32] Similar misregistration may occur elsewhere as a consequence of patient movement between the PET and the CT studies. Artefacts may also occur due to poor injection technique. A paravenous injection may cause spurious lymphatic uptake in ipsilateral axillary nodes. Moreover, local endothelial damage may lead to microembolism of an aggregation of platelets admixed with radiotracer, giving rise to well-defined and intense focal uptake within the lung without any corresponding morphological abnormality on CT (Fig 5).[33,34] Careful injection technique with good venous access and avoidance of blood aspiration can prevent this relatively rare artefact.

Common non-malignant pathological conditions showing increased uptake of FDG

It has been estimated that benign non-physiological lesions with increased uptake of FDG are encountered in more than 25% of PET/CT studies performed in oncological

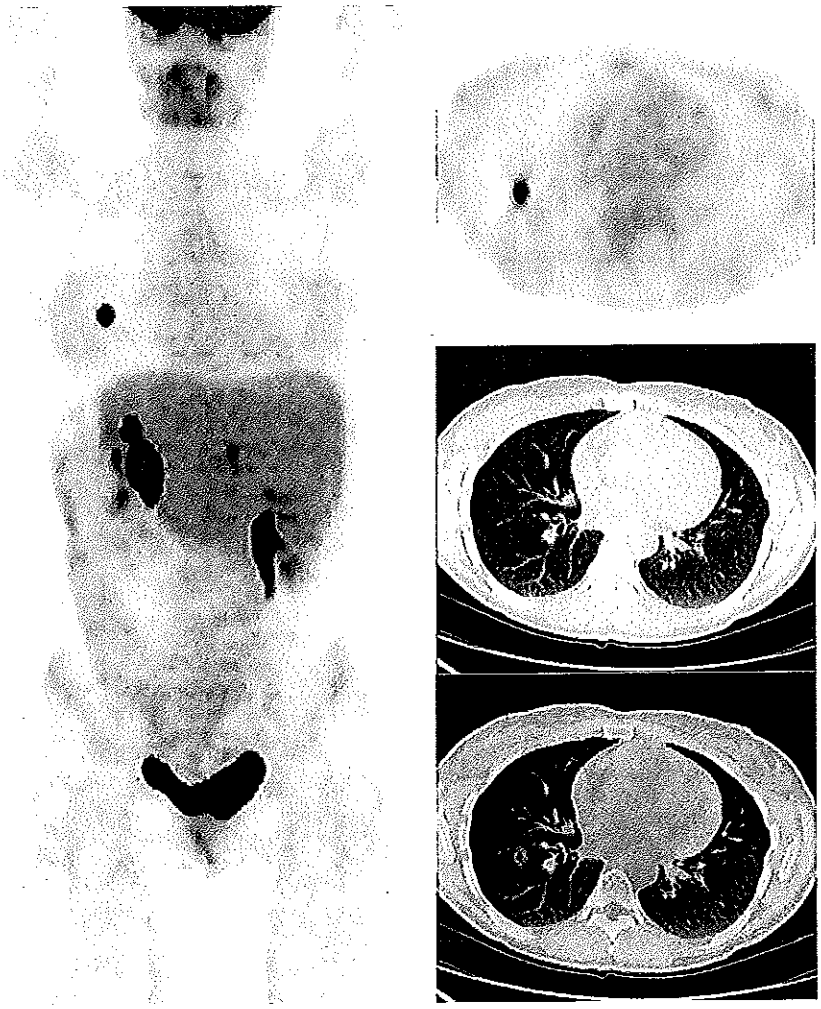

Figure 5 FDG embolus. MIP PET image in a woman with previous right hemi-hepatectomy shows an intense focus of tracer uptake in the right lung. Selected axial PET, CT, and fused PET/CT images fail to show any corresponding CT abnormality. The appearances were felt to be typical of an FDG embolus, and a subsequent follow-up PET/CT several months later was entirely normal.

patients.[9,35] As FDG PET/CT is a whole-body technique, it is not uncommon to find unexpected foci of uptake occurring outside the primary region of interest, and it has been shown that approximately 50% of these findings relate to benign pathological conditions unrelated to the primary tumour.[35] The degree to which further investigation of these findings is undertaken is dependent on a number of factors, which include the diagnostic confidence of the PET/CT reporter, careful review of previous imaging, and multidisciplinary decision-making, based on all the clinical and imaging information available. The following sections provide a practical and systematic overview of the more common benign pathological conditions that may mimic malignancy and potentially affect the accuracy of FDG PET/CT interpretation.

Head and neck

Asymmetric uptake of FDG within the muscles of phonation (vocal cord and cricoarytenoid muscles) may be seen in laryngitis or as a consequence of contralateral vocal cord paralysis.[36] Focal FDG uptake corresponding to a high-attenuation nodule in the parotid gland is an infrequent incidental finding that typically represents a Warthin's tumour; less commonly, focal uptake in the parotid may be due to pleomorphic adenoma. Warthin's tumours may be bilateral (in up to 17%), occur more frequently in smokers, and can be readily confirmed with high-frequency ultrasound (Fig 6).[37,38] Other non-malignant causes of abnormal uptake within the salivary glands include various granulomatous disorders, in particular sarcoidosis.[39] Focal uptake of FDG within the thyroid gland, seen in approximately 4% of patients, is associated with a 30–50% risk of thyroid cancer and requires further evaluation with ultrasound and fine-needle aspiration.[40–42] However, a diffuse increase in activity within both lobes of the gland is a common benign pattern that usually reflects underlying thyroiditis.[40–43]

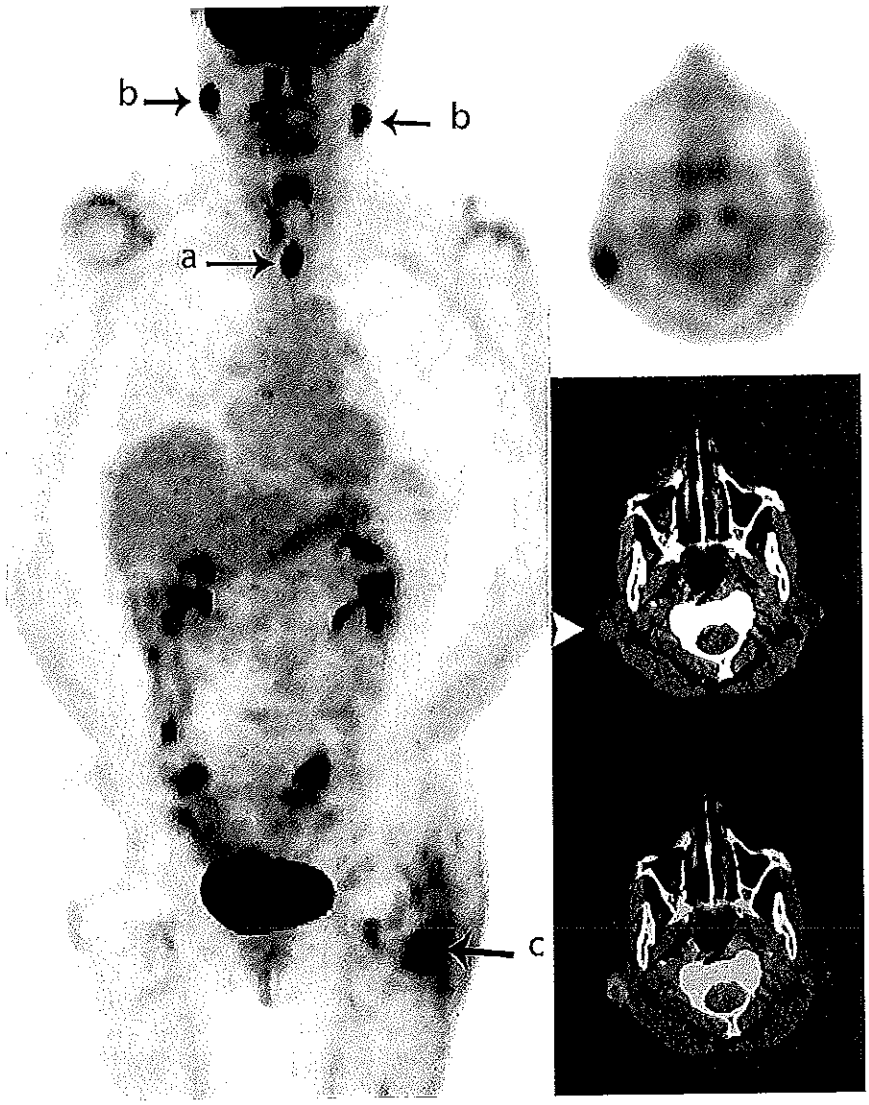

Figure 6 Bilateral Warthin's tumours. MIP PET image in a patient with a primary oesophageal tumour (a). Coincidental bilateral foci of avidly increased tracer uptake were found in both parotid glands (b). Note the post-surgical uptake at the site of recent hip surgery (c). Selected axial PET, CT, and fused PET/CT images show a corresponding high-attenuation nodule in the right parotid gland (arrowhead). This combination of metabolic and morphological findings is typical of a Warthin's tumour, which can be confirmed with high-frequency ultrasound.

Lung and mediastinum

One of the commonest indications for PET/CT in oncological patients is for the staging of non-small cell lung cancer. The clinical impact of FDG PET/CT in this patient group is well established, with additional information obtained in up to 41% of cases compared with conventional imaging alone.[44] FDG PET/CT is also quite accurate in characterizing the nature of solitary pulmonary nodules greater than 8–10 mm in size, with an accuracy approaching 85–93%.[45,46] However, there are many potential causes of false-positive FDG uptake in the thorax that may confound accurate staging or characterization of malignancy.[47–50] Increased FDG uptake has been described in a variety of benign pathological conditions, including acute or chronic pneumonia, atypical infections, mycotic aneurysms, cryptogenic organizing pneumonia, sarcoidosis, following talc pleurodesis, pneumoconiosis, and progressive massive fibrosis, eosinophilic granuloma, hamartoma, and radiation pneumonitis (Figs 7–9). The incidence of some of these inflammatory conditions will obviously vary according to the population studied, and careful correlation with clinical, biochemical, and histological findings, in addition to comparison with previous and serial imaging, can provide much needed clarification in cases where the diagnosis is ambiguous. It is also important to be aware of recent intervention, which can give rise to inflammatory uptake such as mediastinoscopy, thoracoscopy, tracheostomy, and percutaneous biopsy. The use of an adequately completed patient questionnaire at the time of examination can be extremely helpful in this situation.

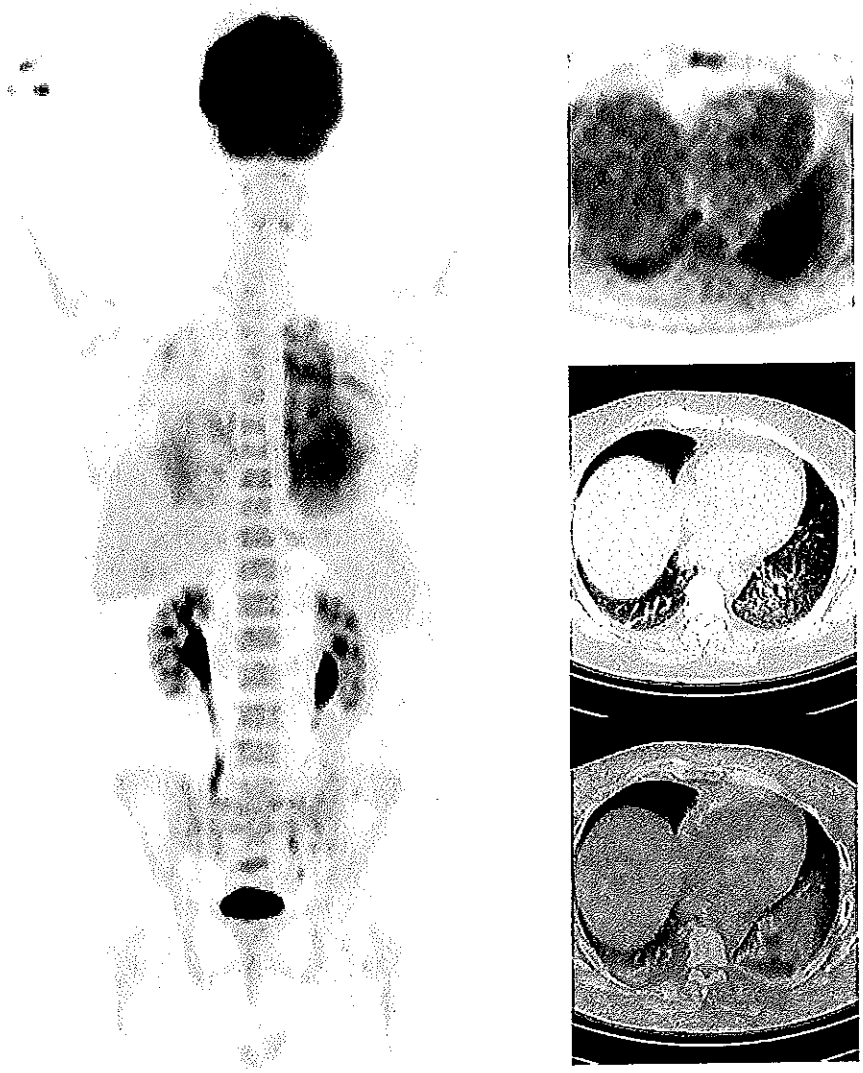

Figure 7 Opportunistic pulmonary infection. MIP PET image in a patient treated for lymphoma shows ill-defined pulmonary FDG uptake bilaterally. Selected axial PET, CT, and fused PET/CT images show that the uptake corresponds to ground-glass opacification and small-airways inflammation, consistent with atypical pulmonary infection. This was treated empirically, with complete clinical and radiological resolution. Note the mild and homogeneous increase in uptake throughout the bone marrow, which is frequently seen following chemotherapy.

Abdomen and pelvis

Physiological uptake of FDG in the bowel takes a diffuse form with no corresponding morphological abnormality on CT. Focal colonic uptake usually requires further evaluation, e.g., with colonoscopy, even in the absence of an obvious morphological correlate, as up to 60–80% of these will turn out to be pre-malignant polyps or adenomas (Fig 10).[51,52] Furthermore, diffuse or segmental uptake with associated bowel wall thickening or pericolic fat stranding can represent inflammatory or infective bowel pathology, such as neutropenic colitis, tuberculosis (TB), and inflammatory bowel disease (Fig 11).[53] Diffuse tracer activity within the oesophago-gastric region and within the anal canal is not infrequently seen on FDG PET/CT and often this is either physiological or due to inflammation, e.g., gastritis related to chemotherapy or inflamed haemorrhoids. In the absence of a structural abnormality on the CT component oesophago-gastric and ano-rectal uptake is almost always benign in nature.[54]

Unequivocal focal uptake of FDG within the liver, in the context of a known primary malignancy, usually indicates metastatic disease. False-positive uptake is recognized in liver abscesses, biliary stasis and cholangitis, infarcts and granulomatous conditions such as sarcoidosis. Moreover, at sites of liver resection and following radiofrequency ablation (RFA),[16] increased FDG activity may be present for up to 2–6 months, especially if there has been post-surgical complication or where the surgical technique includes use of fibrin glue, which can result in localized granulomatous inflammation.[55]

Diffuse splenic uptake, outside the context of lymphoma, may be seen with reactive myeloid changes (e.g., following chemotherapy or treatment with colony-stimulating factor,

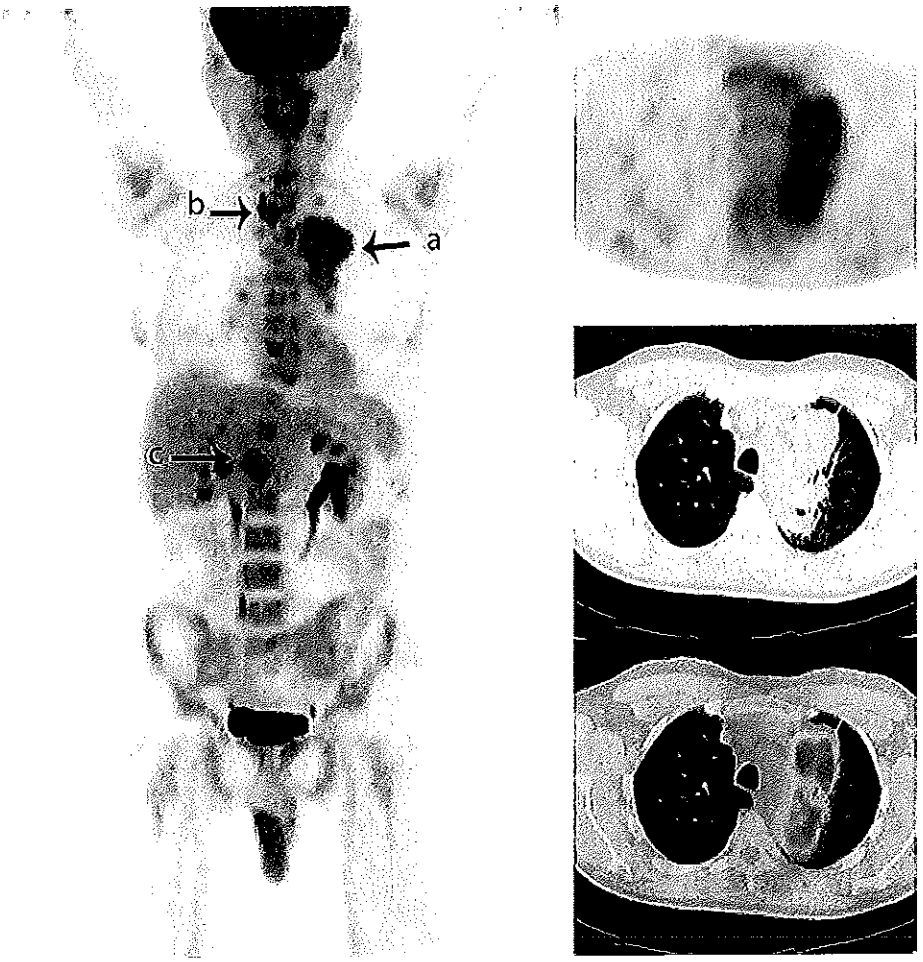

Figure 8 Pulmonary, mediastinal, and nodal tuberculosis masquerading as metastatic lung cancer. MIP PET image in a patient who was suspected of having lung cancer shows an extremely hypermetabolic left upper lobe mass (a) with FDG-avid nodes in the right paratracheal station (b) and below the diaphragm (c). Selected axial PET, CT, and fused PET/CT images confirm a cavitating, FDG-avid, left upper-lobe mass. Bronchoscopic washings and endobronchial ultrasound (EBUS)-guided nodal aspiration yielded a diagnosis of *Mycobacterium tuberculosis* (MTB) and the patient was commenced on triple therapy.

G-CSF), when it is usually also associated with an increase in bone marrow activity, or in patients with systemic inflammation (e.g., sarcoidosis) or infection (e.g., infective mononucleosis).[56,57]

Diffuse pancreatic FDG uptake can be seen in chronic active pancreatitis and the presence of concomitant extrapancreatic uptake by the salivary glands has recently been reported to be sensitive for differentiation of autoimmune pancreatitis from pancreatic malignancy.[58] Focal pancreatic uptake can also be encountered in benign conditions such as haemorrhagic pseudocysts and portal vein thrombosis.[59] Although focal gall bladder FDG activity may indicate the presence of a gall bladder cancer, false-positive uptake has been well described in benign conditions such as cholecystitis and adenomyomatosis (Fig 10).[60]

FDG PET/CT, performed in the post-surgical and post-radiotherapy setting, can achieve high levels of accuracy for detecting recurrent disease.[61] However, careful correlation with the clinical history, tumour markers, and inflammatory serum markers is often required as FDG uptake at sites of surgical and non-surgical intervention (e.g., in the abdominal wall, mesenteric fat, and pre-sacral space) may persist for up to 12 months and beyond, especially if the post-therapeutic period has been complicated by infection or anastomotic breakdown.[62] Focal or linear tracer uptake of FDG is also frequently seen at sites of low-grade inflammation related to therapeutic interventions, such as stoma sites, indwelling lines, and stents.

FDG PET/CT can achieve a sensitivity and specificity in detection of adrenal metastases of 98 and 92%, respectively.[63,64] False-positive FDG uptake may occur in adrenal adenomas, adrenal hyperplasia, angiomyolipoma, and oncocytoma. Other than adrenal metastases, phaeochromocytoma and paraganglionoma usually also exhibit increased uptake of FDG (Fig 12).[65]

FDG uptake in either the endometrium or ovary in post-menopausal women is considered pathological until proven otherwise, and requires gynaecological assessment. Many

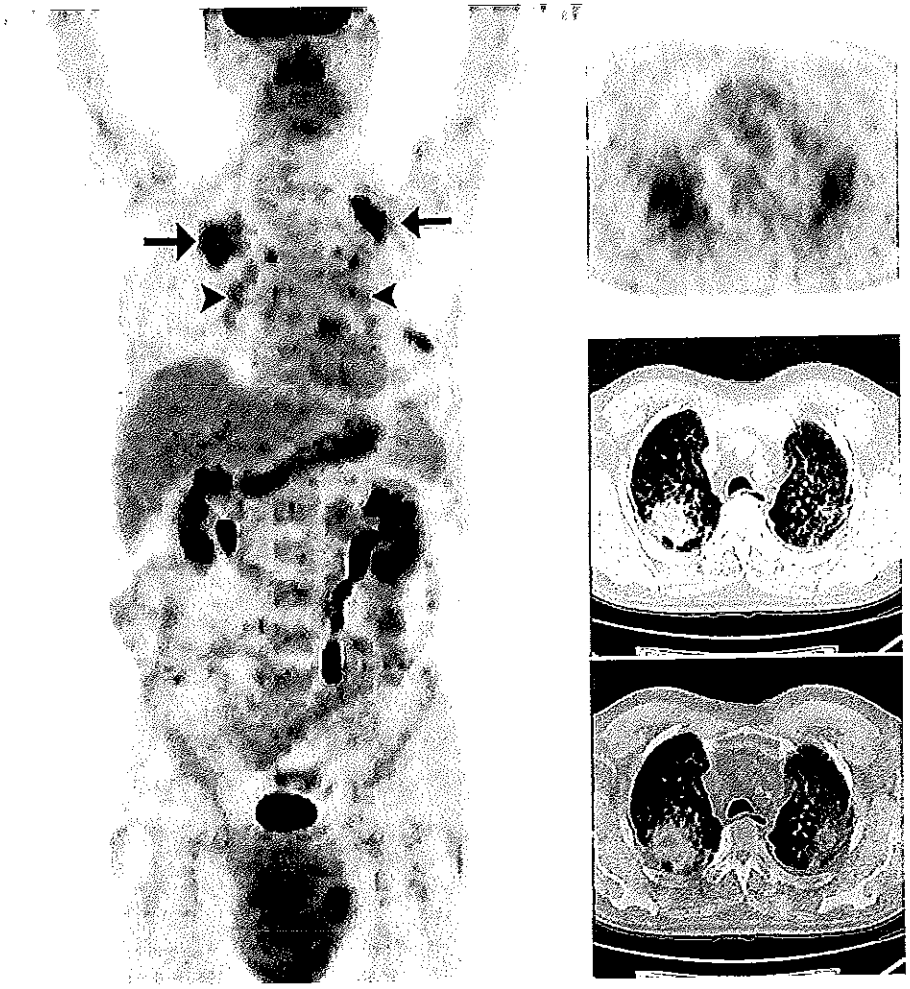

Figure 9 Progressive massive fibrosis (PMF) and anthracosis. MIP PET image in an ex-coal miner shows moderate FDG uptake within both upper lobes (arrows) and a symmetric pattern of low-grade uptake at both pulmonary hila (arrowheads). Selected axial PET, CT, and fused PET/CT images demonstrate pleuro-parenchymal distortion in both upper lobes, with areas of calcification. Comparison with previous imaging confirmed the stability of these changes, which were consistent with PMF and anthracosis.

benign entities in the ovary have also been described as showing FDG uptake, including cystadenoma, dermoid cyst, endometriosis, and schwannoma.[66] Benign peritoneal disease can give rise to abnormal FDG uptake and may mimic malignant peritoneal diseases particularly in the postoperative setting. Diffuse or focal testicular uptake can be seen in the context of epididymo-orchitis.

Bone and joints

PET/CT with FDG is relatively sensitive in the detection of bone metastases, especially in the context of osteolytic lesions.[67,68] However, there can be considerable overlap in the degree of FDG uptake within malignant and benign bone lesions,[69] and false-positive bone uptake can occur in any osseous process that leads to accumulation and turnover of inflammatory cells during the active tissue repair or healing phases, e.g., fracture, surgical resection, active arthropathy, Paget's disease, fibrous dysplasia, and bone infarct (Fig 13).[70] Correlation with the CT findings can improve specificity, and if there is a solitary FDG-avid bone lesion with no definite CT abnormality, this often requires further tests [e.g., magnetic resonance imaging (MRI)] for characterization. Occasionally rare benign inflammatory conditions can cause a combination of bone and joint disease that mimics metastatic disease, one such example where PET/CT may allow a more confident diagnosis is SAPHO (synovitis, acne, pustulosis, hyperostosis and osteitis) syndrome.[71]

Diffusely increased, uniform uptake of FDG within the marrow-containing bones is frequently seen as a reactive phenomenon in patients receiving chemotherapy. This may also be seen on pre-treatment examination images, especially in the context of extremely hypermetabolic or advanced-stage tumours, when it does not usually indicate marrow infiltration.[72] This "reactive marrow hyperplasia" pattern is recognized as a poor prognostic indicator in non-small cell lung cancer, but its significance in the context of other malignancies is not known.[73]

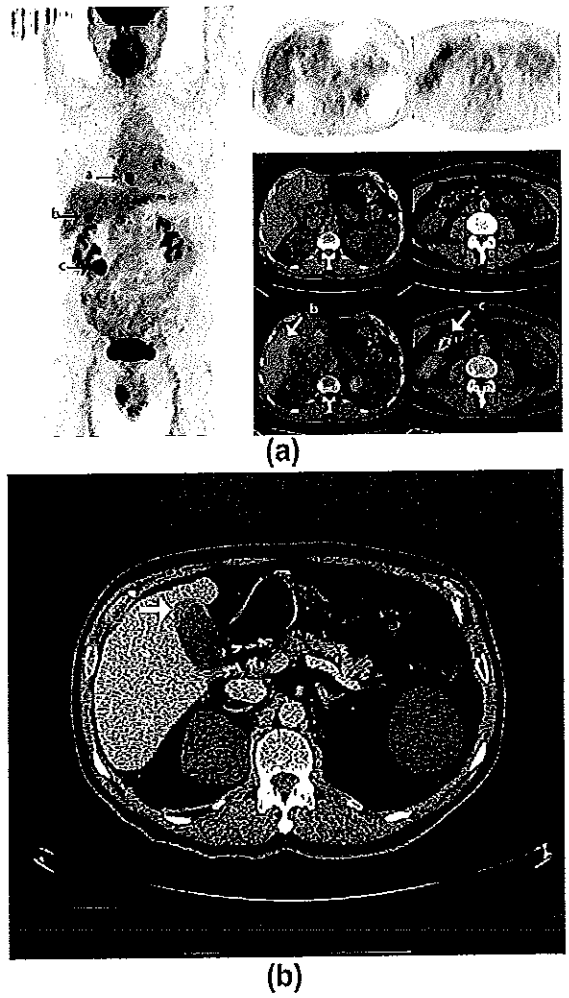

Figure 10 Coincidental detection of colonic polyp and adenomyomatosis of the gall bladder. MIP PET image in a patient with an oesophageal cancer (a) shows focal uptake in the right upper quadrant (b) and in the right paracolic area (c). Selected axial PET, CT, and fused PET/CT images demonstrate that uptake (b) relates to the gall bladder fundus (with focal wall thickening on the contrast-enhanced CT) and uptake (c) localizes to the ascending colon. Cholecystectomy confirmed adenomyomatosis and colonoscopy revealed a 15 mm adenomatous polyp.

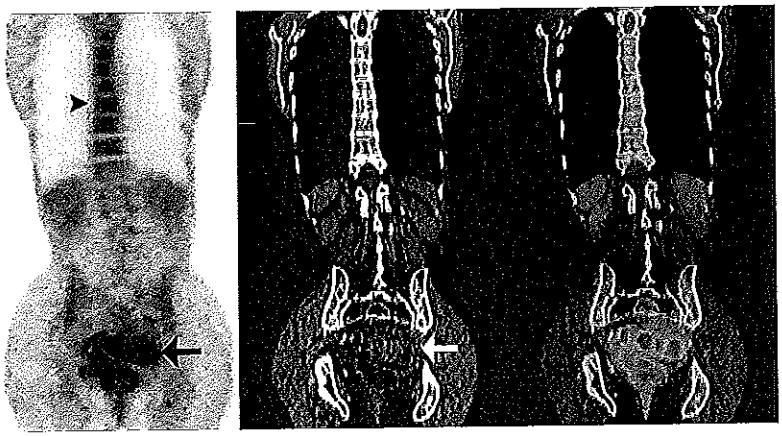

Figure 11 Ulcerative colitis. Coronal PET, CT, and fused PET/CT images in a patient investigated for a solitary pulmonary nodule show segmental uptake within the sigmoid colon with associated mural thickening and pericolic inflammation. Note also the mild and uniform increase in activity throughout the bone marrow. Further clinical evaluation, including flexible sigmoidoscopy, revealed ulcerative colitis, and a normocytic anaemia. The pulmonary nodule was non-FDG avid and felt to be benign.

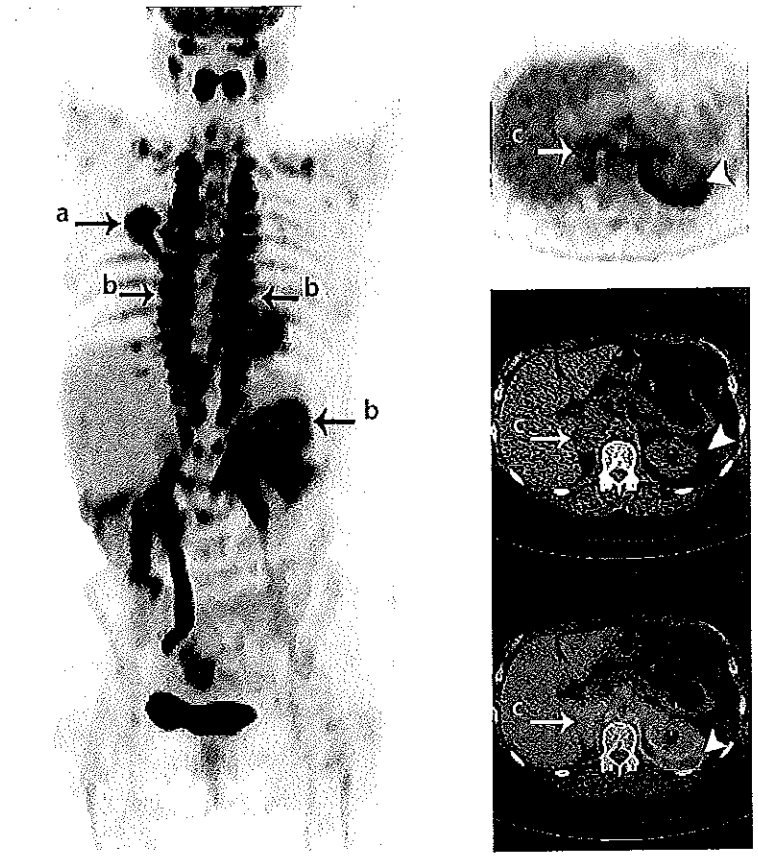

Figure 12 Severe brown adipose tissue activation due to an underlying phaeochromocytoma. MIP PET image in a patient attending for staging of a suspected lung cancer (a) shows intense brown fat activation in supra- and sub-diaphragmatic locations (b). Selected axial PET, CT, and fused PET/CT images depict a right adrenal mass that is mildly FDG avid (c). Biopsy revealed a phaeochromocytoma, with subsequent confirmation of elevated serum and urinary catecholamines. Note the avid brown fat uptake in the perinephric area (arrowhead).

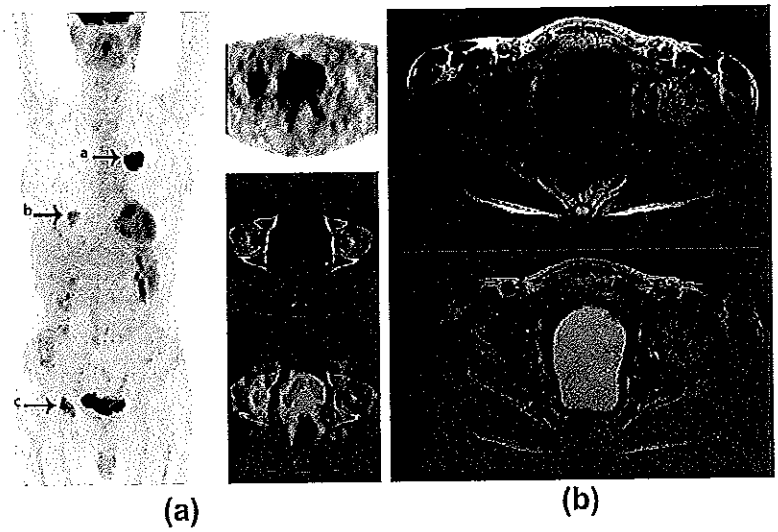

Figure 13 Avascular necrosis of the hip mimicking a bone metastasis. MIP PET image in a patient attending for staging of lung cancer (a) shows a low-grade area of tracer uptake in the right lower lobe (b), which proved to be inflammatory on comparison with previous imaging. In addition, however, there is focal uptake in the right hip (c), which on selected axial PET, CT and fused PET/CT images corresponds to area of osteolysis in the right femoral head involving the fovea capitis. An MRI examination performed subsequently (T1- and T2-weighted, fat-suppressed, axial images shown) demonstrates typical changes of avascular necrosis.

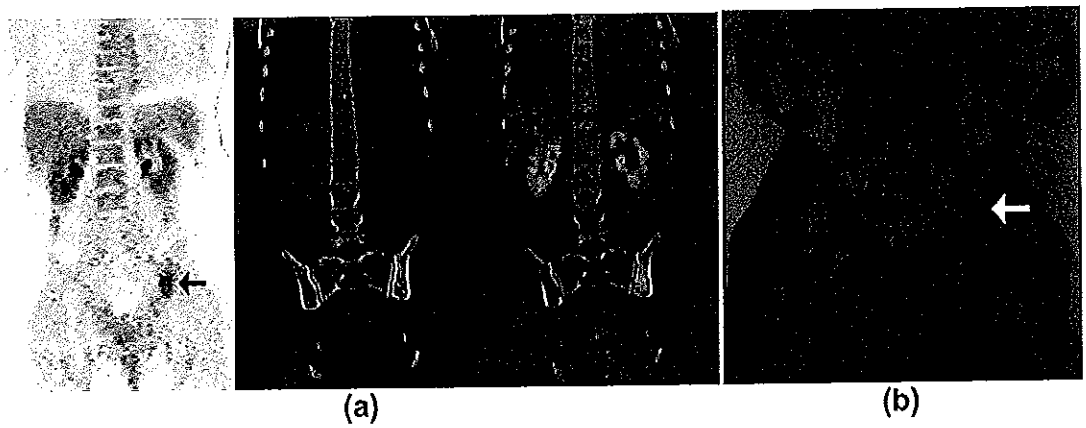

Figure 14 Pelvic insufficiency fracture. Coronal PET, CT, and fused PET/CT images in a patient with previously treated cervical cancer shows linear FDG uptake of moderate intensity within the left iliac bone corresponding to an area of ill-defined medullary sclerosis (arrows). Correlation with MRI (T1-weighted coronal image shown) allowed a confident diagnosis of an insufficiency fracture in this patient with previous radiotherapy and pelvic pain.

Following trauma or surgical intervention, the intensity and duration of activity varies with the location of bone involved, with rib or vertebral uptake normalizing more rapidly than the sternum or pelvic bones (Figs 14 and 15). Postoperative reactive bone uptake may persist for up to 4–12 months, but FDG activity persisting beyond this time should raise concern for a pathological process such as infection or malignancy.[74]

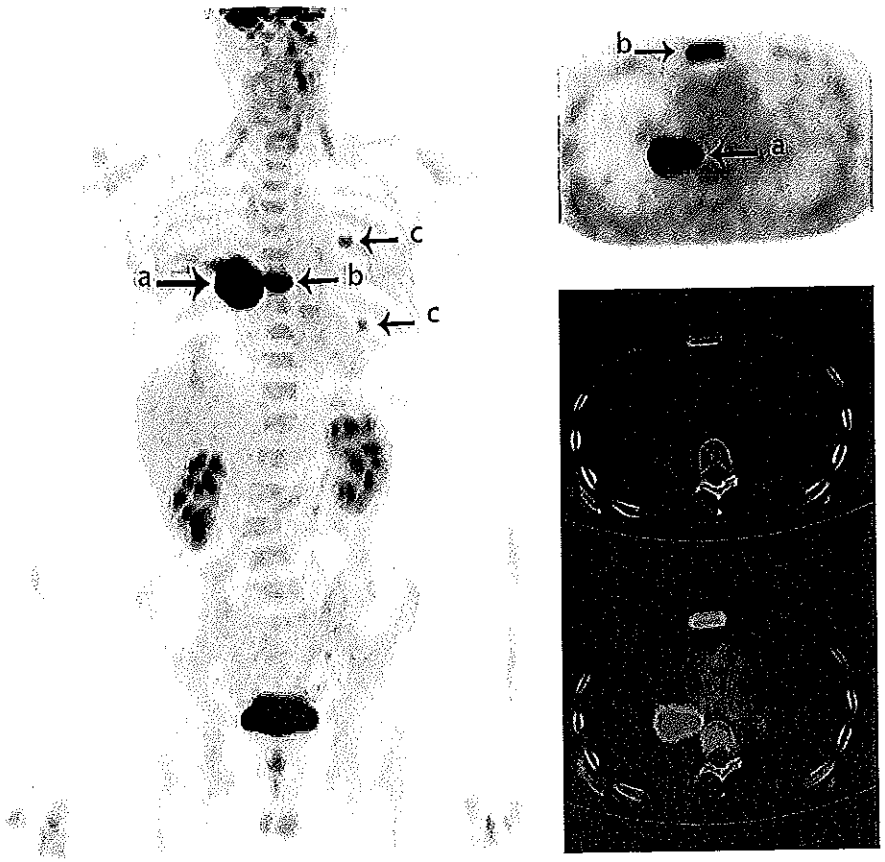

Figure 15 Sternal and rib fractures in a patient with lung cancer. MIP PET image in a patient attending for staging of lung cancer (a) shows moderately avid tracer uptake within the sternum and in a couple of left-sided ribs (b). Selected axial PET, CT, and fused PET/CT images confirm some of these findings. The CT showed healing fractures at the two sites of rib uptake (not shown). The patient had recently undergone cardio-pulmonary resuscitation for life-threatening haemoptysis, and the features were in keeping with traumatic fractures rather than bone metastases.

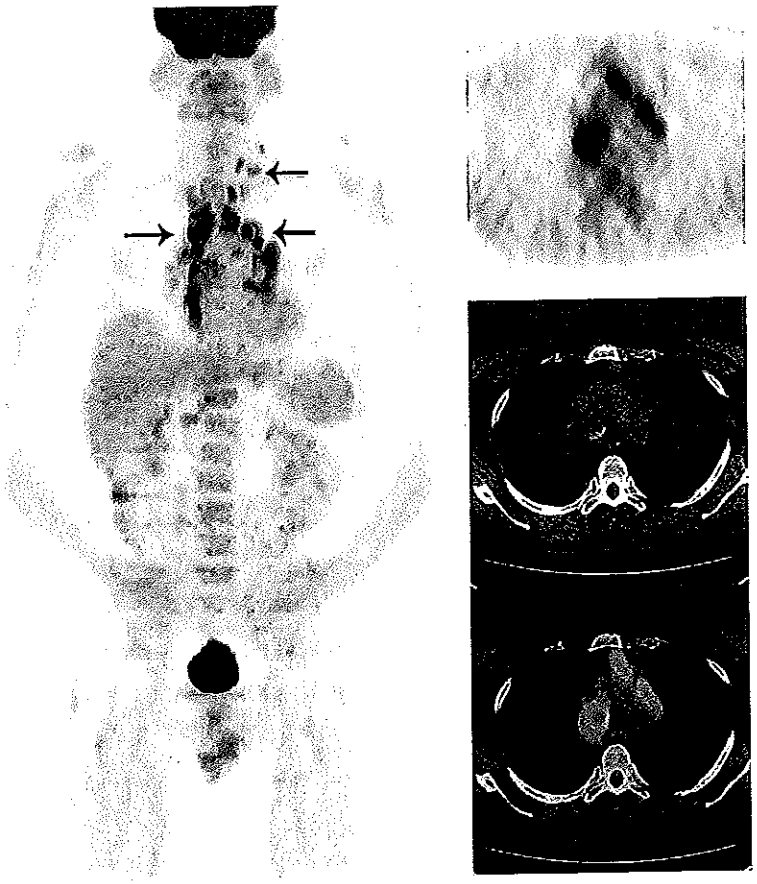

Figure 16 Sarcoidosis. MIP PET image shows the typical symmetric pattern of mediastinal nodal FDG uptake seen in sarcoidosis (arrows). Selected axial PET, CT, and fused PET/CT images confirm these findings. Previous and follow-up imaging showed that these lymph nodes were stable in appearance over several years.

Lymph nodes

Detection of malignant infiltration of lymph nodes is an important requirement in the accurate staging of most cancers, and FDG PET/CT can make a significant contribution to this process by demonstrating tumour involvement in non-pathologically enlarged nodes. However, there are numerous causes of false-positive nodal uptake of FDG. These include inflammatory causes, such as sarcoidosis or sarcoid-like reaction to malignancy, collagen-vascular diseases and anthracosis, and infective causes such as TB, infectious mononucleosis, acquired immunodeficiency syndrome (AIDS), and hepatitis C (Fig 16).[75,76]

Vascular uptake

Inflammation with or without infection within vessels can give rise to abnormal FDG uptake on PET/CT. This can affect either the venous or arterial system and incidental detection frequently changes treatment strategy. Venous thrombosis and intravascular infection are well recognized serious complications associated with central venous catheter use and can lead to increased FDG activity.[77] Similarly acute or chronic pulmonary embolism and infective endocarditis can give rise to abnormal FDG uptake.[78]

Diffuse FDG uptake within arterial vascular grafts, e.g., aortic aneurysm repair is not infrequent and is often physiological (Fig 17). Conversely, focal FDG uptake associated with an irregular graft boundary is an independent significant predictor of vascular prosthesis infection.[79] FDG uptake in large arteries can also be observed and is associated with cardiovascular risk factors. FDG accumulates in plaque macrophages and uptake is correlated with macrophage density. This appearance is most commonly due to large vessel vasculitis or atherosclerosis and may prompt further clinical assessment and alter patient management.[80,81]

Response assessment following chemotherapy and radiotherapy

There is an increasing demand for FDG PET/CT for metabolic response assessment after therapy, which can facilitate more tailored and optimized treatment. However, if performed too soon after chemotherapy or radiotherapy, false-positive inflammatory uptake or false-negative findings due to "tumour stunning" may be encountered. In

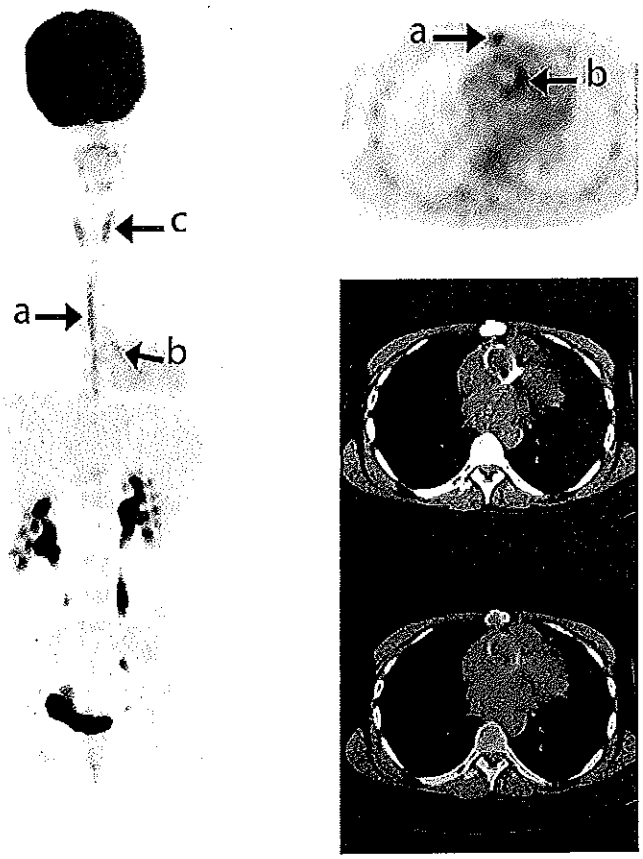

Figure 17 Post-surgical graft uptake. MIP PET image and selected axial PET, CT, and fused PET/CT images in a patient with cardiac surgery 3 months previously show linear uptake within the median sternotomy (a) and circumferential uptake around a composite aortic root replacement graft (b). The uptake around the graft persisted on the non-attenuation corrected (NAC) images, and was considered consistent with a "foreign-body"-type reactive uptake that is usually seen in association with vascular grafts. Note the benign pattern of uptake within the thyroid gland (c), which may be seen in low-grade thyroiditis or even represent physiological thyroid uptake.

order to minimize these unwanted effects, the current recommendations are that FDG PET/CT should be performed at least 2–3 weeks, and preferably 6–8 weeks, after chemotherapy or chemoimmunotherapy, and 8–12 weeks after radiation or chemoradiotherapy.[82]

Conclusion

By providing combined metabolic and morphological information in a single, integrated whole-body examination, FDG PET/CT has had a profound impact on the imaging pathways and management of oncological patients. However, the technique is not perfect, with many potential causes of false-positive FDG uptake. These may be related to unusual physiological patterns, technical artefacts, or benign pathological conditions. In particular, a degree of vigilance should be maintained for the effects of inflammatory and infective conditions, as well as surgical and non-surgical interventions. Attention to detail, meticulous technique, and correlation with clinical and pathological findings can minimize the risk of misinterpretation.

References

1. von Schulthess GK, Steinert HC, Hany TF. Integrated PET/CT: current applications and future directions. *Radiology* 2006;238:405–22.
2. Blodgett TM, Meltzer CC, Townsend DW. PET/CT: form and function. *Radiology* 2007;242:360–85.
3. Hilner BE, Siegel BA, Liu D, et al. Impact of positron emission tomography/computed tomography and positron emission tomography (PET) alone on expected management of patients with cancer: initial results from the national oncologic PET registry. *J Clin Oncol* 2008;26:2155–61.
4. Weber WA. PET for response assessment in oncology: radiotherapy and chemotherapy. *Br J Radiol* 2005;(Suppl. 28):42–9.
5. Poeppel TD, Krause BJ, Heusner TA, et al. PET/CT for staging and follow-up of patients with malignancies. *Eur J Radiol* 2009;70:382–92.
6. Shreve PD, Anzai Y, Wahl RL. Pitfalls in oncologic diagnosis with FDG PET imaging: physiologic and benign variants. *RadioGraphics* 1999;19:61–77.
7. Gorospe L, Raman S, Echeveste J, et al. Whole-body PET/CT: spectrum of physiological variants, artifacts and interpretative pitfalls in cancer patients. *Nucl Med Commun* 2005;26:671–87.
8. Blake MA, Singh A, Setty BN, et al. Pearls and pitfalls in interpretation of abdominal and pelvic PET-CT. *RadioGraphics* 2006;26:1335–53.
9. Metser U, Miller E, Lerman H, et al. Benign non-physiologic lesions with increased ^{18}F-FDG uptake on PET/CT: characterization and incidence. *AJR Am J Roentgenol* 2007;189:1203–10.
10. Cook GJR. Pitfalls in PET/CT interpretation. *Q J Nucl Med Mol Imaging* 2007;51:235–43.

11. Liu Y, Ghesani NV, Zuckier LS. Physiology and pathophysiology of incidental findings detected on FDG-PET scintigraphy. *Semin Nucl Med* 2010;**40**:294–315.
12. Som P, Atkins HL, Bandoypadhyay D, et al. A fluorinated glucose analog, 2-fluoro-2-deoxy-D-glucose (F-18): nontoxic tracer for rapid tumor detection. *J Nucl Med* 1980;**21**:670–5.
13. Warburg O. On the origin of cancer cells. *Science* 1956;**123**:309–14.
14. Wong WL, Gibson D, Sanghera B, et al. Evaluation of normal FDG uptake in palatine tonsil and its potential value for detecting occult head and neck cancers: a PET CT study. *Nucl Med Commun* 2007;**28**:675–80.
15. Heusner TA, Hahn S, Hamami ME, et al. Incidental head and neck (18)F-FDG uptake on PET/CT without corresponding morphological lesion: early predictor of cancer development? *Eur J Nucl Med Mol Imaging* 2009;**36**:1397–406.
16. Nakamoto Y, Tatsumi M, Hammoud D, et al. Normal FDG distribution patterns in the head and neck: PET/CT evaluation. *Radiology* 2005;**234**: 879–85.
17. Blodgett TM, Fukui MB, Synderman CH, et al. Combined PET-CT in the head and neck: part 1. Physiologic, altered physiologic, and artefactual FDG uptake. *RadioGraphics* 2005;**25**:897–912.
18. Kuester LB, Fischman AJ, Fan CM, et al. Lipomatous hypertrophy of the interatrial septum: prevalence and features on fusion ^{18}F fluorodeoxyglucose positron emission tomography/CT. *Chest* 2005;**128**:3888–93.
19. Nasseri F, Eftekhari F. Clinical and radiologic review of the normal and abnormal thymus: pearls and pitfalls. *RadioGraphics* 2010;**30**:413–28.
20. Kawano T, Suzuki A, Ishida A, et al. The clinical relevance of thymic fluorodeoxyglucose uptake in pediatric patients after chemotherapy. *Eur J Nucl Med Mol Imaging* 2004;**31**:831–6.
21. Goutier E, Fourme E, Wartski M. High and typical ^{18}F-FDG bowel uptake in patients treated with metformin. *Eur J Nucl Med Mol Imaging* 2008;**35**:95–9.
22. Ozulker T, Ozulker F, Mert M, et al. Clearance of the high intestinal (18) F-FDG uptake associated with metformin after stopping the drug. *Eur J Nucl Med Mol Imaging* 2010;**37**:1011–7.
23. Lerman H, Metser U, Grisaru D, et al. Normal and abnormal ^{18}F-FDG endometrial and ovarian uptake in pre- and postmenopausal patients: assessment by PET/CT. *J Nucl Med* 2003;**45**:266–71.
24. Nishizawa S, Inubushi M, Okada H. Physiological ^{18}F-FDG uptake in the ovaries and uterus of healthy female volunteers. *Eur J Nucl Med Mol Imaging* 2005;**32**:549–56.
25. Kitajima K, Nakamoto Y, Senda M, et al. Normal uptake of ^{18}F-FDG in the testis: an assessment by PET/CT. *Ann Nucl Med* 2007;**21**:405–10.
26. Goethals I, De Vriendt C, Hoste P, et al. Normal uptake of F-18 FDG in the testis as assessed by PET/CT in a pediatric study population. *Ann Nucl Med* 2009;**23**:817–20.
27. Paidisetty S, Blodgett TM. Brown fat: atypical locations and appearances encountered in PET/CT. *AJR Am J Roentgenol* 2009;**193**:359–66.
28. Shammas A, Lim R, Charon M. Pediatric FDG PET/CT: physiologic uptake, normal variants and benign conditions. *RadioGraphics* 2009;**29**: 1467–86.
29. Garcia CA, van Nostrand D, Atkins F, et al. Reduction of brown fat 2-deoxy-2-[F-18]-fluoro-D-glucose uptake by controlled environmental temperature prior to positron emission tomography scan. *Mol Imaging Biol* 2006;**8**:24–9.
30. Soderlund V, Larsson SA, Jacobsson H. Reduction of FDG uptake in brown adipose tissue in clinical patients by a single dose of propranolol. *Eur J Nucl Med Mol Imaging* 2007;**34**:1018–22.
31. Lucignani G. Respiratory and cardiac motion correction with 4D PET imaging: shooting at moving targets. *Eur J Nucl Med Mol Imaging* 2009; **36**:315–9.
32. Osman MM, Cohade C, Nakamoto Y, et al. Clinically significant inaccurate localization of lesions with PET/CT: frequency in 300 patients. *J Nucl Med* 2003;**44**:240–3.
33. Hany TF, Heuberger J, von Schulthess GK. Iatrogenic FDG foci in the lungs: a pitfall of PET image interpretation. *Eur Radiol* 2003;**13**:2122–7.
34. Ha J-M, Jeong S-Y, Seo Y-S, et al. Incidental focal F-18 FDG accumulation in lung parenchyma without abnormal CT findings. *Ann Nucl Med* 2009;**6**:599–603.
35. Beatty JS, Williams HT, Aldridge BA, et al. Incidental PET/CT findings in the cancer patient: how should they be managed? *Surgery* 2009;**146**: 274–81.
36. Heller MT, Meltzer CC, Fukul MB, et al. Superphysiologic FDG uptake in the non-paralyzed vocal cord: resolution of a false-positive PET result with combined PET/CT imaging. *Clin Positron Imaging* 2000;**3**:207–11.
37. Peter Klussmen J, Wittekindt C, Florian Preuss S, et al. High risk for bilateral warthin tumor in heavy smokers—review of 185 cases. *Acta Otolaryngol* 2006;**126**:1213–7.
38. Lee SK, Rho BH, Won KS. Parotid incidentaloma identified by combined ^{18}F-fluorodeoxyglucose whole-body positron emission tomography and computed tomography: findings at gray-scale and power Doppler ultrasonography and ultrasound-guided fine-needle aspiration biopsy or core biopsy. *Eur Radiol* 2009;**19**:2268–74.
39. Sagowski C, Ussmuller J. Clinical diagnosis of salivary gland sarcoidosis (Heerfordt syndrome). *HNO* 2000;**48**:613–5.
40. Choi Y, Lee KS, Kim HJ, et al. Focal thyroid lesions incidentally identified by integrated ^{18}F-FDG PET/CT: clinical significance and improved characterization. *J Nucl Med* 2006;**47**:609–15.
41. Kwak JY, Kim EK, Yun M, et al. Thyroid incidentalomas identified by ^{18}F-FDG PET: sonographic correlation. *AJR Am J Roentgenol* 2008;**191**: 598–603.
42. Eloy JA, Brett AM, Fatterpaker GM, et al. The significance and management of incidental (^{18}F)fluorodeoxyglucose-positron-emission tomography uptake in the thyroid gland in patients with cancer. *AJNR Am J Neuroradiol* 2009;**30**:1431–4.
43. Yasuda S, Shohsu A, Ide M, et al. Diffuse F-18 FDG uptake in chronic thyroiditis. *Clin Nucl Med* 1997;**22**:341.
44. Lardinois D, Weder W, Hany TF, et al. Staging of non-small-cell lung cancer with integrated positron-emission tomography and computed tomography. *New Engl J Med* 2003;**348**:2500–7.
45. Chin AY, Lee KS, Kim B-T, et al. Tissue characterization of solitary pulmonary nodule: comparative study between helical dynamic CT and integrated PET/CT. *J Nucl Med* 2006;**47**:443–50.
46. Chang CY, Tzao C, Lee SC, et al. Incremental value of integrated FDG-PET/CT in evaluating indeterminate solitary pulmonary nodule for malignancy. *Mol Imaging Biol* 2010;**12**:204–9.
47. Kavanagh P, Stevenson AW, Chen MY, et al. Non-neoplastic diseases in the chest showing increased activity on FDG PET. *AJR Am J Roentgenol* 2004;**183**:1133–41.
48. Shim SS, Lee KS, Kim B-T, et al. Focal parenchymal lung lesions showing a potential of false-positive and false-negative interpretations on integrated PET/CT. *AJR Am J Roentgenol* 2006;**186**:639–48.
49. Su M, Fan Q, Fan C, et al. Lung sequestration and Pott disease masquerading as primary lung cancer with bone metastases on FDG PET/CT. *Clin Nucl Med* 2009;**34**:236–8.
50. Abikhzer G, Turpin S, Bigras JL. Infected pacemaker causing septic lung emboli detected on FDG PET/CT. *J Nucl Cardiol* 2010;**17**:514–5.
51. Kei PL, Vikram R, Yeung HW, et al. Incidental finding of focal FDG uptake in the bowel during PET/CT: CT features and correlation with histopathologic results. *AJR Am J Roentgenol* 2010;**194**:W401–6.
52. Tatlidil R, Jadvar H, Bading JR, et al. Incidental colonic fluorodeoxyglucose uptake: correlation with colonoscopic and histopathologic findings. *Radiology* 2002;**224**:783–7.
53. McDermott S, Skehan SJ. Whole body imaging in the abdominal cancer patient: pitfalls of PET-CT. *Abdom Imaging* 2010;**35**:55–69.
54. Heusner TA, Hahn S, Hamami ME, et al. Gastrointestinal ^{18}F-FDG accumulation on PET without a corresponding CT abnormality is not an early indicator of cancer development. *Eur Radiol* 2009;**19**:2171–9.
55. Donadon M, Bona S, Montorsi M, et al. FDG-PET positive granuloma of the liver mimicking local recurrence after hepatic resection of colorectal liver metastasis. *Hepatogastroenterol* 2010;**57**:138–9.
56. Sugawara Y, Zasadny KR, Kison PV, et al. Splenic fluorodeoxyglucose uptake increased by granulocyte colony-stimulating factor therapy: PET imaging results. *J Nucl Med* 1999;**40**:1456–62.
57. Lustberg MB, Aras O, Meisenberg BR. FDG PET/CT findings in acute adult mononucleosis mimicking malignant lymphoma. *Eur J Haematol* 2008;**81**:154–6.
58. Lee TY, Kim M-H, Park DH, et al. Utility of ^{18}F-FDG PET/CT for differentiation of autoimmune pancreatitis with atypical pancreatic imaging findings from pancreatic cancer. *AJR Am J Roentgenol* 2009;**193**:343–8.
59. Friess H, Langhans J, Ebert M, et al. Diagnosis of pancreatic cancer by 2[^{18}F]-fluoro-2-deoxy-D-glucose positron emission tomography. *Gut* 1995;**36**:771–7.

60. Maldjian PD, Ghessani N, Ahmed S, et al. Adenomyomatosis of the gall bladder: another cause for a "hot" gall bladder on ^{18}F-FDG PET. *AJR Am J Roentgenol* 2007;**189**:W36–8.
61. Even-Sapir E, Parag Y, Lerman H, et al. Detection of recurrence in patients with rectal cancer: PET/CT after abdomino-perineal or anterior resection. *Radiology* 2004;**232**:815–22.
62. Gorenberg M, Bar-Shalom R, Israel O. Patterns of FDG uptake in post-thoracotomy surgical scars in patients with lung cancer. *Br J Radiol* 2008;**81**:821–5.
63. Metser U, Miller E, Lerman H, et al. ^{18}F-FDG PET/CT in the evaluation of adrenal masses. *J Nucl Med* 2006;**47**:32–7.
64. Yun M, Kim W, Alnafisi N, et al. ^{18}F-FDG PET in characterizing adrenal lesions detected on CT or MRI. *J Nucl Med* 2001;**42**:1795–9.
65. Taieb D, Sebag F, Barlier A, et al. ^{18}F-FDG avidity of pheochromocytoma and paraganglionoma: a new molecular imaging signature? *J Nucl Med* 2009;**50**:711–7.
66. Fenchel S, Grab D, Nuessle K, et al. Asymptomatic adnexal masses: correlation of FDG PET and histopathologic findings. *Radiology* 2002; **223**:780–8.
67. Kruger S, Buck AK, Mottaghy FM, et al. Detection of bone metastases in patients with lung cancer: 99mTc-MDP planar bone scintigraphy, ^{18}F-fluoride PET or ^{18}F-FDG PET/CT. *Eur J Nucl Med Mol Imaging* 2009;**36**:1807–12.
68. Cook GJ. PET and PET/CT imaging of skeletal metastases. *Cancer Imaging* 2010;**10**:1–8.
69. Aoki J, Watanabe H, Shinozaki T, et al. FDG PET of primary benign and malignant bone tumours: standardized uptake value in 52 lesions. *Radiology* 2001;**219**:774–7.
70. Su MG, Tian R, Fan QP, et al. Recognition of fibrous dysplasia of bone mimicking skeletal metastases on ^{18}F-FDG PET/CT imaging. *Skeletal Radiol* 2010. doi:10.1007/s00256-010-0999-9.
71. Patel CN, Smith JT, Rankine JJ, et al. F-18 FDG PET/CT can help differentiate SAPHO syndrome (synovitis, acne, pustulosis, hyperostosis, and osteitis) from suspected metastatic bone disease. *Clin Nucl Med* 2009;**34**:254–7.
72. Salaun PY, Gastinne T, Bodet-Milin C, et al. Analysis of ^{18}F-FDG PET diffuse bone marrow uptake in staging of Hodgkin's lymphoma: a reflection of disease infiltration or just inflammation? *Eur J Nucl Med Mol Imaging* 2009;**36**:1813–21.
73. Prevost S, Boucher L, Larivee P, et al. Bone marrow hypermetabolism on ^{18}F-FDG PET as a survival prognostic factor in non-small cell lung cancer. *J Nucl Med* 2006;**47**:559–65.
74. Liu Y. Orthopaedic surgery-related benign uptake on FDG-PET: case examples and pitfalls. *Ann Nucl Med* 2009;**23**:701–8.
75. Chowdhury FU, Sheerin F, Bradley KM, et al. Sarcoid-like reaction to malignancy on whole-body integrated (18)F-FDG PET/CT: prevalence and disease pattern. *Clin Radiol* 2009;**64**:675–81.
76. Jacene HA, Stearns V, Wahl RL. Lymphadenopathy resulting from acute hepatitis C infection mimicking metastatic breast carcinoma on FDG PET/CT. *Clin Nucl Med* 2006;**31**:379–81.
77. Miceli MH, Jones Jackson LB, Walker RC, et al. Diagnosis of infection of implantable central venous catheters by [^{18}F] fluorodeoxyglucose positron emission tomography. *Nucl Med Commun* 2004;**25**:813–8.
78. Sopov V, Bernstine H, Stern D, et al. The metabolic spectrum of venous thrombotic disorders found on PET/CT. *AJR Am J Roentgenol* 2009;**193**: W530–9.
79. Spacek M, Belohlavek O, Votrubova J, et al. Diagnostics of "non-acute" vascular prosthesis infection using ^{18}F-FDG PET/CT: our experience with 96 prostheses. *Eur J Nucl Med Mol Imaging* 2009;**36**:850–8.
80. Chen W, Bural GG, Torigian DA, et al. Emerging role of FDG-PET/CT in assessing atherosclerosis in large arteries. *Eur J Nucl Med Mol Imaging* 2009;**36**:144–51.
81. Otsuka H, Morita N, Yamashita K, et al. FDG-PET/CT for diagnosis and follow-up of vasculitis. *J Med Invest* 2007;**54**:345–9.
82. Juweid ME, Stroobants S, Hoekstra OS, et al. Use of positron emission tomography for response assessment of lymphoma: consensus of the imaging subcommittee of international harmonization project in lymphoma. *J Clin Oncol* 2007;**25**:571–8.

False Positive and False Negative FDG-PET Scans in Various Thoracic Diseases

Jung Min Chang, MD[1]
Hyun Ju Lee, MD[1]
Jin Mo Goo, MD[1]
Ho-Young Lee, MD[2]
Jong Jin Lee, MD[2]
June-Key Chung, MD[2]
Jung-Gi Im, MD[1]

Fluorodeoxyglucose (FDG)-positron emission tomography (PET) is being used more and more to differentiate benign from malignant focal lesions and it has been shown to be more efficacious than conventional chest computed tomography (CT). However, FDG is not a cancer-specific agent, and false positive findings in benign diseases have been reported. Infectious diseases (mycobacterial, fungal, bacterial infection), sarcoidosis, radiation pneumonitis and post-operative surgical conditions have shown intense uptake on PET scan. On the other hand, tumors with low glycolytic activity such as adenomas, bronchioloalveolar carcinomas, carcinoid tumors, low grade lymphomas and small sized tumors have revealed false negative findings on PET scan. Furthermore, in diseases located near the physiologic uptake sites (heart, bladder, kidney, and liver), FDG-PET should be complemented with other imaging modalities to confirm results and to minimize false negative findings. Familiarity with these false positive and negative findings will help radiologists interpret PET scans more accurately and also will help to determine the significance of the findings. In this review, we illustrate false positive and negative findings of PET scan in a variety of diseases.

Index terms:
Computed tomography (CT)
Positron emmosion tomography (PET)
Thoracic diseases

Korean J Radiol 2006;7:57-69
Received December 20, 2004; accepted after revision July 18, 2005.

Department of [1]Radiology and [2]Nuclear Medicine, Seoul National University Hospital, Seoul 110-744, Korea

Address reprint requests to:
Hyun Ju Lee , MD, Department of Radiology, Seoul National University College of Medicine, 28 Yongon-dong, Chongno-gu, Seoul 110-744, Korea.
Tel. (822) 2072-1861
Fax. (822) 743-6385
e-mail: rosaceci@radiol.snu.ac.kr

Differentiation between malignant and benign pulmonary nodules is a common problem encountered by radiologists which has provided the impetus to explore alternative imaging techniques. Accurate diagnosis can reduce unnecessary thoracotomies in patients with benign diseases (1). Metabolic imaging with 2-(18F)-fluoro-2-deoxy-D-glucose positron emission tomography (PET) is being used more and more to differentiate benign from malignant focal lesions and it has been shown to be more efficacious than conventional chest CT (2). It has a unique ability to differentiate benign from malignant nodules, and it offers a different approach to the diagnosis of chest diseases because it exploits fundamental biochemical differences between benign and malignant cells (2).

However, fluorodeoxyglucose (FDG) is not a cancer-specific agent, and false positive findings in benign diseases have been reported in active inflammation or infection, causing false-positive results (1, 2). In addition, the malignant tumors with low metabolic activity (3) or tumors smaller than 1.0 cm in diameter (1) often show false negative results. Furthermore, the accuracy of FDG-PET scans in detecting pulmonary metastases in patients with cancer has not yet been established.

Awareness of the conditions and the mechanisms by which false positive and negative results occur will help radiologists interpret PET scans more accurately and also will help to determine the significance of the findings. In this review, potential sources of false-positive and false-negative findings are illustrated in a variety of lung diseases.

BASIC CONCEPT OF FDG-PET IMAGING

Fluorodeoxyglucose is an analog of glucose and is used as a tracer of glucose metabolism. There are several sites of normal physiologic accumulation of FDG (Fig. 1). It accumulates in various normal organs which use glucose for metabolism, including the brain, muscles, salivary glands, myocardium, gastrointestinal tract, urinary tract, thyroid gland, and gonadal tissues. In additional, increased FDG uptake in brown adipose tissue in the neck has been reported as a false positive result in 2.3–4% of patients. Brown adipose tissue is responsible for cold-induced and diet-induced thermogenesis. Mitochondria in brown adipose tissue exclusively express the thermogenic protein, and FDG uptake in hypermetabolic brown fat can occur, as glucose transporters have been observed in brown adipose tissue (Fig. 2) (2).

The mechanism by which FDG uptake in tumor cells and other pathologic conditions occurs is due to an increased number of glucose transporter proteins and increased intracellular hexokinase and phosphofructokinase levels, which promote glycolysis. In the normal glycolytic pathway, FDG behaves similarly to D-glucose in its transport through the cell membrane and phosphorylation by hexokinase. Once FDG is phosphorylated, structural changes made by a hexose-phosphate bond prevent FDG from being catabolized or transported back into the extracellular space in substantial amounts. This process is called "metabolic trapping," and it makes increased uptake and accumulation of FDG occur within abnormally metabolizing tumor cells (2).

Abnormal areas of FDG accumulation are detected by comparing the uptake with background activity. In the lungs, focal abnormalities that have a greater uptake than the mediastinal blood pool on attenuation corrected images are highly suggestive of malignancy. FDG PET also provides quantitative data in the form of the standardized uptake value (SUV) or standardized uptake ratio (SUR) (2). The SUV is obtained by putting the circular region of interest over the portion of the lesion with the greatest accumulation of FDG (3). The mean SUV is obtained by dividing the activity (μCi/mL) in the region of interest (ROI) by the injected dose in μCi divided by patient weight in grams (3).

SUV = (average ROI activity [μCi /mL]) / (injected dose [μCi] per body weight [g])

Increased body fat elevates the SUV, therefore, correction with lean body mass (SUVLBM) is required to avoid erroneous comparisons that can result from changes in pre- and post-therapy body weight in the same patient (2). The maximum SUV is obtained by using the maximum activity in the ROI instead of the mean activity (3).
Notwithstanding the controversial views, SUVs of 2.5 or greater have been used as a cutoff value indicative of malignancy (3). Gupta et al. (4) reported that FDG-PET is superior to CT, when considering overall sensitivity, specificity, and accuracy of PET for staging mediastinal lymph nodes was 96, 93, and 94%, compared to 68, 65, and 66% with CT.

FALSE POSITIVE FINDINGS

Inflammatory cells such as neutrophil and activated macrophages at the site of inflammation or infection show increased FDG accumulation (5). Active granulomatous processes, other infectious conditions and active fibrotic lesions have also been reported to show increased FDG accumulation and cause false-positive PET scans for malignancy.

Tuberculoma and Tuberculous Lymphadenopathy

Tuberculoma is one of the most well-known diseases that show intense FDG uptake (Fig. 3A). Active granulomatous processes such as tuberculosis have been reported to accumulate FDG (1, 2). Tuberculoma typically appears as a fairly discrete nodule or mass (Fig. 3B) in which repeated extensions of infection have created a central caseous necrosis surrounded by a mantle of epithelioid cells and collagen with peripheral inflammatory cell infiltration (1).

Activated inflammatory cells have markedly increased glycolysis. The hexose monophosphate shunt is stimulated by phagocytosis, with increases of 20–30 times that of baseline values which is the cause of high FDG uptake (6). Tuberculous lymphadenopathy can be understood in the same manner as tuberculoma in the lung parenchyma (Fig. 4).

Elevated glucose levels can accelerate false positive results in inflammatory conditions. It has been suggested that inflammatory cells use more glucose under hyperglycemia than in euglycemia, and therefore, lesions containing such cells are more likely to be interpreted as malignant lesions under such conditions (5).

Sarcoidosis

Sarcoidosis is a chronic multisystem disorder. It can be characterized in affected organs by an accumulation of T lymphocytes and mononuclear phagocytes, noncaseating epithelioid granulomas, and derangements of the normal tissue architecture. The etiology is unknown, but it is thought to be caused by exaggerated cellular immune responses.

Pathologically, the first manifestation of the disease is an accumulation of mononuclear inflammatory cells, mainly CD4+ T helper 1 lymphocytes and mononuclear phagocytes, in the affected organ. This inflammatory process is followed by the formation of granulomas, aggregates of macrophages and their progeny, epithelioid cells, and multinucleated giant cells (7). Active granulomatous conditions with aggregation of inflammatory cells in sarcoidosis results in accumulation of FDG (1–3, 8), and it has been suggested that intensity of FDG uptake may reflect disease activity (9) (Fig. 5).

Cryptococcosis

Cryptococcosis is an infection caused by the yeast-like

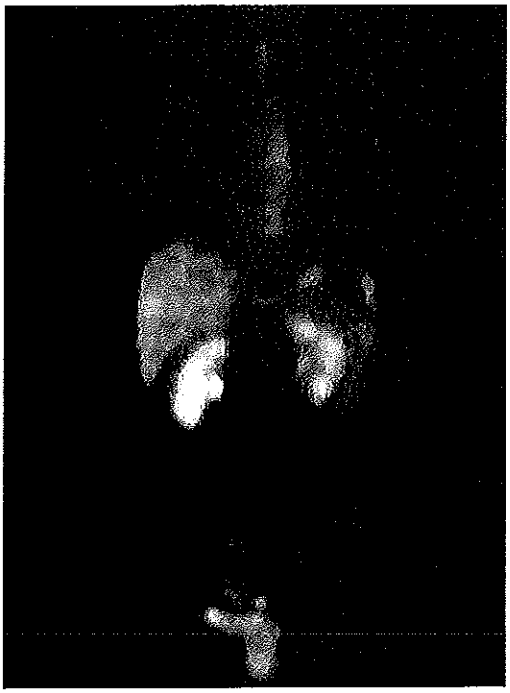

Fig. 1. Normal distribution of FDG.
Coronal FDG-PET image shows physiologic uptake in the liver, kidneys, intestine, and urinary bladder. Also note the minimal uptake in the mediastinum, and bone marrow.

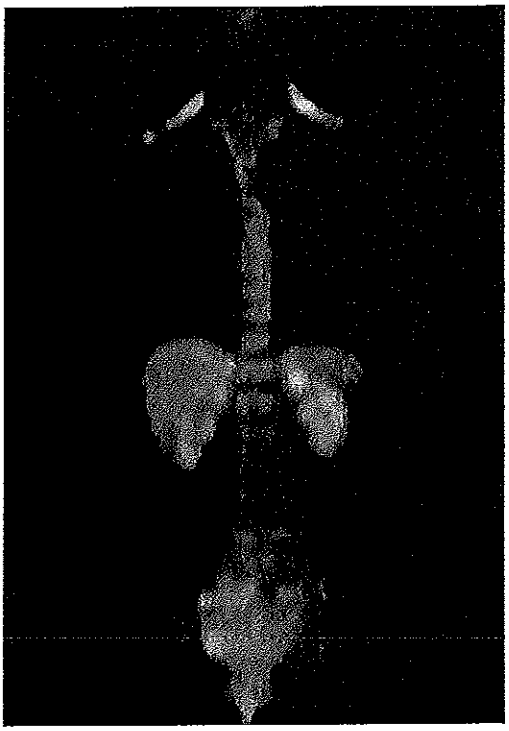

Fig. 2. Normal increased FDG uptake in the shoulder area which represents brown fat.

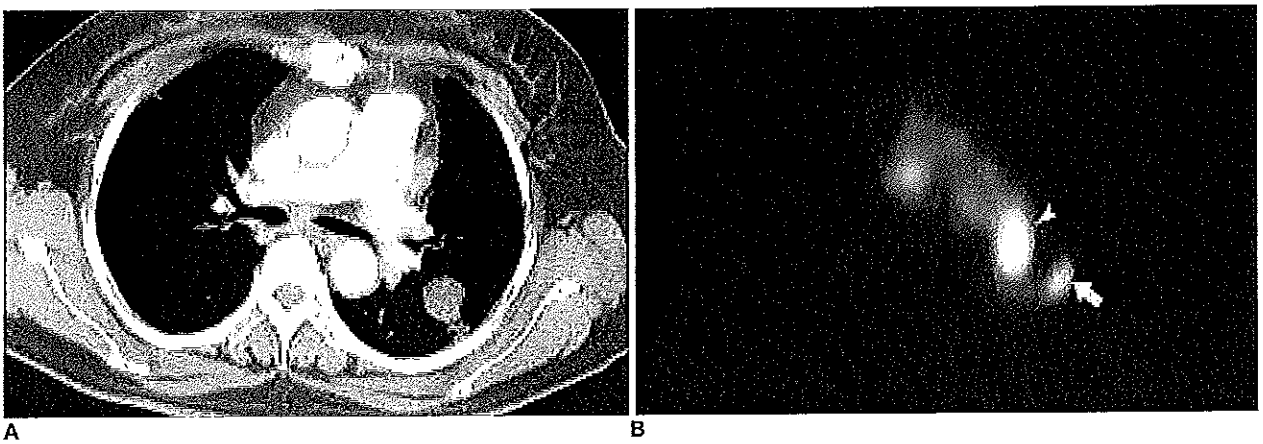

A B

Fig. 3. Tuberculoma in a 53-year-old female.
A. Contrast-enhanced CT scan shows a round mass in the left lower lobe.
B. Axial FDG-PET image shows intense uptake (arrow) in the left upper lobe suggesting a malignant condition with a maximum standardized uptake value of 4.3. The pathologic examination reveals tuberculoma. Another lesion showing high FDG uptake (arrowhead) is a pulmonary artery.

fungus Cryptococcus neoformans. This fungus reproduces by budding and forms round, yeast-like cells. Infection occurs by inhaling the fungus into the lungs. Pulmonary lesions are characterized by intense granulomatous inflammation (10). There are some reports which have showed high FDG uptake causing false positive results in cryptococcosis (8) (Fig. 6).

Paragonimiasis

Paragonimiasis is a food-borne parasitic disease common in south Asia, particularly in Japan, Korea and parts of China (11). Pulmonary paragonimiasis is a disease caused by a lung flake. Once ingested by humans, by eating infected crabs or crayfish, the larvae excyst in the small intestine, penetrate the intestinal wall, and enter the peritoneal cavity. They then penetrate the diaphragm and pleura and enter the lungs. The major target organs for the

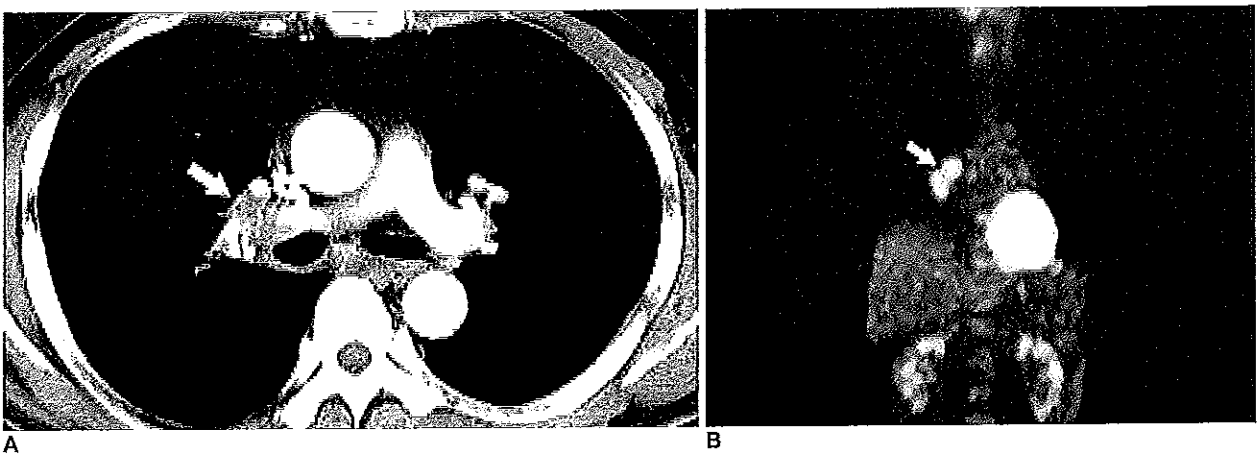

A B

Fig. 4. Tuberculous lymphadenitis in a 56-year-old male.
A. Axial contrast-enhanced CT scan shows right hilar lymph node enlargement (arrow).
B. Coronal FDG-PET scan shows high uptake in the same area (arrow).

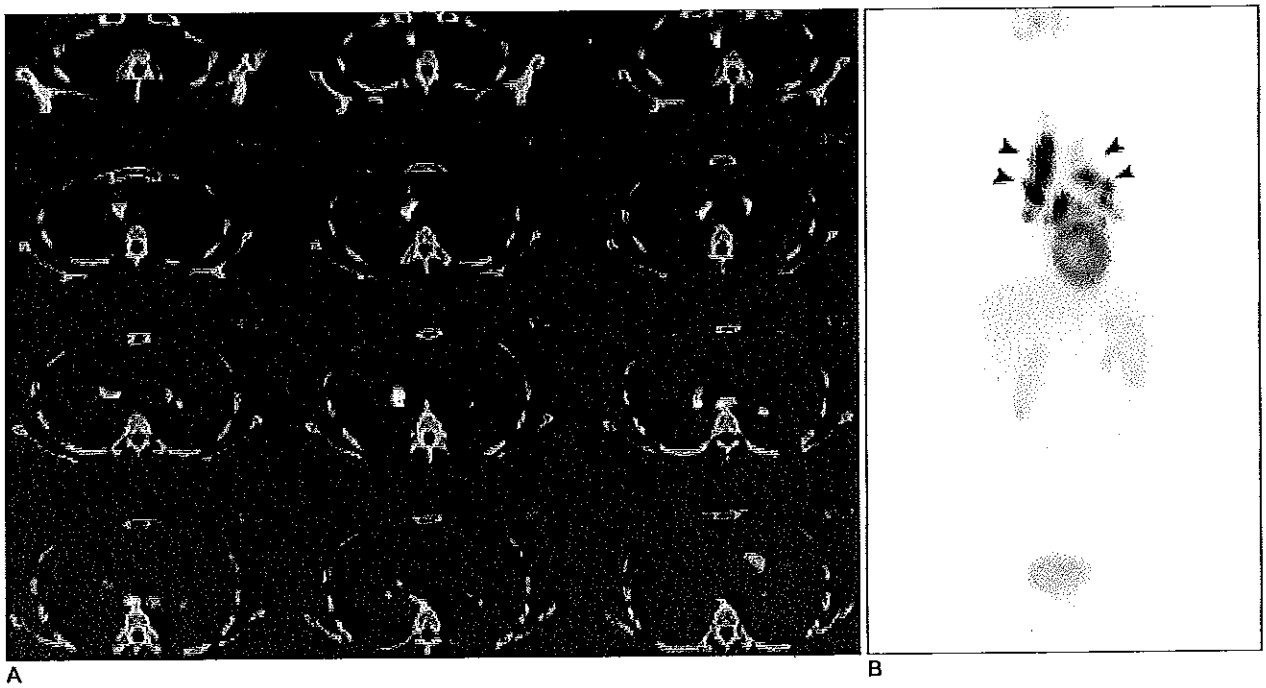

A B

Fig. 5. Sarcoidosis in a 32-year-old male.
A. Axial PET-CT scans show bilateral paratracheal and hilar lymph node enlargement with high FDG uptake.
B. Coronal section of PET shows high FDG uptake with rhamda shape (arrowheads) which is highly suggestive of sarcoidosis. A mediastinoscopic biopsy confirms sarcoidosis.

larvae are the lungs followed by the brain (12).

During the active phase of paragonimiasis, lung tissue surrounding the parasitic cysts may contain evidence of pneumonia, bronchitis, bronchiectasis, and fibrosis (12) (Fig. 7A). Watanabe et al. (11) reported one case of paragonimiasis mimicking lung cancer which showed high FDG uptake (SUV 4.7 at one hour post-injection, and elevation of SUV to 6.2 at two hours). Although the exact causes of FDG accumulation have not yet been proven, we can expect that inflammatory cells including eosinophlic infiltration, active inflammatory responses and viable worms cause high FDG uptake (Fig. 7B).

Other Infectious Conditions

In variable inflammatory conditions including abscesses (Fig. 8), glycolytic metabolism is elevated in the region of leukocytic infiltration associated with inflammatory processes, and consequently FDG uptake is elevated (2). Pneumocystis infections can also cause high FDG-uptake (Fig. 9). These conditions have not been well documented

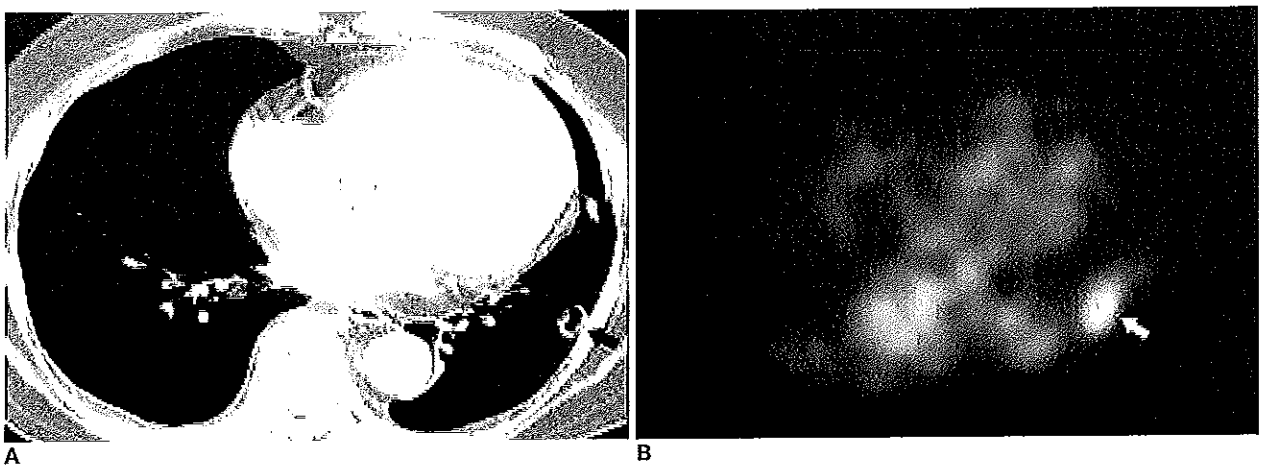

A B

Fig. 6. Cryptococcosis in a 68-year-old female.
A. Contrast-enhanced CT scan shows a cavitary nodule (arrow) in the left lower lobe.
B. Transverse section of a whole body PET image shows increased uptake (arrow) in the left lower lobe and a standardized uptake value of 2.6. The lesion is a round mass-like lesion unlike the CT findings due to respiration artifact.

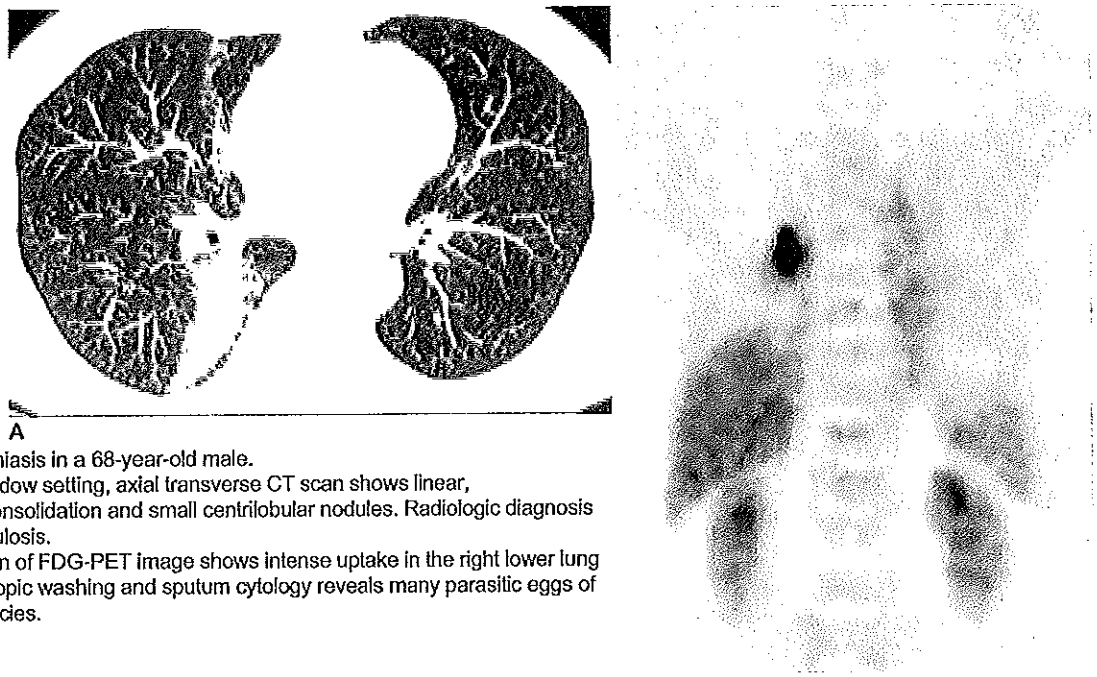

A B

Fig. 7. Paragonimiasis in a 68-year-old male.
A. In the lung window setting, axial transverse CT scan shows linear, wedge shaped consolidation and small centrilobular nodules. Radiologic diagnosis is atypical tuberculosis.
B. Coronal section of FDG-PET image shows intense uptake in the right lower lung zone. Bronchoscopic washing and sputum cytology reveals many parasitic eggs of paragonimus species.

to date. However, in one report (13), patients with fever of unknown origin presented with high FDG uptake in PET imaging, finally proved to be infected by pneumocystis carinii pneumoniae. Inflammatory cells increase the expression of glucose transporters when they are activated, and multiple cytokines and growth factors can facilitate glucose transport without actually increasing the number of glucose transporters (5).

Radiation Fibrosis

Inflammatory processes in radiation fibrosis is caused by infiltration of leukocytes and macrophages and abnormal proliferation of type II pneumocytes, radiation-induced production of local cytokines such as platelet-derived growth factor, tumor necrosis factor, and transforming growth factor β in the radiation field are based on these inflammatory morphologic changes. Consequently, increased FDG uptake in the affected region would be expected (Fig. 10) (14).

Pneumoconiosis with Combined Massive Fibrosis

Pneumoconiosis is a tissue reaction to the presence of an

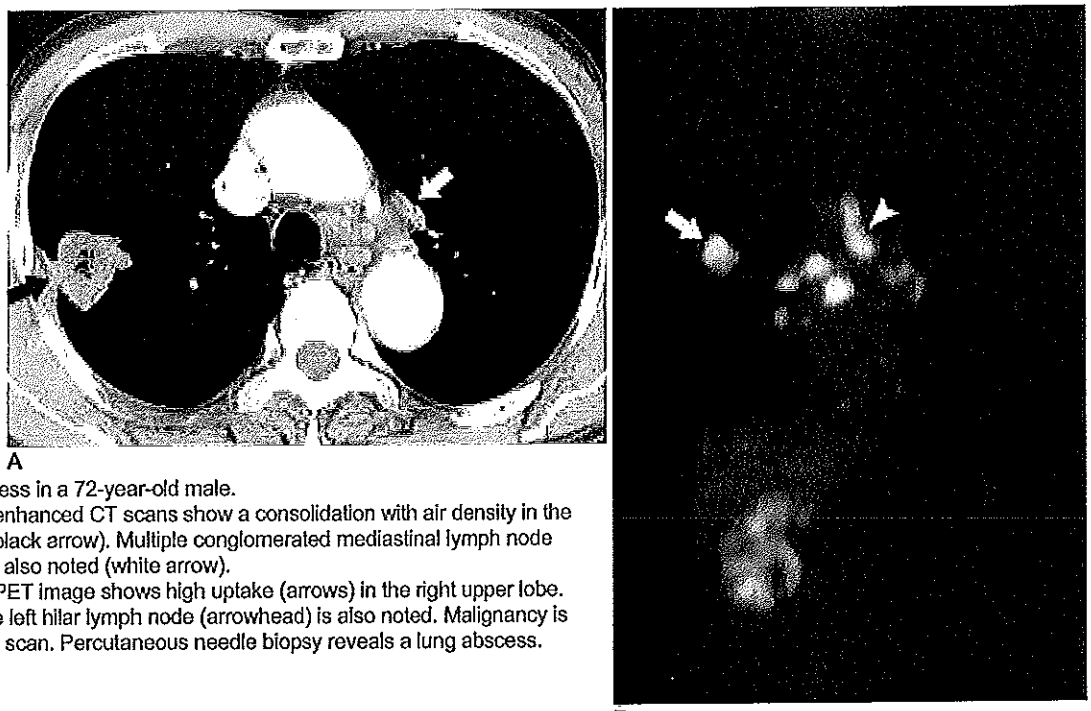

A B

Fig. 8. Lung abscess in a 72-year-old male.
A. Axial contrast enhanced CT scans show a consolidation with air density in the right upper lobe (black arrow). Multiple conglomerated mediastinal lymph node enlargements are also noted (white arrow).
B. Coronal FDG-PET image shows high uptake (arrows) in the right upper lobe. High uptake in the left hilar lymph node (arrowhead) is also noted. Malignancy is suspected in PET scan. Percutaneous needle biopsy reveals a lung abscess.

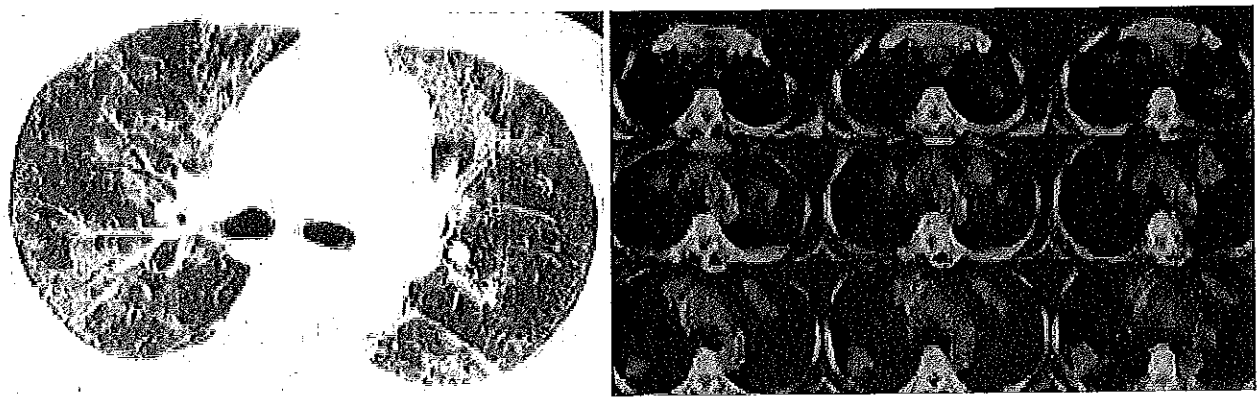

A B

Fig. 9. Pneumocystis carinii infection in a 61-year-old female.
A. In the lung window setting of chest CT, multifocal ground-glass opacities are noted. The patient had been diagnosed with systemic lupus erythematosus, and cytoxan and steroid pulse therapy was performed.
B. PET-CT shows multifocal hypermetabolic lesions with an standardized uptake value of between 4.0–5.8 in both lung parenchymas.

accumulation of dust in the lungs. One clinicopathologic form of this reaction is fibrosis, while the other form consists of aggregates of particle-laden macrophages with minimal or no accompanying fibrosis, a reaction that is typically seen with inert dusts such as iron, tin, and barium (15) (Fig. 11). FDG-PET studies have revealed increased uptake in pneumoconiosis and progressive massive fibrosis. Some of this uptake is perhaps related to the presence of inflammatory cells such as macrophages, as well as fibroblasts (5).

Fig. 11. Progressive massive fibrosis in a 58-year-old male. Coronal FDG-PET image shows increased uptake in right upper lobe (arrow) and a mean standardized uptake value of 6.4.

Sclerosing Hemangioma

Sclerosing hemangioma is widely believed to arise from type II pneumocyte and bronchial epithelial lining. It is a benign lesion with a good prognosis. However, in some cases it shows local invasion, multiplicity and lymph node metastasis. The CT findings of scelrosing hemangiomas are well defined, round or oval shaped, enhanced mass with or without punctuate calcification. There has been only one case report of FDG-PET findings of sclerosing hemangioma, and in this report it shows intermediate FDG

A B

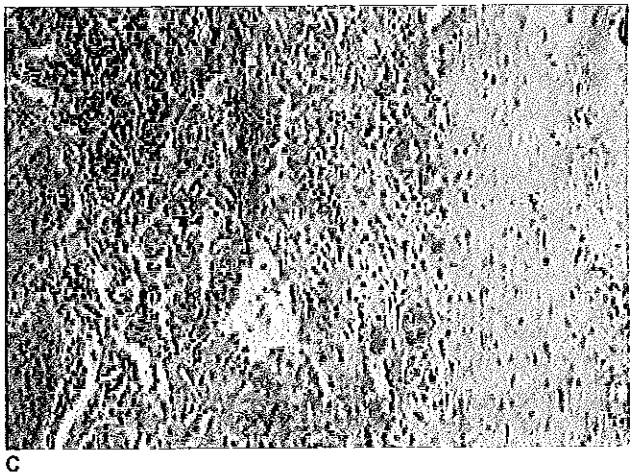

C

Fig. 10. Radiation fibrosis in a 61-year-old male by radiation therapy due to lung cancer.
A. Axial CT scan shows consolidation in the left lower lobe, suggesting lung cancer recurrence.
B. Axial PET image shows increased uptake in the left lower lobe (arrow) which was mistaken for lung cancer recurrence.
C. Microscopic image reveals severe fibrosis with inflammatory cell accumulation.

uptake (SUV= 3.0) (16) (Fig. 12).

Granulation Tissue around Tumors

Even within tumors, FDG uptake is not completely confined to the tumor cells themselves. The newly formed granulation tissue around the tumor and the macrophages infiltrating the marginal areas surrounding the necrotic area of the tumor show a high uptake of FDG. Some authors have suggested that about 24% of the FDG concentration in a tumor mass is derived from non-tumor tissue (17).

FALSE NEGATIVE CONDITIONS

Tumors with low activity are well-known major causes of false negative findings. This can be easily understood considering the FDG PET is metabolic imaging using the activity of lesion.

Another major cause of false negative findings for malignancy is tumor size. It is likely a result of a loss in measured activity as the nodule size diminishes due to the roughly 1-cm resolution of the PET systems frequently used (partial volume effect) (2).

Bronchioloalveolar Carcinoma (BAC)

Bronchioloalveolar carcinomas appear as areas of ground-glass opacity, nodules, masses, or areas of ground-glass opacity plus consolidation, on high-resolution CT scans. On pathologic examination, bronchioloalveolar carcinomas are well differentiated, having moderate degrees of nuclear atypism, mild degrees of mitotic figure, desmoplasia, and necrosis. These mild degrees of atypism,

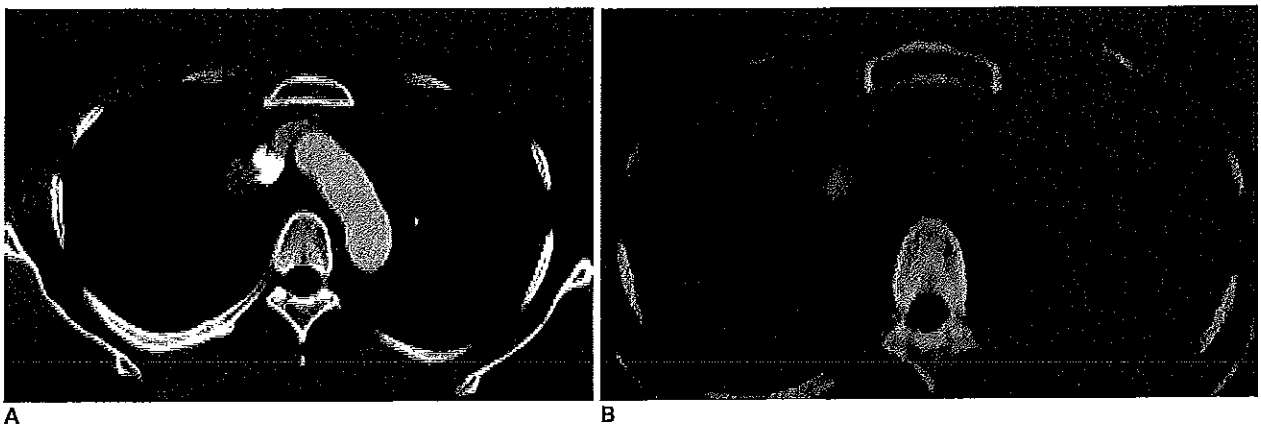

A B

Fig. 12. Sclerosing hemangioma in a 43-year-old female.
A. Axial contrast-enhanced CT shows a round well demarcated, highly enhancing mass in the right lateral side of the superior vena cava in the right upper lobe.
B. FDG-PET fusion CT image shows increased uptake in the lesion with a maximum standardized uptake value of 3.4.

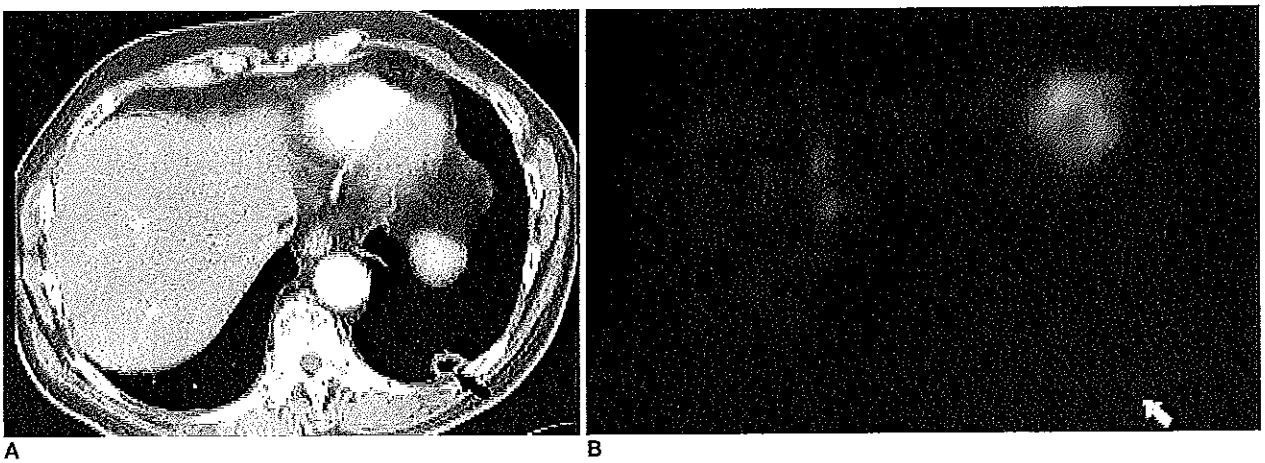

A B

Fig. 13. Bronchioloalveolar carcinoma in a 75-year-old male.
A. Contrast-enhanced CT shows a cavitary lesion in the left lower lobe (arrow).
B. Transverse FDG-PET image of the transverse scan shows subtle uptake (arrow) in the left lower lobe with a maximum standardized uptake value of 1.7.

mitosis, and desmoplasia may be the causes of lower peak SUVs than those of other lung carcinomas. Several reports (18) have revealed lower FDG uptake in BAC than adenocarcinomas in the lungs. Thus, bronchioloalveolar carcinomas can be potential causes of false negative findings of malignancy on FDG PET scans (Fig. 13). Furthermore, mucinous bronchioloalveolar cell carcinomas, which often contain abundant mucin, exhibit significantly lower peak SUVs compared with those of squamous cell carcinomas, adenocarcinomas, and other cell types. In

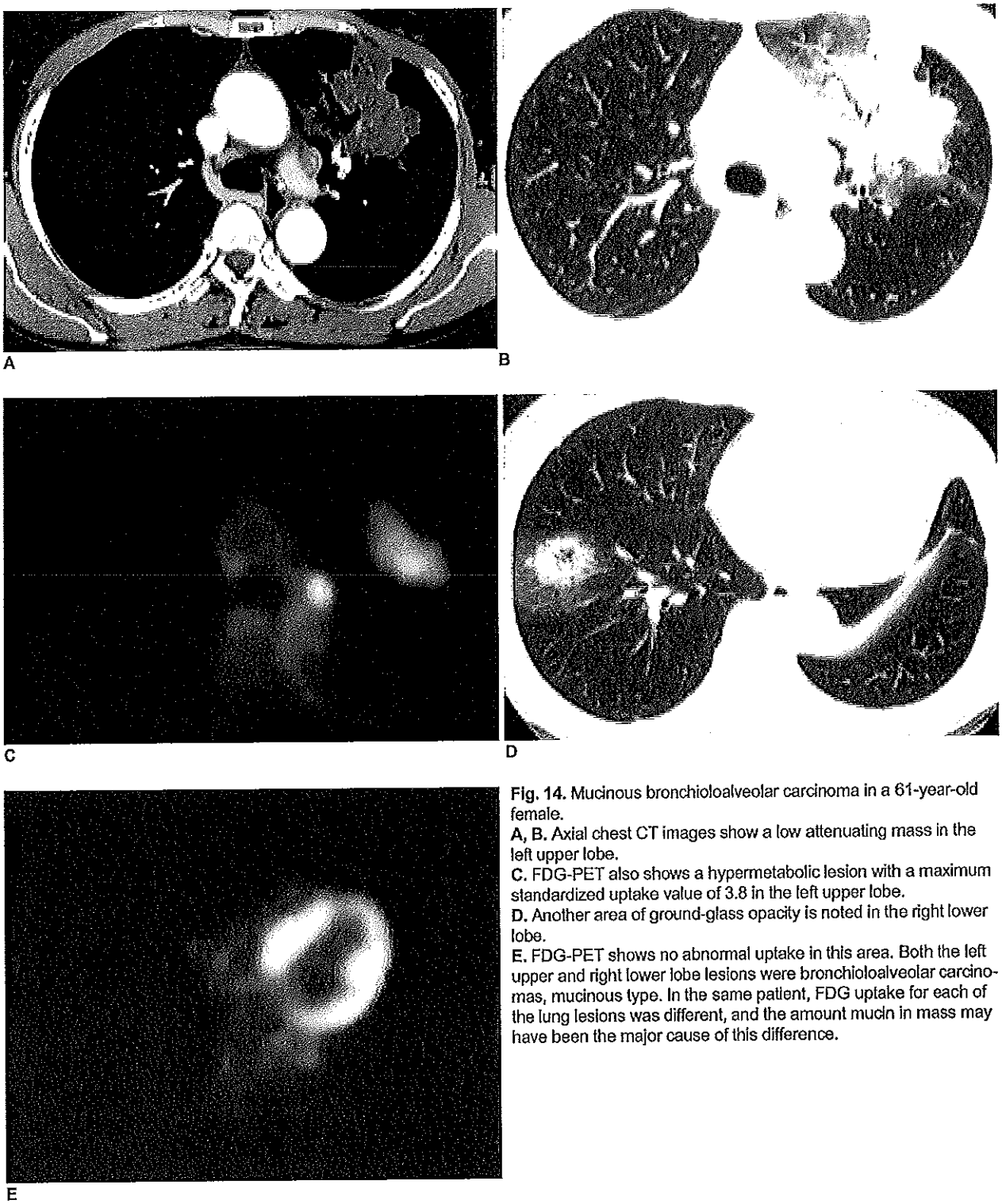

Fig. 14. Mucinous bronchioloalveolar carcinoma in a 61-year-old female.
A, B. Axial chest CT images show a low attenuating mass in the left upper lobe.
C. FDG-PET also shows a hypermetabolic lesion with a maximum standardized uptake value of 3.8 in the left upper lobe.
D. Another area of ground-glass opacity is noted in the right lower lobe.
E. FDG-PET shows no abnormal uptake in this area. Both the left upper and right lower lobe lesions were bronchioloalveolar carcinomas, mucinous type. In the same patient, FDG uptake for each of the lung lesions was different, and the amount mucin in mass may have been the major cause of this difference.

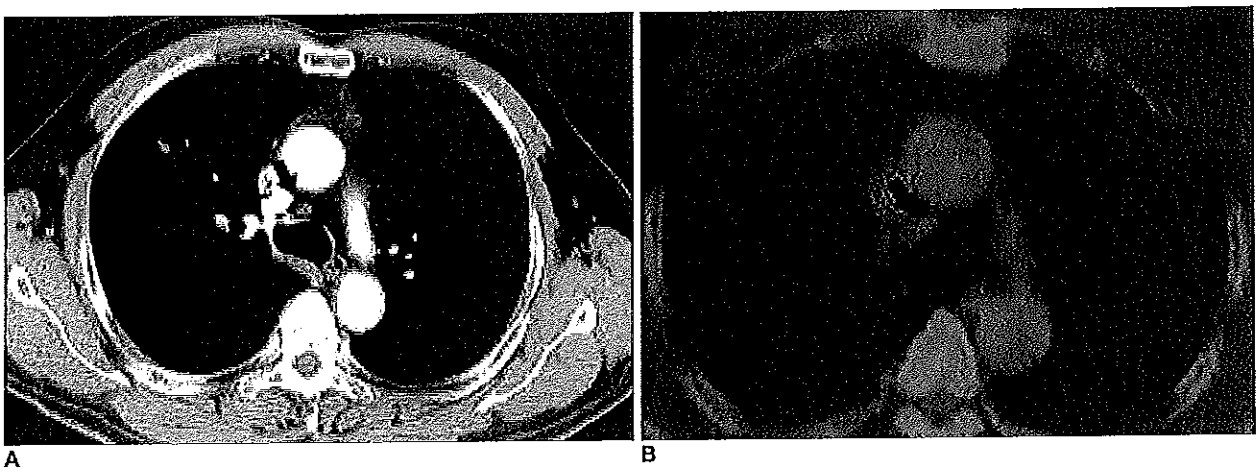

A B

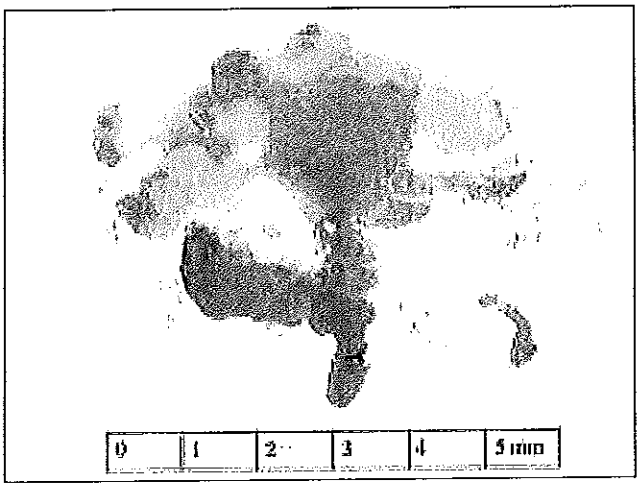

C

Fig. 15. Small malignant mediastinal lymph node in a 56-year-old male.
A. Axial contrast-enhanced CT shows a nodular lesion in the right upper lobe with a lymph node of less than 1 cm in the right paratracheal area (arrow).
B. FDG-PET fusion CT shows no increased uptake due to the small size of the lesion (arrow).
C. Pathology reveals a 0.6 cm lymph node with metastatic tumor cells.

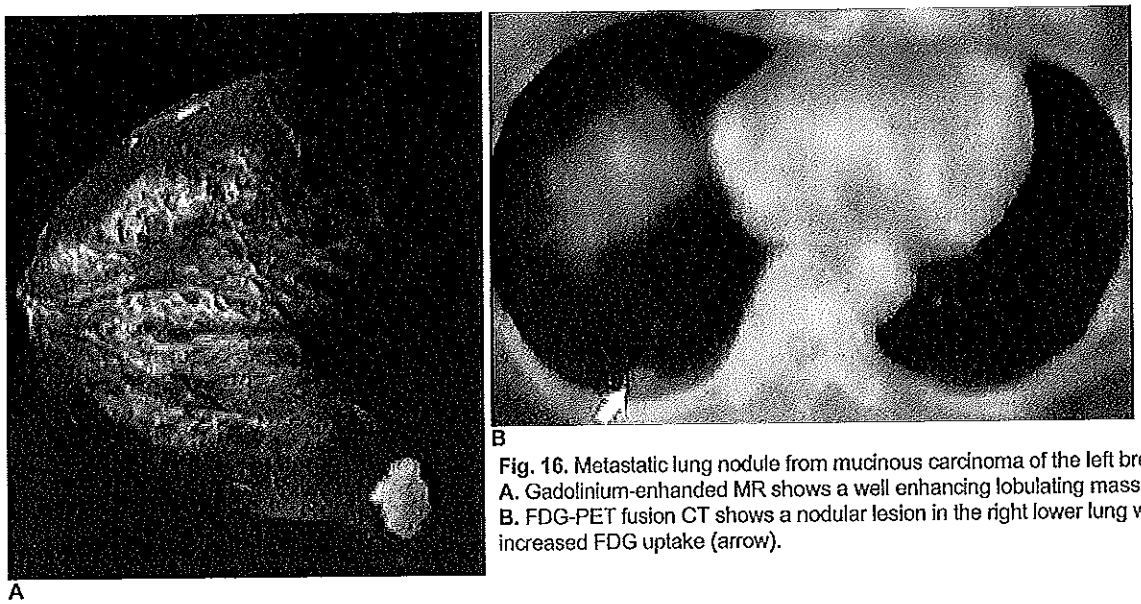

A B

Fig. 16. Metastatic lung nodule from mucinous carcinoma of the left breast.
A. Gadolinium-enhanded MR shows a well enhancing lobulating mass.
B. FDG-PET fusion CT shows a nodular lesion in the right lower lung without increased FDG uptake (arrow).

such cases, not only histologic grade, but also the amount of mucin component in the tumor (Fig. 14) is closely related with FDG-uptake (18).

Small Size Lesion

When lesions are smaller than 1 cm, these lesions may not show high FDG uptake in the lungs or mediastinum. This is the result of the 1-cm resolution of PET systems frequently used (partial volume effect) (2). Spatial resolution limitations of FDG PET have been shown to be the causative factor of false negative PET scans (Fig. 15).

Metastatic Lung Nodule of Extrapulmonary Neoplasm

Metastasis of tumors with a mucinous component can result in low FDG uptake (18). The relative cellularity of tumors is important in the detection of disease using FDG PET. Consequently, low cellularity in these tumors caused by the presence of mucin results in lower FDG uptake (19). For example, lung metastasis of a mucinous carcinoma of the breast (Fig. 16) may not show high FDG uptake. Other metastatic tumors such as mucinous adenocarcinomas of gastrointestinal origin can also show false negative findings in PET scans. Also, a metastatic mass from a renal cell carcinoma (20) (Fig. 17), and some invasive ductal and lobular breast carcinomas (21) are well reported to result in false negative findings.

Chemotherapy Related Factor

In several previous reports, it has been well documented that FDG uptake usually decreases after chemotherapy, and this correlates with therapeutic response. Decreased FDG uptake after irradiation is mainly due to the reduced number of metabolically active tumor cells. However, a decrease of FDG PET does not always predict a good response because FDG can differentiate metabolically active cells from dead cells, but cannot differentiate biologically viable from metabolically active cells (22) (Fig. 18).

Carcinoid Tumor

Carcinoid tumors arise from the dispersed neuroen-

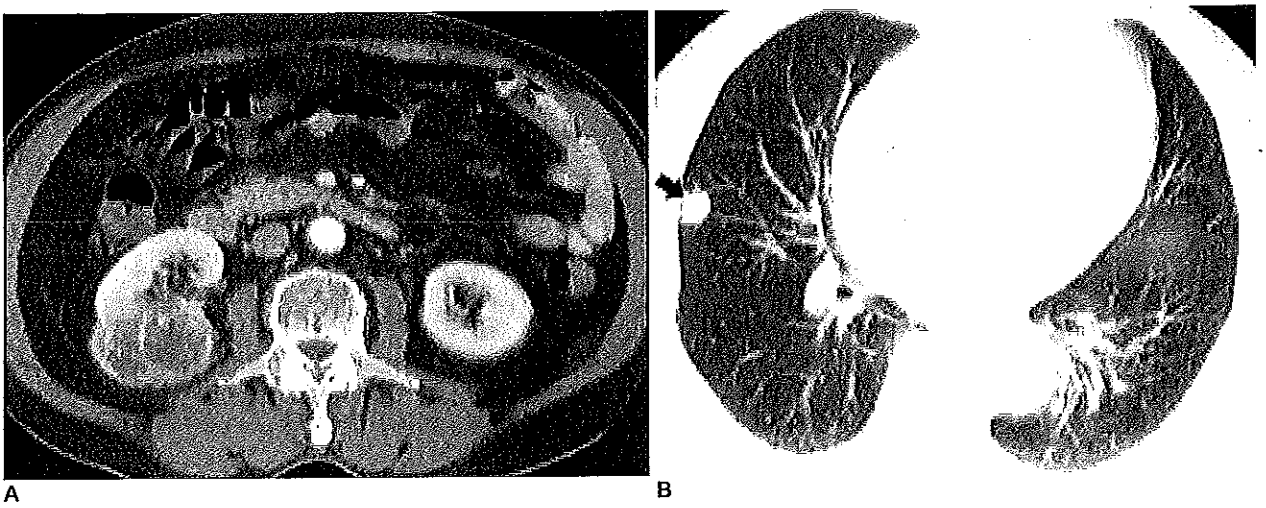

A B

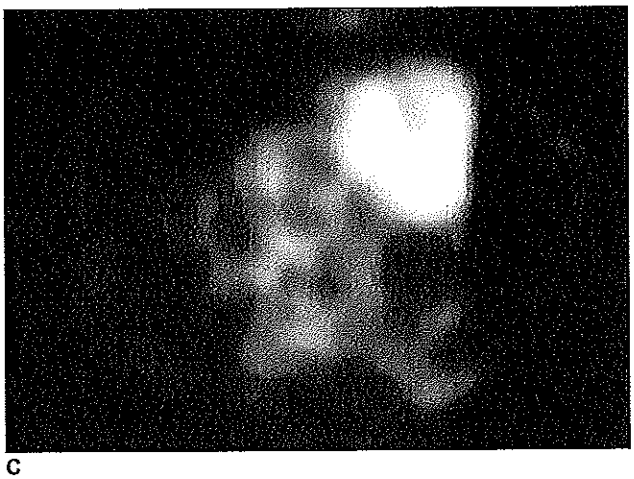

C

Fig. 17. Metastasis from renal cell carcinoma in an 83-year-old male.
A. Axial contrast-enhanced CT scans shows a mass lesion in the right kidney suggesting renal cell carcinoma.
B. Axial CT scan of lung window setting shows a lung nodule in the right middle lobe (arrow).
C. A selected transverse section of whole body-PET image shows no demonstrable uptake in the right lung.

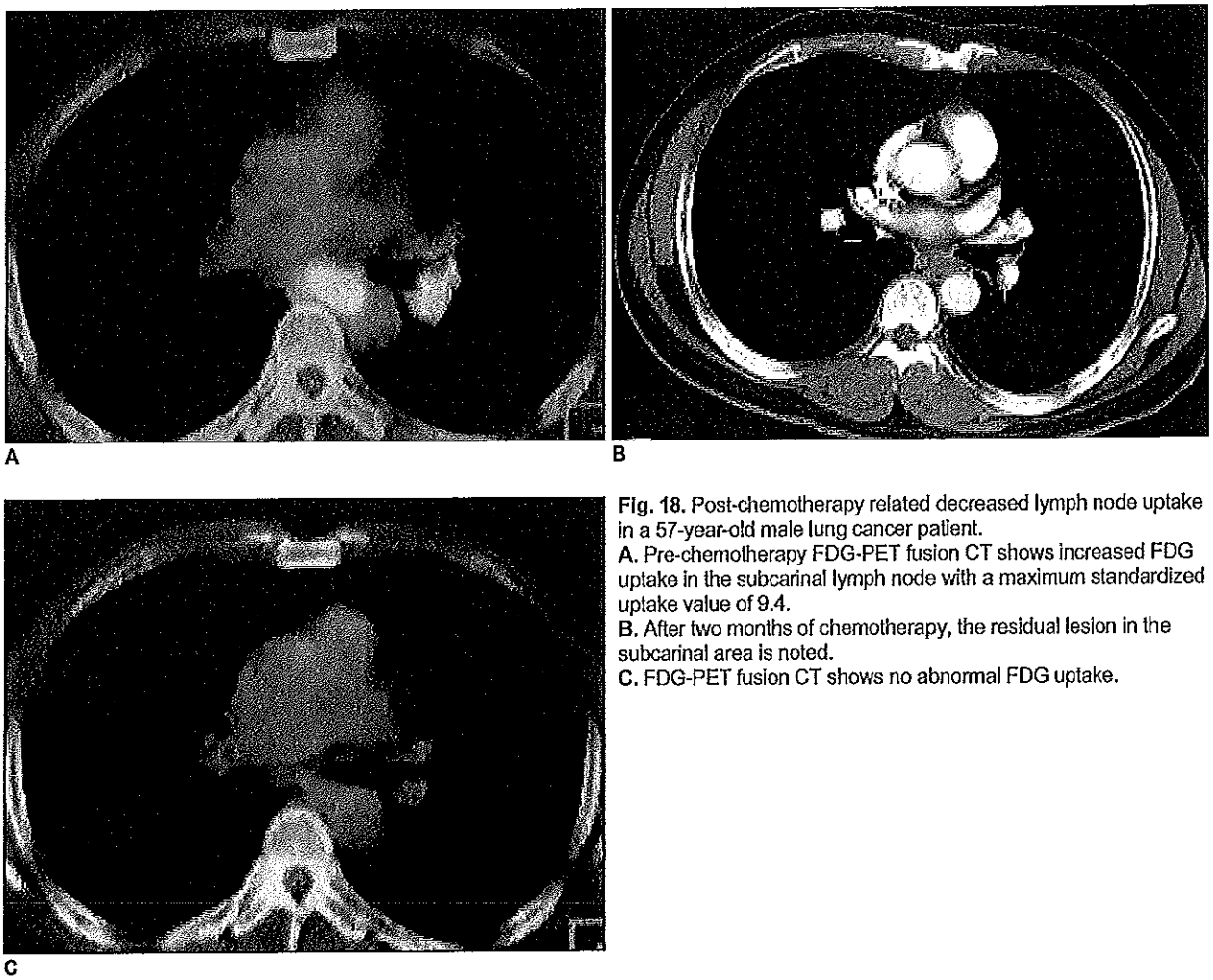

Fig. 18. Post-chemotherapy related decreased lymph node uptake in a 57-year-old male lung cancer patient.
A. Pre-chemotherapy FDG-PET fusion CT shows increased FDG uptake in the subcarinal lymph node with a maximum standardized uptake value of 9.4.
B. After two months of chemotherapy, the residual lesion in the subcarinal area is noted.
C. FDG-PET fusion CT shows no abnormal FDG uptake.

docrine system, and are classified as typical and atypical, depending on the degree of cellular atypia. In a previous report, the SUV in a carcinoid tumor was 1.0–2.3, which is the result of low metabolic activity. The reason for the low metabolic activity in the carcinoid tumor is unknown (23).

Hyperglycemia

The biodistribution of FDG can be affected by blood glucose levels. In situations of high blood glucose levels, circulating blood glucose uptake in pathologic lesions increase and this prevents FDG uptake because of the competitive reaction (5). Therefore, a large amount of glucose in the blood is taken up in the tumor tissue which interferes FDG uptake in the tumor, resulting in a false negative finding. Specifically, in type II diabetic patients insulin may be used to manipulate glucose levels. However, there is still no agreement as to adjusting glucose levels in diabetic patients (2).

CONCLUSION

Metabolic imaging with FDG-PET is beginning to play important role in the management of oncologic diseases. In addition, it plays a complementary role in accurate overall evaluation of malignant diseases. However, false positive FDG uptake or false negative PET scans are frequently encountered. Proper interpretation and accurate characterization of an abnormality can be accomplished only if one is aware of possible false positive and negative conditions.

References

1. Goo JM, Im JG, Do KH, Yeo JS, Seo JB, Kim HY, et al. Pulmonary tuberculoma evaluated by means of FDG PET: findings in 10 cases. *Radiology* 2000;216:117-121
2. Kostakoglu L, Agress H, Goldsmith SJ. Clinical role of FDG PET in evalutaion of cancer patients. *RadioGraphics* 2003;23:315-340
3. Trukington TG, Coleman RE. Clinical oncologic PET: An

Introduction. *Semin Roentgenol* 2002;37:102-109
4. Gupta NC, Graeber GM, Bishop HA. Comparative efficacy of positron emission tomography with fluorodeoxyglucose in evaluation of small (< 1 cm), intermediate (1 to 3 cm), and large (> 3 cm) lymph node lesions. *Chest* 2000;117: 773-778
5. Alavi A, Gupta N, Alberini JL, Hickeson M, Adam LE, Bhargava P, et al. Positron emission tomography imaging in nonmalignant thoracic disorders. *Semin Nucl Med* 2002;32: 293-321
6. Amerein PC, Larson SM, Wagner HN Jr. An automated system for measurement of leukocyte metabolism. *J Nucl Med* 1975;15:352-355
7. Crystal RG. *Disorders of the immune system, connective tissue, and joints, sarcoidosis.* In: Braunwald E, Fauci AS, Kasper DL, Hauser SL, Longo DL, Jameson JL, eds. *Harrison's principle of internal medicine,* 15th ed. NewYork: McGraw-Hill, 2001;1969-1970
8. Bakheet SM, Powe J. Benign causes of 18-FDG uptake on whole body imaging. *Semin Nucl Med* 1998;28:352-358
9. Brudin LH, Valind SO, Rhodes CG, Pantin CF, Sweatman M, Jones T, et al. Fluorine-18 deoxyglucose uptake in sarcoidosis measured with positron emission tomography. *Eur J Nucl Med* 1994;21:297-305
10. Bennett JE. *Cryptococcosis.* In: Braunwald E, Fauci AS, Kasper DL, Hauser SL, Longo DL, Jameson JL, eds. Harrison's principle of internal medicine 15th ed. NewYork: McGraw-Hill, 2001;1174-1175
11. Watanabe S, Nakamura Y, Kariatsumari K, Nagata T, Sakata R, Zinnouchi S, et al. Pulmonary paragonimiasis mimicking lung cancer on FDG-PET imaging. *Anticancer Res* 2003;23:3437-3440
12. Im JG, Kong Y, Shin YM, Yang SO, Song JG, Han MC, et al. Pulmonary paragonimiasis: clinical and experimental studies. *RadioGraphics* 1993;13:575-586
13. Lorenzen J, Buchert R, Bleckmann C, Munchow N, Bohuslavizki KH. A search for the focus in patients with fever of unknown origin: is positron-emission tomography with F-18-fluorodeoxyglucose helpful? *Rofo Fortschr Geb Rontgenstr Neuen Bildgeb Verfahr* 1999;171:49-53
14. Lin P, Chu J, Pocock N. Fluorine -18 FDG dual-head gamma camera coincidence imaging of radiation pneumonitis. *Clin Nucl Med* 2000;25:866-869
15. Speizer FE. *Environmental lung diseases.* In: Braunwald E, Fauci AS, Kasper DL, Hauser SL, Longo DL, Jameson JL, eds. *Principle of internal medicine,* 15th ed. NewYork: McGraw-Hill, 2001;1470-1471
16. Hara M, Iida A, Tohyama J, Miura N, Shiraki N, Itoh M, et al. FDG-PET findings in sclerosing hemangioma of the lung: a case report. *Radiat Med* 2001;19:215-218
17. Kubota R, Yamada S, Kubota K, Ishiwata K, Tamahashi N, Ido T. Intratumoral distribution of fluorine-18-fluorodeoxyglucose in vivo: high accumulation in macrophages and granulation tissues studied by microautoradiography. *J Nucl Med* 1992;33:1972-1980
18. Kim B, Kim Y, Lee K, Yoon SB, Cheon EM, Kwon OJ, et al. Localized form of bronchioloalveolar carcinoma: FDG PET findings. *AJR Am J Roentgenol* 1998;170:935-939
19. Berger KL, Nicholson SA, Dehdashti F, Siegel BA. FDG PET evaluation of mucinous neoplasms: correlation of FDG uptake with histopathologic features. *AJR Am J Roentgenol* 2000;174: 1005-1008
20. Montravers F, Grahek D, Kerrou K, Younsi N, Doublet JD, Gattegno B, et al. Evaluation of FDG uptake by renal malignancies (primary tumor or metastases) using a coincidence detection gamma camera. *J Nucl Med* 2000;41:78-84
21. Avril N, Rose CA, Schelling M, Dose J, Kuhn W, Bense S, et al. Breast imaging with positron emission tomography and fluorine-18 fluorodeoxtglucose: use and limitations. *J Clin Oncol* 2000;18:3495-3502
22. Ryu JS, Choi NC, Fischman AJ, Lynch TJ, Mathisen DJ. FDG-PET in staging and restaging non-small cell lung cancer after neoadjuvant chemoradiotherapy: correlation with histopathology. *Lung Cancer* 2002;35:179-187
23. Erasmus JJ, McAdams HP, Patz EF Jr, Coleman RE, Ahuja V, Goodman PC. Evaluation of primary pulmonary carcinoid tumors using FDG PET. *AJR Am J Roentgenol* 2004;182:559-567

MOLECULAR IMAGING AND BIOLOGY

Published Online: 16 December 2010

Mol Imaging Biol (2011) 13:1051–1060
DOI: 10.1007/s11307-010-0459-x

REVIEW ARTICLE

Clinical Utility of FDG–PET and PET/CT in Non-malignant Thoracic Disorders

Sandip Basu,[1] Babak Saboury,[2] Tom Werner,[2] Abass Alavi[2]

[1]*Radiation Medicine Centre (BARC), Tata Memorial Hospital Annex, Parel, Bombay, 400012, India*
[2]*Division of Nuclear Medicine, Hospital of University of Pennsylvania, 3400 Spruce Street, Philadelphia, PA, 19104, USA*

Abstract

There have been several endeavors made to investigate the potential role of 2-deoxy-2-[^{18}F] fluoro-D-glucose positron emission tomography (FDG-PET) (and tracers) and PET-computed tomography imaging in various benign disorders, particularly those related to thoracic structures. These various conditions can be broadly categorized into three groups: (a) infectious diseases (mycobacterial, fungal, bacterial infection), (b) active granulomatous disease such as sarcoidosis, and (c) other non-infectious/inflammatory conditions or proliferative disorders (e.g., radiation pneumonitis, post-lung transplant lymphoproliferative disorders, occupational pleuropulmonary complications, and post-surgical conditions), all of which can demonstrate varying degrees of FDG uptake on PET scans based upon the degree of inflammatory activity. This article reviews the current state of this very important application of FDG–PET imaging.

Key words: FDG, PET, PET/CT, Non-malignant thoracic disorders, Tuberculosis, Sarcoidosis

Introduction

It is clear that several benign conditions, in addition to cancer, can demonstrate increased 2-deoxy-2-[^{18}F] fluoro-D-glucose (FDG) accumulation and therefore are considered as false-positive results for malignancy. In the oncological setting, differentiation between malignant and benign thoracic pathologies is a dilemma, and therefore it is important to be aware of these non-specific findings in FDG–positron emission tomography (PET) studies to make an appropriate diagnosis. These can be broadly categorized into three groups: (a) infectious disorders (mycobacterial, fungal, bacterial infection), (b) active granulomatous disease such as sarcoidosis, and (c) other non-infectious inflammatory conditions or proliferative disorders (e.g., radiation pneumonitis, post-lung transplant lymphoproliferative processes, occupational pleuropulmonary complications, and post-surgical conditions), all of which can demonstrate varying degrees of FDG uptake on PET scans due to inflammatory reactive response. Among these, false-positive FDG–PET imaging has been primarily described in the setting of granulomatous processes such as sarcoidosis or mycobacterial infection.

It is proposed that the inflammatory cells such as neutrophils and activated macrophages at the site of inflammation or infection are responsible for the accumulation of FDG. As experience with FDG–PET has evolved over the past few years, the need for alternative tests or certain maneuvers for enhancing its specificity in these scenarios is increasingly being realized. Furthermore, these observations have resulted in exploring the potential utility of this test, FDG–PET, in the setting where suspected diagnosis can be made and its activity can be characterized for monitoring therapeutic response.

FDG–PET Characteristics Indicating Benign and Malignant Etiology in Non-specific Mediastinal and Hilar Foci

Several investigators have examined the variables for determining benign or malignant nature of non-specific uptake in the mediastinum and hilar nodes on FDG–PET scan (Table 1). The parameters or factors that have been

Correspondence to: Abass Alavi; *e-mail:* abass.alavi@uphs.upenn.edu

Table 1. Factors utilized for correct characterization of uptake in the mediastinal and hilar nodes in FDG–PET scan

(a) SUVmax (especially after partial volume correction of the estimated value, which has been overlooked in most published data in the literature),
(b) Dual-time-point and delayed PET imaging (a critical test for distinguishing between malignant and benign disorders),
(c) Symmetry of the lesions,
(d) Site of the primary tumor,
(e) Node size and characteristics as determined by reviewing the CT,
(f) Absence/presence of FDG-avid foci in non-hilar mediastinal nodes ("purity" of the lesions)
(g) Time course of FDG uptake among repeat scans

utilized include (a) the maximum standard uptake value (SUVmax), especially after partial volume correction of the measured value, (b) dual-time-point PET imaging (Fig. 1), (c) symmetry, (d) site of the primary tumor, (e) node size and characteristics as revealed by the computed tomography (CT), (f) absence/presence of FDG-avid foci in non-hilar mediastinal nodes, and (g) the degree of stability of uptake between the scans in those who participated in more than two studies in their disease course. It is important to remember that respiratory motions can result in significant image misregistration on PET–CT scans and SUV calculation of thoracic lesions. Therefore, every effort should be made to account for such technical factors in interpreting the findings on these scans.

In a recent retrospective study [1], investigators analyzed 51 patients with cancer with bilateral hilar node FDG–PET uptake. On a univariate analysis, variables associated with malignancy were degree of SUVmax, absence/presence of FDG-avid sites in non-hilar mediastinal nodes, symmetry, the primary tumor, node size determined by CT, and, in those who had participated in two studies, stability of uptake over time. After multivariate analysis, the first two variables (e.g., SUVmax and absence/presence of FDG-avid foci in non-hilar mediastinal nodes) were found to be independent predictors. These authors concluded that in patients with non-pulmonary malignancies, especially colorectal carcinoma, foci of symmetric and mild uptake limited to the hilar regions are likely related to a benign etiology if they are stable on two sequential PET studies despite intervening anticancer therapy.

In another study [2] which compared FDG–PET and transesophageal endosonography with fine needle aspiration (EUS–FNA) in 40 patients for characterization of mediastinal nodes, the sensitivity, specificity, and accuracy of PET were 100, 54.5, and 87.5%, respectively, whereas those of the EUS–FNA were 79.3, 100, and 85%, respectively. It was observed that the combination of FDG–PET and EUS–FNA avoided invasive procedures (mediastinoscopies or staging surgery) in 34 patients. The authors concluded that combined EUS–FNA and FDG–PET imaging are complementary diagnostic procedures by enhancing the high sensitivity of FDG–PET with the high specificity of EUS–FNA for accurate diagnosis in the setting of enlarged mediastinal lymph nodes in patients with known malignancies.

Tuberculosis

Tuberculomas are discrete nodules, usually less than 3 cm in diameter, in which repeated infection has caused a core of

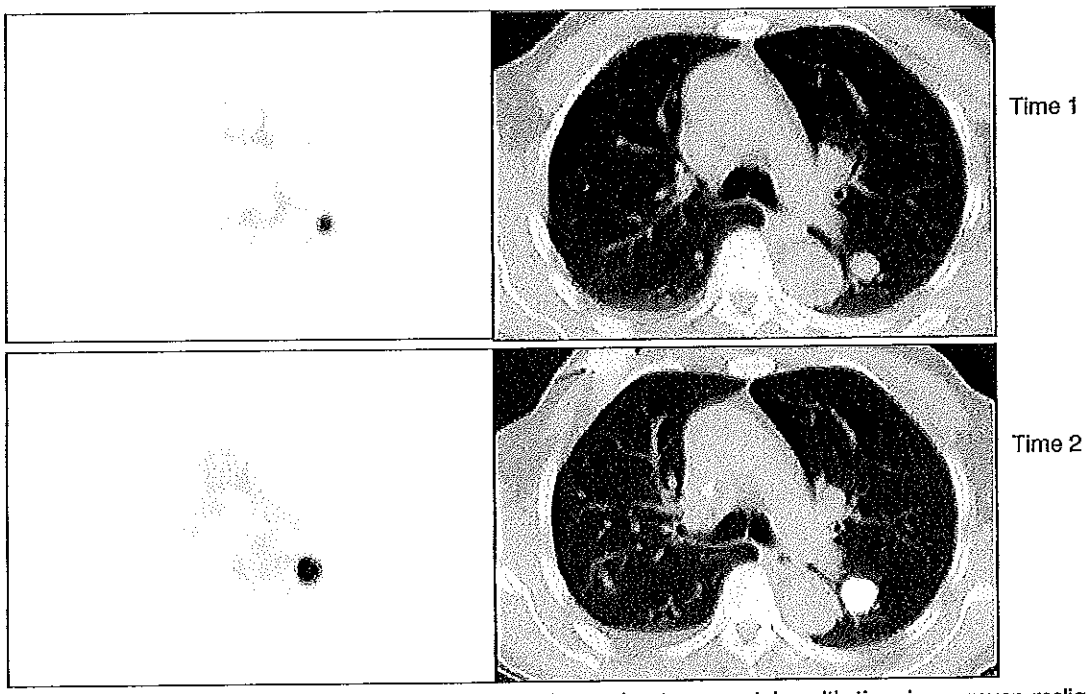

Fig. 1. Dual-time-point FDG–PET/CT imaging demonstrating increasing tracer uptake with time in a proven malignant lung nodule.

caseous necrosis surrounded by zone of epithelioid cells and collagen with peripheral round cell infiltration. Small, discrete shadows in the vicinity of the main lesion, known as "satellite lesions", are observed in as many as 80% of cases [3, 4]. The promising features of FDG–PET imaging in the management of patients with this disorder are (a) its potential role for assessing therapeutic response especially in certain locations such as spinal tuberculosis, (b) its ability to detect unsuspected distant sites of infection because of the whole body nature of this imaging technique, (c) its role in guiding for a biopsy site (combined PET/CT, in particular, may be very useful for this purpose), and (d) diagnosis of suspected recurrence and residual disease following successful therapy. It is important to note that this role for FDG–PET has a geographical relevance as developing countries have high prevalence of tuberculosis and, therefore, the probability of false-positive FDG–PET results are high in the Asian population compared to that of the Europeans or North Americans.

Sarcoidosis: Pulmonary and Cardiac Sarcoidosis

Sarcoidosis is a chronic granulomatous multiorgan disease of unknown etiology that most frequently involves the lungs which is the major cause of morbidity in these patients. The disease is characterized in affected organs by an accumulation of T lymphocytes and mononuclear phagocytes, non-caseating epithelioid granulomas, and derangements of the normal tissue architecture. Histopathologically, the initial event in the disease is the accumulation of mononuclear inflammatory cells, mainly CD4+ T helper 1 lymphocytes and mononuclear phagocytes, in the affected organ which eventually looks to the formation of granulomas, aggregates of macrophages and their progeny, epithelioid cells, and multinucleated giant cells.

The initial pulmonary lesions consist of mononuclear cell infiltration of interstitial tissue of the lung which is followed by formation of granulomas characteristic of this disease. The majority of granulomas resolve in their course, but in some, fibrosis ensues giving rise to tissue dysfunction. Disease activity in sarcoidosis can be best assessed by detecting and quantifying the degree of inflammatory and granulomatous reactions that occur in the lungs and elsewhere in the body. Since both sarcoidosis and lymphomas affect lymphoid systems throughout the body, the pattern noted on the FDG–PET images is non-specific and cannot differentiate between the two distinct entities (Fig. 2). However, in a patient with proven diagnosis of sarcoidosis, the extent of involvement and quantification of the disease activity can be more accurately assessed by FDG–PET than with ^{67}Ga scintigraphy and other single gamma-emitting tracers. This is due to the high quality of the images generated by PET with superior spatial and contrast resolutions compared to those acquired with single photon emission computed tomography (SPECT).

Fig. 2. Whole-body FDG–PET demonstrating avid FDG uptake in the mediastinal nodes and bilateral lungs in a proven case of sarcoidosis.

PET/CT in Sarcoidosis

To evaluate the role of FDG–PET/CT in sarcoidosis, Braun et al. [5] retrospectively assessed 20 consecutive patients with biopsy-proven sarcoidosis. For thoracic, sinonasal, and pharyngo-laryngeal localizations, the sensitivity of FDG–PET/CT was 100%, 100%, and 80%, respectively, for these sites. Overall sensitivity for all 36 biopsy-proven localizations improved from 78% to 87% after excluding skin involvement. When (67) Ga scintigraphy and (18) F-FDG PET/CT were compared for the 12 patients who underwent both examinations, the overall sensitivity of ^{67}Ga scintigraphy was 58% and 79%, and by using FDG–PET improved to 67% and 86% after excluding all sites of skin involvement. The authors concluded that FDG–PET/CT provides a complete morpho-functional cartography of active inflammatory sites and is useful to follow the efficacy of treatment in patients with sarcoidosis, particularly in its atypical, complex, and multisystem forms.

Cardiac Sarcoidosis

Diagnosis of cardiac involvement by sarcoidosis continues to be a challenge to the attending physician and usually relies on a combination of clinical and imaging findings. In one

of the earlier reports [6], sudden death due to unsuspected cardiac involvement has been found to occur in up to 35% of affected individuals. While ^{67}Ga scan and ^{99m}Tc-methoxyisobutylisonitrile (^{99m}Tc-MIBI) myocardial perfusion scintigraphy have been utilized for detection of myocardial involvement, they are relatively insensitive in the early stages of the disease, possibly delaying therapy which can pose substantial risks. Delayed-enhanced cardiac MRI and PET imaging are the most promising emerging diagnostic modalities in this setting, and the role of other non-invasive modalities like ultrasonic tissue characterization [7, 8] and iodine-123-labeled 15-(*p*-iodophenyl)-3*R*,*S*-methylpentadecanoic acid scintigraphy [9] have also been investigated.

The use of both FDG–PET and perfusion scanning with ^{13}N–NH_3 was reported by Yamagishi et al. [10] in a series of 17 patients with cardiac sarcoidosis. In these patients, the perfusion defects demonstrated minimal change following steroid treatment, while the FDG abnormalities largely resolved. This suggests that with effective treatment, there was an improvement from an active inflammatory granulomatous process to a healed scar.

Okumura et al. [11] studied cardiac PET using ^{18}F-FDG under fasting conditions for identification of cardiac sarcoidosis and assessment of disease activity. They observed a higher frequency of abnormal myocardial segments on FDG–PET than ^{99m}Tc-MIBI SPECT [mean number of abnormal segments per patient=6.6±3.0 vs. 3.0±3.2 (mean±SD), $P<0.05$]. The sensitivity of fasting FDG–PET in detecting cardiac sarcoidosis was 100%, significantly higher than that of ^{99m}Tc-MIBI SPECT (63.6%) or ^{67}Ga scintigraphy (36.3%). These authors concluded that FDG–PET can detect the early stage of cardiac sarcoidosis, in advance of myocardial impairment due to widespread disease involvement.

Ishimaru et al. [12] evaluated the value of FDG–PET in detecting cardiac sarcoidosis in 32 patients and 30 controls. These authors observed that focal FDG uptake of the heart on PET images is a characteristic feature of patients with sarcoidosis and FDG–PET has the potential to detect cardiac sarcoidosis that cannot be diagnosed by (67)Ga or (99m) Tc-MIBI scintigraphy.

Occupational Pleuropulmonary Disorders

Pneumoconioses include coal worker's pneumoconiosis, silicosis, asbestosis, and berylliosis, of which silicosis and asbestosis are the two major types. Data on the PET appearance of pneumoconiosis has been reported in the literature. FDG uptake has been observed in pneumoconiosis and progressive massive fibrosis. This uptake may be related to the presence of inflammatory cells such as macrophages, as well as fibroblasts [13]. Avid FDG uptake in the right ventricle coupled with enhanced intercostal muscle hypermetabolism has been reported to indicate the severity of the disease [14, 15]. The role of FDG in the diagnosis of malignancy in the setting of pneumoconiosis is unclear. Controversial results (mainly case studies) have been described. Shukuya et al. [16] described significantly increased uptake in a nodular lesion that turned out to be only pneumoconiosis. On the other hand, the reports by Bandoh et al. [17] and Williams et al. [18] demonstrated a case where FDG–PET was able to clearly distinguish the lung cancer from progressive massive fibrosis, suggesting a potential usefulness of FDG–PET in cancer screening in patients with pneumoconiosis. More data needs to be accrued on this topic in the future.

In a comparative study of the ability of C^{11}methionine (MET) and FDG–PET to diagnose lung cancer in patients with pneumoconiosis, Kanegae et al. [19] examined 26 subjects who underwent both whole-body MET–PET and FDG–PET on the same day. The first group was a lung cancer group, which consisted of 15 patients, including those with pneumoconiosis with multiple nodules (13 cases), hemoptysis (one case), and positive sputum cytology (one case). The second group was a no-malignancy control group, consisting of 11 patients with pneumoconiosis. Significant correlations between nodule size and the SUV(max) of the two PET tracers were observed in the control group. The larger the nodule size, the greater were the degree of these tracers uptake (MET—r=0.771, $P<0.0001$; FDG—r=0.903, $P<0.0001$). The SUV(max) of MET was significantly lower than that of FDG in the pneumoconiotic nodules ($P<0.0001$). Lung cancer was found in five of 19 nodules (two with adenocarcinoma, one with squamous cell carcinoma, one with small cell carcinoma, and one with large cell carcinoma) in the first group. As for nodules equal to or less than 3 cm in diameter, the SUV(max) of MET was significantly higher in the lung cancer than in the pneumoconiotic nodules, with 3.48±1.18 (mean±SE) for the lung cancer and 1.48±0.08 for the pneumoconiotic nodules ($P<0.01$), similar to the SUV (max) of FDG, with 7.12±2.36 and 2.85±0.24 ($P<0.05$), respectively. On the basis of the criteria for the control group, FDG and MET identified lung cancer with sensitivities of 60% and 80%, specificities of 100% and 93%, accuracies of 90% and 90%, positive predictive values of 100% and 80%, and negative predictive values of 88% and 93%, respectively. The authors concluded that nodules with an intense uptake of MET and FDG relative to their size should be carefully observed because of a high risk for lung cancer.

The FDG uptake pattern has also been described in the setting of progressive massive fibrosis secondary to pulmonary silicosis [20]. Chronic exposure to free silica results in nodular lung fibrosis that may be progressive in the absence of further exposure, with coalescence and formation of non-segmental conglomerates of irregular collagen-containing masses characteristic of progressive massive fibrosis. These patients are reported to have a significantly enhanced risk of tuberculosis or atypical mycobacterial infection.

FDG–PET imaging has been described in benign pleural conditions most commonly with regard to its utility in distinguishing benign from malignant disease in occupational pneumoconioses. It has been reported to be useful in distinguishing benign from malignant disease in asbestos-related pleural disorders.

In an attempt to differentiate pleural malignancies from the asbestos exposure related benign lesions viz. pleural plaques, diffuse pleural thickening, and benign asbestos-related pleural effusion, Melloni et al. [21] examined 30 patients exposed to asbestos who underwent ^{18}FDG imaging *via* coincidence detection. All primary malignant mesotheliomas accumulated FDG, and, in two patients, the findings were superior to those of CT, allowing early detection. In two cases, lung carcinomas with malignant pleural effusion were also detected. There were five false-positive coincidence detection emission tomography results: three unilateral pleural thickening, one rounded atelectasis, and one benign lung nodule. All patients with pleural plaques showed no significant ^{18}FDG uptake. Malignant diseases were detected by ^{18}FDG-coincidence imaging with a sensitivity of 89% and specificity of 71%. The authors concluded that coincidence detection emission tomography (using a two-detector system) is a useful non-invasive method to identify malignant mesothelioma in selected subjects exposed to asbestos.

In another study, the role of FDG dual-head gamma-camera coincidence imaging (FDG-CI) was examined in 15 consecutive patients with CT scan evidence of pleural thickening, fluid, plaques, or calcification for its ability to detect malignant pleural mesothelioma [22]. FDG-CI demonstrated a sensitivity of 88% whereas that of CT was 75%. FDG-CI identified extrathoracic metastases in five patients, excluding them from surgical therapy. The authors concluded that FDG-CI appears to be an accurate method to diagnose and to define the extent of disease in diffuse malignant pleural mesothelioma.

We have examined the potential of dual time point FDG–PET imaging in differentiating malignant from benign pleural disease. In this prospective evaluation study [23], 55 consecutive patients referred for the evaluation of suspected malignant pleural mesothelioma (MPM) and recurrence of MPM underwent two sequential PET scans (dual-time-point imaging). The mean±SD of the SUVmax1, SUVmax2, and Δ%SUVmax in both newly diagnosed and recurrent MPM were significantly higher than those of benign pleural disease group ($P<0.0001$). It was also observed that there is increasing uptake of ^{18}F-FDG over time in pleural malignancies, whereas the uptake in benign pleural disease generally stays stable or decreases over time. The study results indicated that the dual-time-point imaging may help in differentiating benign from malignant pleural disease by increasing the sensitivity and is also helpful for guiding the biopsy site for diagnosis.

Post-lung Transplant Lymphoproliferative Disorder in Lung Transplant Recipients: Implications for Disease Staging with FDG–PET

Post-transplantation lymphoproliferative disorder (PTLD) is encountered as a complication in 4% to 8% of lung transplant recipients. Accurate estimation of disease extent is an important prognostic factor that allows selection of optimal therapy in this disease. Marom et al. [24] had examined the utility of FDG–PET imaging to stage lung transplant recipients with posttransplantation lymphoproliferative disorder. The study results indicated that FDG can show foci of uptake, particularly in extrathoracic sites that are not evident on conventional imaging. The authors concluded that FDG–PET allows more accurate staging of PTLD, thereby yielding useful prognostic information and guiding therapy.

Other Infective Pathologies Reported in Literature

In addition to tuberculosis, FDG–PET has been known to concentrate in a number of other infective pathologies that are known to infect lung or other thoracic locations, e.g., cryptococcosis [25], paragonimiasis, and Pneumocystis infections [26]. Watanabe et al. [27] reported one case of paragonimiasis mimicking lung cancer, which showed high FDG uptake (SUV 4.7 at 1 h post-injection and 6.2 at 2 h).

Other Non-infective Benign Conditions

Radiation fibrosis is due to infiltration of leukocytes and macrophages and abnormal proliferation of type II pneumocytes, radiation-induced production of local cytokines such as platelet-derived growth factor, tumor necrosis factor, and transforming growth factor in the radiation field. In this process, there is increased FDG uptake in the affected region [28]. There has been one case report of FDG–PET uptake in sclerosing hemangioma [29], and in this report it showed moderate degree FDG uptake (SUVmax of 3). FDG–PET findings may be non-specific in different types of thymic lesions (e.g., commonly encountered diffuse low to moderate uptake in the postchemotherapy thymic rebound), although thymic carcinomas tend to be extremely FDG avid.

FDG Uptake in Vessel Wall: Atherosclerosis and Vasculitis

FDG uptake in the atherosclerotic large vessels has been observed in several reports. It is generally thought that increased glucose uptake and metabolism in the plaque macrophages accounts for the visualization of vulnerable atherosclerosis lesion by FDG–PET imaging.

Based on the data available, it is apparent that FDG–PET imaging combined with CT holds great promise for assessing atherosclerosis in large arteries. The high sensitivity and optimal quantification provided by this imaging modality has the potential for early diagnosis and accurate evaluation of response to treatment. Our group has investigated the frequency of FDG uptake in the large arteries in relation to the atherogenic risk factors [30, 31]. FDG–PET imaging, by its inherent ability to quantify the metabolic activity of the

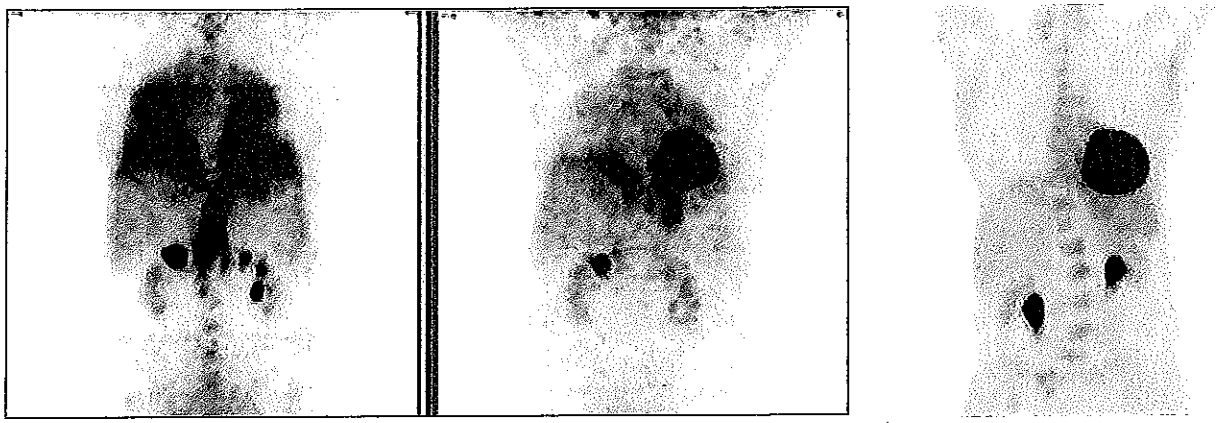

Fig. 3. FDG–PET maximum intensity projection images (antero-posterior view) demonstrating the FDG uptake during the treatment course in a patient with *Mycobacterium avium–intercellulare* (MAI) infection.

intended physiological or disease process, can assess the disease activity in vulnerable plaques throughout the whole body, defined as atheroburden by our group [32, 33]. This objective parameter can be utilized to predict the risk of plaque rupture and to monitor the effects of therapy. In a population of 149 subjects, the mean SUVs of the ascending aorta, aortic arch, descending thoracic aorta, iliac arteries, and femoral arteries increased with age ($P<0.01$) [32]. In this study, inner and outer wall contours of the aortic wall were drawn on each axial CT image and the respective wall areas of four aortic segments (ascending, arch, descending, and abdominal) were calculated as net wall areas by subtracting the inner surface area from the outer surface area. Net aortic wall areas were multiplied by the slice thickness to yield aortic wall volumes. The products of aortic wall volumes and mean SUVs over each segment were calculated for each segment and called "atherosclerotic burden" or "atheroburden" (AB) values as a means for integrating structural and functional data into a single quantitative value.

FDG–PET appears to have great potential in the diagnosis and monitoring response to treatment in patients with vasculitis. Large-vessel vasculitis accounts for about 6% in an unselected population of fever of unknown origin (FUO) patients and up to 17% in elderly FUO patients, so nuclear medicine specialists need to be aware of this diagnosis. The value of FDG–PET in the diagnosis of large-vessel vasculitis and the assessment of activity and extent of disease is being increasingly emphasized in literature. The modality has been examined in almost all forms of vasculitis like giant cell arteritis [34–37], Takayasu's arteritis [38–40], polymyalgia rheumatica [41, 42], Behcet disease [43–45], systemic lupus erythematosus [46–49], polyarteritis nodosa, and Wegener's granulomatosis [50]. Several of these types involve the large thoracic vessels, and FDG–PET imaging has not only proven to be a sensitive tool for assessing disease activity but in some disorders this imaging modality has provided an objective evidence for the longstanding notion of vasculitic nature of the diseases such as polymyalgia rheumatica [41] or uncommon involvement like papillary muscle inflammation in Takayasu's arteritis [40].

Myocardial Viability

The use of FDG–PET to determine myocardial viability remains a very important technique and is considered the gold standard for this purpose. Patients with viable ischemic myocardium diagnosed by a flow/metabolism mismatch (decreased flow with preserved glucose metabolism) represent a high-risk subgroup for serious coronary events in the near future and are candidates for myocardial revascularization. With the widespread availability of this modality there has been a growing interest in the use of

Fig. 4. a Comparison of MIP FDG–PET images of a patient with sarcoidosis performed in 2009 (*left*) and 2010 (*right*) reveals no significant difference in the extent and degree of FDG uptake in the thoracic structure (a). In fact, SUV of a comparable lesion in the mid-mediastinum was 5.83 and 5.75, respectively, which is almost identical. b The same images with segmentation using an iterative thresholding algorithm [Region Of interest Visualization, Evaluation and Registration (ROVER); ABX, Radeberg, Germany] permits generating significant data with regard to the size of the lesions and their metabolic activities. These include the volume, SUVmax, SUVmean, partial volume corrected SUVmean (cSUVmean), metabolic volume product (MVP), and corrected MVP as recorded above. These values clearly demonstrate a substantial reduction in the overall metabolic burden of the disease which was not apparent from standard approach.

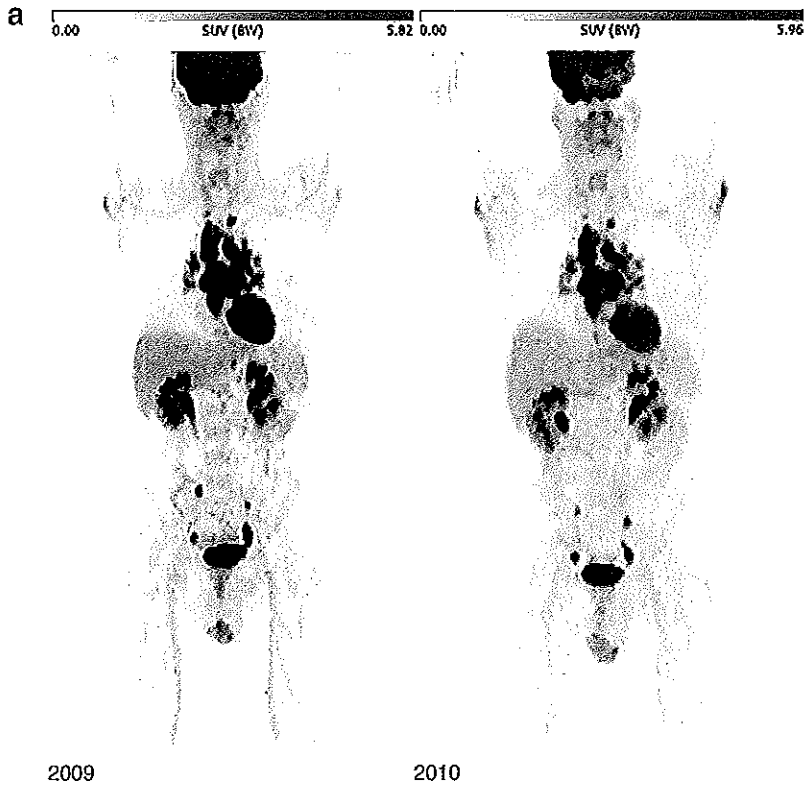

	Volume	SUVmax	SUVmean	cSUVmean	MVP	cMVP
2009	216.06	11.98	6.17	13.34	1333.73	2882.24
2010	131.46	10.59	5.30	12.29	696.75	1615.87

cardiac PET for the evaluation of patients with coronary artery disease due to its ability to detect changes in left ventricular function from rest to peak exercise and to quantify myocardial perfusion (in milliliters per minute per gram of tissue).

Therapeutic Response Monitoring

As in malignancies, FDG–PET holds great promise for determining the effects of therapy for a variety of benign disorders. Hence, in several reports, FDG–PET has been proposed as an effective tool in the evaluation of the therapeutic efficacy in infectious disease (Fig. 3). The change of FDG activity following antibiotics has been postulated as an effective way to determine the efficacy of the anti-tuberculosis therapy [51]. Chamilos et al. [52] examined the utility of this modality in 16 non-neutropenic patients with invasive mold infections. The results indicated the importance of FDG–PET in guiding the duration of treatment in most patients (n=8). The role of FDG–PET in monitoring therapeutic efficacy has also been described in the setting of invasive aspergillosis [53], candidal lung abscess following antifungal therapy [54], and *Pneumocystis carinii* pneumonia [55]. Similar promising results have been obtained in non-infectious inflammatory conditions also (discussed under each subheading). The promise of FDG–PET in early monitoring of therapeutic response has also been highlighted in extensive sarcoidosis at 6 weeks following the initiation of corticosteroid therapy [56].

Promising Future Role of FDG–PET in the Assessment of Lung and Airway Inflammation

FDG–PET is a non-invasive imaging technique that has significant potential to quantify pulmonary inflammation with high sensitivity. Pulmonary FDG–PET imaging has demonstrated enhanced FDG uptake in chronic obstructive pulmonary disease [57] and acute lung injury [58]. Also, high pulmonary uptake of FDG has been observed in patients with head injury, who are at risk of developing acute respiratory distress syndrome, but who had no lung symptoms at the time of the scan [59]. It is suggested that FDG–PET imaging can be successfully exploited to study various inflammatory pulmonary disorders and is likely to provide objective means to assess alveolar inflammation in a wide variety of diffuse lung diseases. The feasibility to monitor the extent and activity of the alveolitis during the course of the disease can be utilized for follow-up evaluation to therapy and also can be employed as a biomarker in new drug development. Furthermore, FDG uptake in the intercostal muscles has been found to be associated with COPD, asthma, recent heart failure, interstitial lung disease (post-external radiotherapy) and pulmonary embolism, and atelectasis with pleural effusion, whereas prominent visualization of right ventricle (RV) has been observed to occur in the setting of pulmonary hypertension (PH) [14, 15]. This uptake in the ICM and RV uptake can subserve as a valuable surrogate marker in the treatment-monitoring scenario of a variety of obstructive and restrictive airway diseases and in PH, respectively.

Future Direction: Combined Structure–Function Approach of Global Disease Assessment

The promise of assessing global metabolic burden in monitoring global disease activity in these systemic disorders cannot be overemphasized. Though presently this technique is under active investigation and refinement, it is likely to be employed in the near future. An example of this approach is depicted in Fig. 4a and b.

Conclusion

FDG as a surrogate marker of disease activity can be effectively utilized for assessing a variety of benign diseases and disorders including infection and inflammation due to enhanced glycolysis in these settings. Awareness of the conditions and the mechanisms for such findings will assist the physicians responsible to interpret FDG–PET scan accurately. FDG has proven to be an excellent tracer to detect inflammation in the setting of either infectious or non-infectious inflammatory processes.

Conflict of Interest Statement. The authors declare that they have no conflict of interest.

References

1. Karam M, Roberts-Klein S, Shet N, Chang J, Feustel P (2008) Bilateral hilar foci on 18F-FDG PET scan in patients without lung cancer: variables associated with benign and malignant etiology. J Nucl Med 49 (9):1429–1436
2. Bataille L, Lonneux M, Weynand B, Schoonbroodt D, Collard P, Deprez PH (2008) EUS–FNA and FDG–PET are complementary procedures in the diagnosis of enlarged mediastinal lymph nodes. Acta Gastroenterol Belg 71(2):219–229
3. Sochocky S (1958) Tuberculoma of the lung. Am Rev Tuberc 78 (3):403–410
4. Palmer PE (1979) Pulmonary tuberculosis—usual and unusual radiographic presentations. Semin Roentgenol 14(3):204–243
5. Braun JJ, Kessler R, Constantinesco A, Imperiale A (2008) (18)F-FDG PET/CT in sarcoidosis management: review and report of 20 cases. Eur J Nucl Med Mol Imaging 35(8):1537–1543, Epub 2008 Apr 17
6. Silverman KJ, Hutchins GM, Bulkley BH (1978) Cardiac sarcoid: a clinicopathologic study of 84 unselected patients with systemic sarcoidosis. Circulation 58:1204–1211
7. Pandya C, Brunken RC, Tchou P, Schoenhagen P, Culver DA (2007) Detecting cardiac involvement in sarcoidosis: a call for prospective studies of newer imaging techniques. Eur Respir J 29(2):418–422
8. Hyodo E, Hozumi T, Takemoto Y et al (2004) Early detection of cardiac involvement in patients with sarcoidosis by a non-invasive method with ultrasonic tissue characterisation. Heart 90:1275–1280
9. Kaminaga T, Takeshita T, Yamauchi T, Kawamura H, Yasuda M (2004) The role of iodine-123-labeled 15-(p-iodophenyl)-3R, S-methylpentadecanoic acid scintigraphy in the detection of local myocardial involvement of sarcoidosis. Int J Cardiol 94:99–103

10. Yamagishi H, Shirai N, Takagi M et al (2003) Identification of cardiac sarcoidosis with ^{13}N–NH_3/^{18}F-FDG PET. J Nucl Med 44:1030–1036
11. Okumura W, Iwasaki T, Toyama T, Iso T, Arai M, Oriuchi N, Endo K, Yokoyama T, Suzuki T, Kurabayashi M (2004) Usefulness of fasting 18F-FDG PET in identification of cardiac sarcoidosis. J Nucl Med 45 (12):1989–1998
12. Ishimaru S, Tsujino I, Takei T, Tsukamoto E, Sakaue S, Kamigaki M, Ito N, Ohira H, Ikeda D, Tamaki N, Nishimura M (2005) Focal uptake on 18F-fluoro-2-deoxyglucose positron emission tomography images indicates cardiac involvement of sarcoidosis. Eur Heart J 26(15):1538–1543, Epub 2005 Apr 4
13. Alavi A, Gupta N, Alberini JL, Hickeson M, Adam LE, Bhargava P, Zhuang H (2002) Positron emission tomography imaging in non-malignant thoracic disorders. Semin Nucl Med 32(4):293–321
14. Basu S, Alavi A (2007) Avid FDG uptake in the right ventricle coupled with enhanced intercostal muscle hypermetabolism in pneumoconiosis. Clin Nucl Med 32(5):407–408
15. Basu S, Alzeair S, Li G, Dadparvar S, Alavi A (2007) Etiopathologies associated with intercostal muscle hypermetabolism and prominent right ventricle visualization on 2-deoxy-2[F-18]fluoro-D-glucose-positron emission tomography: significance of an incidental finding and in the setting of a known pulmonary disease. Mol Imaging Biol 9(6):333–339
16. Shukuya T, Naka G, Kawana A, Sugiyama H, Kobayashi N, Kudo K, Yago Y, Tamegai Y, Kubota K (2006) Pneumoconiosis associated with an esophageal ulcer and uptake revealed in FDGPET. Intern Med 45 (5):293–296, Epub 2006 Apr 3
17. Bandoh S, Fujita J, Yamamoto Y, Nishiyama Y, Ueda Y, Tojo Y, Ishii T, Kubo A, Ishida T (2003) A case of lung cancer associated with pneumoconiosis diagnosed by fluorine-18 fluorodeoxyglucose positron emission tomography. Ann Nucl Med 17(7):597–600
18. Williams HT, Solis V, Dillard TA, Gossage JR Jr, Freant LJ (2008) Malignancy in kaolin pneumoconiosis found with F-18 FDG positron emission tomography. Clin Nucl Med 33(1):4–7
19. Kanegae K, Nakano I, Kimura K, Kaji H, Kuge Y, Shiga T, Zhao S, Okamoto S, Tamaki N (2007) Comparison of MET–PET and FDG–PET for differentiation between benign lesions and lung cancer in pneumoconiosis. Ann Nucl Med 21(6):331–337, Epub 2007 Aug 27
20. O'Connell M, Kennedy M (2004) Progressive massive fibrosis secondary to pulmonary silicosis appearance on F-18 fluorodeoxyglucose PET/CT. Clin Nucl Med 29(11):754–755
21. Melloni B, Monteil J, Vincent F, Bertin F, Gaillard S, Ducloux T, Verbeke S, Maubon A, Vandroux JC, Bonnaud F (2004) Assessment of 18F-fluorodeoxyglucose dual-head gamma camera in asbestos lung diseases. Eur Respir J 24(5):814–821
22. Gerbaudo VH, Sugarbaker DJ, Britz-Cunningham S, Di Carli MF, Mauceri C, Treves ST (2002) Assessment of malignant pleural mesothelioma with (18)F-FDG dual-head gamma-camera coincidence imaging: comparison with histopathology. J Nucl Med 43(9):1144–1149
23. Mavi A, Basu S, Cermik TF, Urhan M, Bathaii M, Thiruvenkatasamy D, Houseni M, Dadparvar S, Alavi A (2009) Potential of dual time point FDG–PET imaging in differentiating malignant from benign pleural disease. Mol Imaging Biol 11(5):369–378
24. Marom EM, McAdams HP, Butnor KJ, Coleman RE (2004) Positron emission tomography with fluoro-2-deoxy-d-glucose (FDG–PET) in the staging of post transplant lymphoproliferative disorder in lung transplant recipients. J Thorac Imaging 19(2):74–78
25. Bakheet SM, Powe J (1998) Benign causes of 18-FDG uptake on whole body imaging. Semin Nucl Med 28:352–358
26. Lorenzen J, Buchert R, Bleckmann C, Munchow N, Bohuslavizki KH (1999) A search for the focus in patients with fever of unknown origin: is positron-emission tomography with F-18-fluorodeoxyglucose helpful? Rofo Fortschr Geb Rontgenstrahlen Neuen Bildgeb Verfahr 171:49–53
27. Watanabe S, Nakamura Y, Kariatsumari K, Nagata T, Sakata R, Zinnouchi S et al (2003) Pulmonary paragonimiasis mimicking lung cancer on FDG–PET imaging. Anticancer Res 23:3437–3440
28. Lin P, Chu J, Pocock N (2000) Fluorine-18 FDG dual-head gamma camera coincidence imaging of radiation pneumonitis. Clin Nucl Med 25:866–869
29. Hara M, Iida A, Tohyama J, Miura N, Shiraki N, Itoh M et al (2001) FDG–PET findings in sclerosing hemangioma of the lung: a case report. Radiat Med 19:215–218
30. Yun M, Yeh D, Araujo LI et al (2001) F-18 FDG uptake in the large arteries: a new observation. Clin Nucl Med 26(4):314–319
31. Yun M, Jang S, Cucchiara A et al (2002) 18F FDG uptake in the large arteries: a correlation study with the atherogenic risk factors. Semin Nucl Med 32(1):70–76
32. Bural GG, Torigian DA, Chamroonrat W, Alkhawaldeh K, Houseni M, El-Haddad G, Alavi A (2006) Quantitative assessment of the atherosclerotic burden of the aorta by combined FDG–PET and CT image analysis: a new concept. Nucl Med Biol 33(8):1037–1043, Epub 2006 Oct 4
33. Bural GG, Torigian DA, Chamroonrat W, Houseni M, Chen W, Basu S, Kumar R, Alavi A (2008) FDG–PET is an effective imaging modality to detect and quantify age-related atherosclerosis in large arteries. Eur J Nucl Med Mol Imaging 35(3):562–569
34. Walter MA, Melzer RA, Schindler C, Muller-Brand J, Tyndall A, Nitzsche EU (2005) The value of [^{18}F]FDG–PET in the diagnosis of large-vessel vasculitis and the assessment of activity and extent of disease. Eur J Nucl Med Mol Imaging 32:674–681
35. Blockmans D, De CL, Vanderschueren S, Knockaert D, Mortelmans L, Bobbaers H (2006) Repetitive ^{18}F-fluorodeoxyglucose positron emission tomography in giant cell arteritis: a prospective study of 35 patients. Arthritis Rheum 55:131–137
36. Hautzel H, Sander O, Heinzel A, Schneider M, Müller HW (2008) Assessment of large-vessel involvement in giant cell arteritis with 18F-FDG PET: introducing an ROC-analysis-based cutoff ratio. J Nucl Med 49(7):1107–1113, Epub 2008 Jun 13
37. Meller J, Strutz F, Siefker J et al (2003) Early diagnosis and follow-up of aortitis with F-18 FDG PET and MRI. Eur J Nucl Med Mol Imaging 30:730–736
38. Webb M, Chambers A, Al-Nahhas A et al (2004) The role of F-18-FDG PET in characterising disease activity in Takayasu arteritis. Eur J Nucl Med Mol Imaging 31:627–634
39. Hara M, Goodman PC, Leder RA (1999) FDG-PET finding in early-phase Takayasu arteritis. J Comput Assist Tomogr 23:16–18, Full Text via CrossRef
40. Dumarey N, Tang BN, Goldman S, Wautrecht JC, Matos C, Unger P, Nortier J (2007) Papillary muscle inflammation in Takayasu's arteritis revealed by FDG–PET. Eur Heart J 28(8):1011
41. Blockmans D, Maes A, Stroobants S et al (1999) New arguments for a vasculitic nature of polymyalgia rheumatica using positron emission tomography. Rheumatology (Oxford) 38:444–447
42. Moosig F, Czech N, Mehl C et al (2004) Correlation between 18-fluorodeoxyglucose accumulation in large vessels and serological markers of inflammation in polymyalgia rheumatica: a quantitative PET study. Ann Rheum Dis 63:870–873
43. Wildhagen K, Meyer GJ, Stoppe G, Heintz P, Deicher H, Hundeshagen H (1989) PET and MR imaging in a neuro-Behçet syndrome. Eur J Nucl Med 15(11):764–766
44. Mineura K, Sasajima T, Kowada M, Shishido F, Uemura K, Nagata K (1989) Sequential PET studies in neuro-Behçet's syndrome. J Neurol 236(6):367–370
45. Terada T (1991) Magnetic resonance imaging in neuro-Behçet's disease—comparison with clinical, X-ray CT, and PET findings. Ryumachi 31(2):175–183
46. Otte A, Weiner SM, Hoegerle S, Wolf R, Juengling FD, Peter HH, Nitzsche EU (1998) Neuropsychiatric systemic lupus erythematosus before and after immunosuppressive treatment: a FDG PET study. Lupus 7(1):57–59
47. Weiner SM, Otte A, Schumacher M, Klein R, Gutfleisch J, Brink I, Otto P, Nitzsche BU, Moser E, Peter HH (2000) Diagnosis and monitoring of central nervous system involvement in systemic lupus erythematosus: value of F-18fluorodeoxyglucose PET. Ann Rheum Dis 59(5):377–385
48. Stoppe G, Wildhagen K, Meyer GJ, Schober O (1989) Use of fluorodeoxyglucose PET in the diagnosis of central nervous system lupus erythematosus and a comparison with CT and MRI. Nuklearmediziner 28(5):187–192
49. Meyer GJ, Schober O, Stoppe G, Wildhagen K, Seidel JW, Hundeshagen H (1989) Cerebral involvement in systemic lupus erythematosus (SLE): comparison of positron emission tomography (PET) with other imaging methods. Psychiatry Res 29(3):367–368
50. Wildhagen K, Stoppe G, Meyer GJ, Heintz P, Hundeshagen H, Deicher H (1989) Imaging diagnosis of central nervous system involvement in panarteritis nodosa. Z Rheumatol 48(6):323–325
51. Park IN, Ryu JS, Shim TS (2008) Evaluation of therapeutic response of tuberculoma using F-18 FDG positron emission tomography. Clin Nucl Med 33(1):1–3

52. Chamilos G, Macapinlac HA, Kontoyiannis DP (2008) The use of 18F-fluorodeoxyglucose positron emission tomography for the diagnosis and management of invasive mould infections. Med Mycol 46(1):23–29
53. Ozsahin H, von Planta M, Muller I, Steinert HC, Nadal D, Lauener R, Tuchschmid P, Willi UV, Ozsahin M, Crompton NE, Seger RA (1998) Successful treatment of invasive aspergillosis in chronic granulomatous disease by bone marrow transplantation, granulocyte colony-stimulating factor-mobilized granulocytes, and liposomal amphotericin-B. Blood 92:2719–2724
54. Bleeker-Rovers CP, Warris A, Drenth JP, Corstens FH, Oyen WJ, Kullberg BJ (2005) Diagnosis of Candida lung abscesses by 18F-fluorodeoxyglucose positron emission tomography. Clin Microbiol Infect 11:493–495
55. Win Z, Todd J, Al-Nahhas A (2005) FDG–PET imaging in *Pneumocystis carinii* pneumonia. Clin Nucl Med 30:690–691
56. Basu S, Asopa RV, Baghel NS (2009) Early documentation of therapeutic response at 6 weeks following corticosteroid therapy in extensive sarcoidosis: promise of FDG–PET. Clin Nucl Med 34(10):689–690
57. Jones HA, Marino PS, Shakur BS, Morrell NW (2003) *In vivo* assessment of lung inflammatory cell activity in patients with COPD and asthma. Eur Respir J 21:567–573
58. Chen DL, Schuster DP (2004) Positron emission tomography with 18F-fluorodeoxyglucose to evaluate neutrophil kinetics during acute lung injury. Am J Physiol Lung Cell Mol Physiol 286:L834–L840
59. Jones HA, Clark JC, Minhas PS, Kendall IV, Downey SP, Menon DK (1998) Pulmonary neutrophil activation following head trauma. Am J Respir Crit Care Med 157:A349

FRÅN

STOCKHOLMS LÄNS LANDSTING

Karolinska Universitetssjukhuset
Karolinska Universitetslaboratoriet
Klin Pat/Cyt lab

Tfn

B: 11002-521-SV1
S: 11002-521-SV1
F: 11002-521-S03
R: 1026-7246757-2
L: T9332-11

SVAR PATOLOGI/CYTOLOGI

Appendix 6a

TILL

Karolinska Universitetssjukhuset
Öron-,näs- och halskliniken, Huddinge
Avdelning B82
141 86 STOCKHOLM

Regnr

T9332-11

Provtagningstid:	2011-05-26 15:07	Remittent:	Gert Henriksson
Ankomstid lab:	2011-05-27	SNABBSVAR:	Tfn: 3195

Preparatets natur: Px trachealslh 1 cm ovan tumören
Frågeställning: Ca?

Anamnes: Mucoepidermoid ca trachea

SVAR

UTLÅTANDE
2011-05-31 T9332/2011
2011-442098

I snitten från px av trachea ses en liten slemhinneflaga med respiratorisk epitelbeklädnad och med sparsamt lätt inflammerat stroma. Inga hållpunkter för malignitet.
DIAGNOS
Tumörfri slemhinneflaga från trachea.
BIOBANKSINFORMATION
Provet får användas för samtliga, enligt biobankslagen, godkända ändamål.

Bela Bozoky 2011-05-31

----------slut----------

Framställd
2011-05-31 16:25

FRÅN

STOCKHOLMS LÄNS LANDSTING
Karolinska Universitetssjukhuset
Karolinska Universitetslaboratoriet
Klin Pat/Cyt lab

Tfn

B: 11002-521-SV1
S: 11002-521-SV1
F: 11002-521-S03
R: 1026-7246777-0
L: T9333-11

SVAR PATOLOGI/CYTOLOGI

Appendix 6b

TILL

Karolinska Universitetssjukhuset
Öron-,näs- och halskliniken, Huddinge
Avdelning B82
141 86 STOCKHOLM

Regnr
T9333-11

Provtagningstid:	2011-05-26 15:10	Remittent:	Gert Henriksson
Ankomstid lab:	2011-05-27	SNABBSVAR:	Tfn: 3195

Preparatets natur: Px trachealslh 2 cm ovan tumören
Frågeställning: Ca?

Anamnes: Mucoepidermoid ca trachea. Px 2 cm ovan.

SVAR

UTLÅTANDE
2011-05-31 T9333/2011
2011-442098

I snitten från px trachea ses två små slemhinneflagor med respiratorisk epitelbeklädnad och med sparsamt stroma. Löst liggande deskvamerat respiratorisk epitelbeklädnad samt granulocyter kan nämnas.

Inga tecken på malignitet.

Hållpunkter för ursprung av granulocyter förekommer ej.
DIAGNOS
Tumörfri px från trachea.
BIOBANKSINFORMATION
Provet får användas för samtliga, enligt biobankslagen, godkända ändamål.

Bela Bozoky 2011-05-31
----------slut----------

Framställd
2011-05-31 16:28

STOCKHOLMS LÄNS LANDSTING

SVAR BENMÄRGSUNDERSÖKNING

Appendix 6c

FRÅN
Karolinska Universitetssjukhuset
Karolinska Universitetslaboratoriet
Klin Pat/Cyt lab

Tfn

B: 11002-521-SV1
S: 11002-521-SV1
F: 11002-521-S03
R: 1026-7244860-6
L: MC1024-11

TILL
Karolinska Universitetssjukhuset
Öron-,näs- och halskliniken, Huddinge
Avdelning B82
141 86 STOCKHOLM

Regnr
MC1024-11

Provtagningstid: 2011-05-27 13:00
Ankomstid lab: 2011-05-27

Remittent: Jan-Erik Juto
SNABBSVAR: Tfn: 80371

Preparatets natur: Benmärg
Frågeställning: micrometastaser från mucoepidermoid cancer i bronk / mediastinum

Datum för senast givna cytostatika

Provtagningsställe	Provtagningsteknik	Provtagare (om annan än remissutfärdare)
Crista	Biopsi	

Lymfkörtlar	Lever	Mjälte	B-SR (mm)	P-CRP (mg/L)	M-komponent, typ, storlek

B-Hemoglobin (g/L)	B-Leukocyter (x10(9)/L)	B-Trombocyter (x10(9)/L)	Erc(B)-MCV (fL)	B-Reticulocyter (x10(9)/L)	P-Järn (umol/L)
134-170 150	3,5-8,8 2,7	145-348 252			

S-Ferritin (DxI) ug/L	S-Ferritin (ModE) ug/L

B-Celler (Differentialräkning, diff)

Erytroblaster (x10(9)/L)	Övriga leukocyter x10(9)/L	Blastceller (x10(9)/L)	Promyelocyter (x10(9)/L)	Myelocyter (x10(9)/L)	Metamyelocyter (x10(9)/L)
Neutrofila granulo x10(9)/L	Eosinofila granulo x10(9)/L	Basofila granulo x10(9)/L	Lymfocyter (x10(9)/L)	Monocyter (x10(9)/L)	Plasmaceller (x10(9)/L)

Anamnes: Undersökning snarast!!
Debulking av intraluminal tracheo-bronkialt växande mucoepidermoid cancer, med stor peroperativ blödning som via öppen thoraxkirurgi stoppas. Haft därefter tuberkulosinfektion med behandling och sedan fulldos strålbehandling.
Nu lokalt recidiv i trachea-bronk.
Utredning inför planerad radikal kirurgi med transplantation av luftvägs-graft.
Nu utredning inför

SVAR

Tidigare utlåtande

2011-05-27 MC1024/2011

2011-442098

Preliminärt svar från benmärg och perifert blodutstryk.

Framställd
2011-05-31 14:57

STOCKHOLMS LÄNS LANDSTING

FRÅN
Karolinska Universitetssjukhuset
Karolinska Universitetslaboratoriet
Klin Pat/Cyt lab

Tfn

B: 11002-521-SV1
S: 11002-521-SV1
F: 11002-521-S03
R: 1026-7244860-6
L: MC1024-11

TILL
Karolinska Universitetssjukhuset
Öron-,näs- och halskliniken, Huddinge
Avdelning B82
141 86 STOCKHOLM

SVAR BENMÄRGSUNDERSÖKNING

Regnr
MC1024-11

I benmärgsutstryken ses måttligt hög cellhalt, med representation av samtliga poeser. Cytologiskt kan några märgfrämmande celler ej säkert påvisas. I utstryken dominerar myelopoes, som visar tecken till komplett utmognad och innehåller 1% blaster samt upp till 8,5% promyelocyter/promonocyter. Andelen monocyter är lätt ökad. Inga tydliga dysplasitecken.

Erytropoes är rikligt företrädd, med en diskret cellfraktion, där ses megaloblastiska drag eller lätt oregelbundna kärnor.

Lymfocytpopulation består av 8,5% lymfocyter och 2% plasmaceller.

I utstryken ses flertal stora megakaryocyter; de flesta av dem har loberade kärnor.

I utstryken från perifert blod ses endast diskret poikilocytos men inga avvikelser i leukocytpopulationen. Inga omogna celler.

Således lätt aktiverad benmärg, cytologiskt utan mikrometastaser. Komplettering och definitiv bedömning ska dock ske efter undersökningen av snittmaterialet.

Tidigare diagnos

Preliminär: Cellrika benmärgsutstryk cytologiskt utan märgfrämmande celler.

Framställd
2011-05-31 14:57

FRÅN

STOCKHOLMS LÄNS LANDSTING
Karolinska Universitetssjukhuset
Karolinska Universitetslaboratoriet
Klin Pat/Cyt lab

Tfn

B: 11002-521-SV1
S: 11002-521-SV1
F: 11002-521-S03
R: 1026-7244860-6
L: MC1024-11

SVAR BENMÄRGSUNDERSÖKNING

TILL

Karolinska Universitetssjukhuset
Öron-,näs- och halskliniken, Huddinge
Avdelning B82
141 86 STOCKHOLM

Regnr
MC1024-11

BIOBANKSINFORMATION

Provet får användas för samtliga, enligt biobankslagen, godkända ändamål.

KOMPLETTERANDE UTLÅTANDE

2011-05-31 MC1024/2011

2011-442098

16 mm lång benmärgsbiopsi med cellhalt på hematopoetisk vävnad upp till 40%, representation av alla poeser. Fåtaliga små lymfocytaggregat kan påvisas. Megakaryocytpopulation är riklig och cytologiskt ordinär, utan aggregatbildning. Inga märgfrämmande celler.

I benmärgsaspiratet ses rikliga vävnadsfragment med genomsnittlig cellhalt på 40% och liknande morfologisk presentation som i biopsi. Inga synliga metastaser. Järnfärgningar utfaller positiva. I utstryken hittas inga kompletta ringsideroblaster.

Således morfologiskt ordinär benmärg, utan tecken till malignitet.

DIAGNOS

Slutlig: Benmärg morfologiskt utan hållpunkter för malignitet.

BIOBANKSINFORMATION

Provet får användas för samtliga, enligt biobankslagen, godkända

Framställd
2011-05-31 14:57

FRÅN

Karolinska Universitetssjukhuset
Karolinska Universitetslaboratoriet
Klin Pat/Cyt lab

Tfn

B: 11002-521-SV1
S: 11002-521-SV1
F: 11002-521-S03
R: 1026-7244860-6
L: MC1024-11

TILL

Karolinska Universitetssjukhuset
Öron-,näs- och halskliniken, Huddinge
Avdelning B82
141 86 STOCKHOLM

Regnr

MC1024-11

ändamål.

Monika Klimkovska 2011-05-31

----------slut----------

Karolinska Universitetssjukhuset 11001412308
Thoraxkliniken, Solna
N14 Thorax-IVA
171 76 Stockholm
tel: 08-517 748 04 fax:08-517 757 44

Appendix 7

* 2011-06-09 09:12 Jan Liska, Läk S - N14/24 Thiva/Thima (låst)

OPERATIONSBERÄTTELSE

Preop. bedömn.

36-årig man, tidigare väs frisk, ursprungligen från Eritrea, boende på Island sedan 2 år tillbaka. För 19 månader sedan sökt p g a stridorös andning, utredning visade en tumör i distala delen av trachea med nästintill totalstopp. Man gjorde då akut kirurgi för att avlägsna tumören via bronkoskopi. I samband med denna åtgärd perforerades trachea och även en lungartärgren samt vena azygos. Tillståndet ledde till omedelbar exploration via sternotomi och man kunde laga skadan med hjälp av hjärt/lungmaskinstöd. Dessutom exstirperades tumören lokalt. Efter förlängd vårdtid återhämtade sig pat mycket bra. Har sedan dess haft ett recidiv som strålbehandlats, har också haft en episod med miliar tuberkulos som är utläkt nu. Tumören har recidiverat och är av lågt diff mykoepidermoid cancer och har nu återigen andningsbesvär. Utredning med CT och PET-CT samt bronkoskopi visar att tumören är recessabel och att det inte föreligger någon misstanke på metastasering. Han remitteras därför hit för åtgärd i form av trachealresektion inkluderande carina samt rekonstruktion med en polymerprotes som förbehandlats med pats egna stamceller och slemhinna.

Assistent

Tomas Gudjarsson (thoraxkirurg från Reykjavik)
Jan Liska (Thoraxkirurgkliniken, Karolinska Univ sjh)
Paolo Macchiarini
K-H Grinnemo

Diagnos enl ICD-10

C339 Malign tumör i luftstrupen

Operationsdatum

11-06-09

Operations- åtgärdskod

GBC06 Resektion och rekonstruktion av trakea med protes
GBC13 Resektion och rekonstruktion av carina med protes
GBB00 Trakeostomi

Operationsförlopp

Resternotomi med cirkelsåg, i samband med denna liten skada på vena anonyma som ombesörjs med en 4-0 Prolene. Fridissektion av högerhjärtat och aorta ascendens (Liska). Fridissektionen fortsätter sedan (Macciarini) av cava superior, vena anonyma samt trachea proximalt, när man kommer till baksidan av vena cava finns här framför allt adherenser från tidigare operation samt strålfibros. Det går inte att få fritt utan att man delar av cavan mot detta område

Karolinska Universitetssjukhuset 11001412308
Thoraxkliniken, Solna
N14 Thorax-IVA
171 76 Stockholm
tel: 08-517 748 04 fax:08-517 757 44

längst ned. Innan dess ligeras vena azygos intrapleuralt. När man delat cavan från det fibrotiska området kring trachea på längden kan man lätt sy över denna med fortlöpande 5-0 Prolene. Ingen lumeninskränkning på cavan. Fortsatt dissektion av arteria pulmonalis på höger sida och utmed trachea proximalt inga bekymmer. I samband med dissektion av bifurkationen får man en skada på arteria pulmonalis som delas över kärltänger på höger sida alldeles mot carinaområdet. Så småningom kan sedan både höger huvudbronk och vänster huvudbronk fridissikeras. Man ser ingen makroskopisk överväxt av tumörvävnad, däremot en hel del fibrösa förändringar till följd av tidigare operationsingrepp samt strålning. Trachea delas av cirka 4-5 cm ovan carina och höger huvudbronk alldeles intill ovanlobsbronkens avgång. Vänster huvudbronk delas av cirka 1,5 cm från carina. Makroskopiskt ingen tumörväxt vilket även verifieras vid fryssnitt. Under tiden som dr Macciarini preparerar trachealprotesen sutureras pulmonalisartären (Liska) medelst interposition av ett 9 mm:s Dacrongraft. Får en tillfredsställande och bra anastomos med gott flöde i pulmonalisartären. Pat ventileras omväxlande med syrgaskateter i vänster huvudbronk samt en endotracheal tub som läggs via operationssåret. Tillfredsställande syresättning. Stabil cirkulation. Något förhöjda koldioxidvärden, i övr u a. Dr Macciarini syr sedan ner trachealprotesen. Börjar med anastomosen mot höger bronk som är tämligen mödosam. Syr först en fortlöpande rad posteriort och därefter enstaka suturer i den anteriora delen med 3-0 Prolene. Övergår sedan till den vänstra bronkanastomosen som sys på samma sätt. I samband med att man satt de enstaka suturerna i den anteriora delen fås återigen en skada på pulmonalisartären. Efter att kärltänger placerats här får så småningom det tätt. Fortsätter nu att avsluta denna bronkanastomos. Syr sedan den proximala tracheala anastomosen på samma sätt som de tidigare anastomoserna d v s fortlöpande sutur i bakväggen och framtill med enstaka suturer. Anastomosen blir harmonisk och bronkoskopiskt föreligger fina förhållanden med öppna anastomoser, inget påtagligt luftläckage. Övergår sedan till att reparera lungartären återigen (Liska). Då vi försöker exponera området där kärltången har satts tidigare börjar det blöda ymnigt. Vi beslutar då att genomföra reparation av lungartären genom att anbringa en kärltång på cava inferior och banda cava superior d v s genom en inflödesocklusion då vi planerar att göra reparationen när högerhjärtat är tomt. Risk finns vid ECMO-behandling i samband med en ev reparation för luftläckage in oxynatorn vilket är delitärt varför vi beslutar ang denna tidigare nämnda processen. Under inflödesocklusionen får pat naturligtvis

lågt blodtryck då minimalt med blod går över till vänsterhjärtat men vi kan hålla ett systoliskt tryck kring 35-40 med en märkligt nog tämligen god saturation. När det är minimal blödning i lungartären till följd av denna åtgärd kan vi sedan reparera densamma med pledgeterade suturer, efter en process på 4-5 minuter kan vi återigen släppa på blodflödet till hjärtat och pat återhämtar sig mycket snabbt. Lägger Flo-Seal, Tiesel och Surgicel i det reparerade området. Ingen kvarstående blödning. Sedan fortsätter operationen med att först lägger upp oment kring anastomosområdet mellan trachea och protesen samt vid bifurkationen. Slutligen slutes sternum efter dränageläggning i etager liksom bukincisionen. Avslutningsvis läggs en tracheostomi (P Macchiarini). Pat överstår ingreppet väl och vid överflyttning till IVA har pat stabil cirkulation och tillfredsställande ventilation.

---------- slut utskrift ----------

STOCKHOLMS LÄNS LANDSTING

SVAR PATOLOGI/CYTOLOGI

Appendix 8

FRÅN
Karolinska Universitetssjukhuset
Karolinska Universitetslaboratoriet
Klin Pat/Cyt lab

Tfn

B: 11002-521-SV1
S: 11002-521-SV1
F: 11002-303-HS1
R: 1026-7302226-9
L: T10094-11

TILL
Karolinska Universitetssjukhuset
Öron-,näs- och halskliniken, Huddinge
Avdelning B82
141 86 STOCKHOLM

Regnr
T10094-11

Provtagningstid: 2011-06-09 17:38
Ankomstid lab: 2011-06-10

Remittent: Jan-Erik Juto
Tfn:

Preparatets natur: Lgll / ärrvävnad ?
Frågeställning: Fibros? Tumörvävnad??

Anamnes: Op av recidiverande mucoepidermoid cancer i distala trachea. Radikalt syftande operatyion.
Tar ut ett fibrotiskt vävnadsstycke med lokalisation vä sida lateralt vid avgången för vänster huvudbronk.
Utgör prep till undersökning.
Strålbehandlad: Ja, år 2009

SVAR

UTLÅTANDE
2011-07-11 T10094/2011
2011-442098

2 x 1 x 0,6 cm stor lymfkörtel med slät och homogen snittyta. All material har bäddats.

Histologiskt ses en antrakotisk lymfkörtel med reaktiva förändringar i form av sinus histiocytos och follikel hyperplasi. Inga hållpunkter för malignitet i det undersökta materialet.

Dr. Monika Klimkovska konsulterad.

DIAGNOS
Reaktiv lymfadenit.
BIOBANKSINFORMATION
Provet får användas för samtliga, enligt biobankslagen, godkända ändamål.

Katalin Dobra 2011-07-11

----------slut----------

Framställd
2011-07-11 17:10

Karolinska Universitetssjukhuset 11002521SV1
Öron-,näs- och halskliniken, Huddinge
Avdelning B82
141 86 STOCKHOLM
tel: 08-585 877 91 fax:08-585 873 25

Appendix 9

* 2011-07-08 16:48 Gert Henriksson, Läk H - ÖNH-avd B82 (signerad)

EPIKRIS

Patientansvarig läkare Gert Henriksson (läk) /1cqq/

Vårdtid 11-05-24--11-07-08

Diagnos enl ICD-10 C339 Malign tumör i luftstrupen
Z430 Tillsyn av trakeostomi

Vårdförlopp Pat som vid ankomst till ÖNH-kliniken 11-05-24, efter det att han 19 mån tidigare erhållit stridor och undersökts på Reykjavik, Island, där man funnit en mucoepidermoid cancer distalt i trachea. Bronkoskopisk op, där man tar bort delar av cancern inifrån. Vid samma ingrepp får man en blödning, varför öppen thoraxkirurgi krävs för att stoppa blödningen. Därefter behandlad för lungtuberkulos och fått behandlingar under några månader för detta. Gått över till strålbehandling 66 Gy. Tumören har initialt gått tillbaka, men fått recidiv av tumör med viss stridor våren 2011. Pat har nu bedömts av prof Paolo Macchiarini för exstirp av trachea och proxmiala bronker och isättande av konstgjord trachea med implantat med införande av stamceller för optimerad tracheobroncheal anastomosering. Genomgått en preoperativ bronkoskopi 11-05-26, där man finner den distala trachealtumören liggandes till hö framåt med förträngning ner mot hö och vä huvudbronk. Det finns sedan tidigare thoraxkirurgi någon slags sutur med vitaktigt mothåll inne i distala trachea, som en rest efter tidigare thoraxkirurgiskt ingrepp i kombination med bronkoskopiskt ingrepp på Reykjavik. Vi tar px i anslutning till den preoperativa bronkoskopin, vilket visar tumörfria förhållanden, cirka 4 och 5 cm ovanför carina. Härefter kvarstannar pat och ytterligare preoperativ utredning genomförs inför det thoraxkirurgiska ingreppet 11-06-09. Se op-berättelse av dr Jan Liska 11-06-09. I samband med insättandet av den konstgjorda luftstrupen med avgångar med anastomosering både i proximala hö huvudbronk och proximala vä huvudbronk genomförs också en tracheostomi för att underlätta uppföljande bronkoskopier. Pat ligger på IVA postoperativt och genomgår dagliga bronkoskopier med försök till rengöring med bronksköljvätska fram till 11-06-23. Se IVA-epikris daterad 11-06-09--23 för detaljer. Postoperativt har man funnit candida i det delvis intorkade sekretet i den konstgjorda luftstrupen. Under den postoperativa tiden, när pat ligger på IVA, insatt på Meronem fram

Karolinska Universitetssjukhuset 11002521SV1
Öron-,näs- och halskliniken, Huddinge
Avdelning B82
141 86 STOCKHOLM
tel: 08-585 877 91 fax:08-585 873 25

till 11-06-26. Pat dekanyleras av prof Macchiarini 11-06-22. Uppföljande odling från sista bronkoskopin på IVA visar inväxt av Stenotrophomonas maltophilia, varför pat sätts in på trimsulfa. Efter det att pat överförts till vanlig vårdavd förbättras han successivt. Lokalbehandling med metylrosanilin motsvarande tracheostomat pga viss granulationspolypbildning där. Postoperativt har vi funnit en vä-sidig stämbandspares, vilket kan vara av övergående karaktär. Pat har hes röst, något läckande, pga detta. Om fortsatta besvär med vä-sidig stämbandspares kan det behövas kompletterande behandling av foniater i form av hyaluronsyreinj eller liknande vä stämband. Vid hemgång är stomat helt sammandraget. Postoperativ uppföljning med slät-rtg av lungor och slutligen CT thorax 11-07-06 visar liknande bild, där hö ovanlob ser något tätare ut och är lätt sammanfallen. Detta korrelerar till bronkoskopisk bild där ovanlobsavgången i sidled är något sammanfallen. Lung-rtg visar också genomgående förhöjd diafragma hö sida, vilket kan överensstämma med frenicuspåverkan. Vä-lungan genomgående välventilerad. Se i övrigt CT thorax-svar 11-07-06 för ytterligare detaljer. Pat går hem i gott skick.

Tillägg:

Rak bronkoskopi i narkos med rengöring av sekret från det tracheobronchiella graftet genomfördes 11-06-21 och 11-06-30. CT-bilderna 11-07-06 visar att det finns ett litet luftläckage motsvarande den distala anastomosen vid vä huvudbronk. Pat överförs till hemsjukhuset på Island och företar resa från Arlanda till Island med thoraxkirurgen, dr Tomas Gudjarsson, som också varit med vid thoraxingreppet 11-06-09.

Aktuella läkemedel vid hemgång:
T Nexium 40 mg, 1 x 1
Mixtur Laktulos 30 ml, 1 x 1
Brustabl Solvezink, 1 x 1
Bactrim forte, 1 x 2, fr.o.m. den 28/6 (förslagsvis sammanlagt 2 v behandling).
Brustabl Alvedon 500 mg, 1 x 4
T Diflucan (förslagsvis utsättning inom ytterligare 1 v).

Kopia till Dr Tomas Gudmansson, Landspitali-sjukhuset, Reykjavik.

---------- slut utskrift ----------

Karolinska Universitetssjukhuset 11002521SV1
Öron-,näs- och halskliniken, Huddinge
Avdelning B82
141 86 STOCKHOLM
tel: 08-585 877 91 fax:08-585 873 25

Appendix 10

* 2011-11-21 08:40 Jan-Erik Juto, Läk H - ÖNH-avd B82 (låst)

INTAGNINGSANT.

Patientansvarig läkare Jan-Erik Juto (läk) /1f3x/

Intagningsorsak Inkommer för en bronkoskopi och borttagning av förändring i ingången till intermediärbronken efter att ha op radikalt för en lågdifferentierad mucoepidermoid cancer i trakea juni 2011 med insättande av plastgraft. Sammantaget har efter radikalop vistats först på rehabilitering och sedan 2 mån tillbaka hemskriven till privatboende i Reykjavik. Bor tillsammans med familj, fru och barn från Eiritrea i Reykjavik.

Först under op var man tvungen att grafta hö lungartär förutom att man satte in plastgraften i trakea och övre delen av hö huvudbronk men väl ovanför ovanlobsbronken.

Pat har kontrollerats i Reykjavik av professor Tomas Gudbjartsson, thoraxkirurg, som också medverkade vid op i juni.

Pat har utvecklat en granulationsliknande förändring distalt om graften i höjd med ovanlobsbronken den man har biopserat ifrån och enl telefonuppgift från Reykjavik icke malignt utfall vid undersökning. Man önskar nu en rensning av granulationen där material förstås bör sändas till PAD för undersökning och även odling bör tagas från luftrören.

Läkemedelsavstämning Medicinfri sedan 2 mån tillbaka, då fått en kur med ett Trimetoprimpreparat som utsattes efter fullbordad kur 2 v sedan.

Status

Allmäntillstånd	Ser lite medtagen ut. Går obehindrat. Produktivt spute. Uppger att han gått ner cirka 7 kg efter op.
Munhåla och svalg	Retningsfria slemhinnor.
Halsens mjukdelar	Palperas u a. Välläkt sår efter trakeostomat och ingrepp i thorax.
Hjärta	Regelbunden rytm, cirka 110 slag/min.
Blodtryck	90/70 mmHg i vila vä arm.
Lungor	Inga andningsljud på hö sida. Relativt rena andningsljud på vä sida.

Karolinska Universitetssjukhuset 11002521SV1
Öron-,näs- och halskliniken, Huddinge
Avdelning B82
141 86 STOCKHOLM
tel: 08-585 877 91 fax:08-585 873 25

E580-001A

Bedömning

Man som kommer för revision av luftväg efter luftvägskirurgi pga cancer med insättning av en graft i trakea av plast. Inkommer för rengöring, odling och preparat för PAD. Op som planerats i jetventilation och rak bronkoskopi.

---------- slut utskrift ----------